Memo

To: Perry Wood

From: Team 9: Matt Gerlich, Alex Hawley, Phillip Kinsley, Heather Kutz, Kevin Montoya, and Erik Nelson

Date: December 13, 2013

Subject: Human Powered Vehicle Project Proposal

To address the need of a form of transportation that combines the benefits of bicycling commuting with the practicality of automobiles the team has designed and analyzed a vehicle to compete in the American Society of Mechanical Engineers Human Powered Vehicle Challenge.

This project has the clients of the American Society of Mechanical Engineers and the Northern Arizona University student section advisor, Perry Wood. Each of these clients presented the team with objectives and constraints in which the vehicle is designed around. The most significant of these design objectives were for the vehicle to be capable of high speeds, have an improved coefficient of drag over traditional bicycles, and protect the rider from the outside environment.

Presented in this project proposal is the team's vehicle design that meets all of the given requirements. The vehicle's design is a three-wheeled, recumbent style vehicle enclosed by a full fairing. It will be powered using a standard bicycle drivetrain with an integrated reverse gear. The practicality of an automobile is addressed in the design with the ability to carry cargo, a weather proof fairing, and a lighting system that includes brake lights, turn signals and a headlight. The design also accommodates a large range of riders through an adjustable seat position.

The team will begin construction and physical testing of the vehicles design in January, with the Human Powered Vehicle Challenge occurring in April. The design presented throughout this proposal will cost approximate $5,972.78 to build and test. A detailed breakdown of the costs can be seen in this proposal.

The following project proposal includes a detailed introduction to the project, the design concepts considered, engineering analysis of the designs, and a cost analysis of the vehicle.

With Regards,

Team 9: Matt Gerlich, Alex Hawley, Phillip Kinsley, Heather Kutz, Kevin Montoya, and Erik Nelson

Human Powered Vehicle Challenge

By
Matt Gerlich, Alex Hawley, Phillip Kinsley,
Heather Kutz, Kevin Montoya, Erik Nelson
Team 9

Project Proposal

Document

Submitted towards partial fulfillment of the requirements for
Mechanical Engineering Design I – Fall 2013

Department of Mechanical Engineering
Northern Arizona University
Flagstaff, AZ 86011

TABLE OF CONTENTS

NOMENCLATURE

Symbol	Description	Units
A	Area	in^2
b	base	in
c	Distance from neutral axis to extreme fiber	in
C	Airfoil length	in
C_d	Coefficient of drag	
C_R	Coefficient of rolling resistance	
d	Diameter	in
E	Modulus of elasticity	ksi
F	Applied force	lbs
f	Frictional force	lbf
F_d	Drag force	N
g	Acceleration due to gravity	m/s^2
h	height	in
$\overline{h_l}$	Average convection coefficient	W/m^2K
I	Moment of inertia	in^4
k	Theoretical stress concentration factor	
k_{cd}	Thermal conductivity	W/mK
L	Length	in
l	length	M
M	Moment	lb-in
m	Mass	Kg
N	Normal force	lbf
$\overline{Nu_l}$	Average Nusselt number	
q	Notch sensitivity	
Re_l	Reynolds number at maximum length	
$Re_{l,c}$	Critical Reynolds number	
s	Slope of a hill	°
t	Thickness coefficient	
V	Velocity	m/s
V_w	Wind velocity	m/s
W	Power	Watts
x	X coordinate of airfoil	in
y_t	Y coordinate of air foil	in
η	Drive train efficiency	
μ_s	Coefficient of static friction	
ρ	Density	$slug/in^3$

LIST OF FIGURES

LIST OF TABLES

ABSTRACT

As the world population expands in both stature and volume, the demand on existing transportation systems is continually increasing. These loads pollute our environments and often times are extremely expensive. With this is mind, a team of undergraduate mechanical engineering students set out to design a vehicle functioning on human power that can act as a viable, healthy, alternative form of transportation. Such an alternative must be capable of traveling at speeds in excess of 40mph, while still being able to safely navigate the obstacles of typical automobile environments. Similar vehicles have been developed previously, but none have adequately combined the benefits of bicycle commuting, while offering the practicality of automobiles.

The design of a human powered vehicle was broken into six key subsections: Frame, Fairing, Steering, Ergonomics, Drivetrain, and Innovation. An alloy frame of 6061-T6 aluminum was developed to support the weight of the occupant and maintain appropriate spatial and geometry relationships of critical components. Steering components that allow for a turning radius as low as 12.3 feet are mounted to this internal frame along with the occupant's seating. The position of the rider was optimized for maximum power output using a stationary fixture to measure rider power output over a range of operating positions. A drive train constructed of traditional cycling components allows the vehicle to travel at speeds ranging from zero to 45 MPH for a typical occupant, with much higher speeds possible for physically fit drivers. To further increase the vehicle's maximum speeds a low drag shell encompasses the entire vehicle, giving it aerodynamic properties a fifth that of a typical commuting bicycle and rider. Innovative features not typically found on human power vehicles were included such as complete lighting systems and remote operated ventilation systems.

The designed assembly will have its' performance as a traffic worthy vehicle evaluated on road tests at the Human Powered Vehicle Challenge (HPVC) hosted by the American Society of Mechanical Engineers (ASME). The design of this vehicle occurred during a five month span and the fabrication of a fully functional prototype spanned another five months. While the cost of development was in excess of $5000 dollars it is projected that a production version of such a vehicle could also sell for a price significantly cheaper than an automobile.

1.0 INTRODUCTION

Team 9 was given the opportunity to build and compete in the HPVC sponsored by the ASME. The HPVC consists of creating a human powered vehicle that can be used as an alternative form of transportation in everyday life. During the competition, the team will be competing in multiple events that evaluate the design, innovation, endurance, and speed of the vehicle. In the design section, the team will be required to submit a report that describes the engineering analysis and work that went into the design of the overall vehicle.

In order to define the problem, the team worked with the client Perry Wood, to identify the project need, goal, as well as the project's objectives and constraints. For the team to begin the design process the operating conditions were evaluated as well as a state of the art review was conducted. After evaluating the problem and its' specific requirements the team generated concepts for important aspects of the design, as well as conducted analysis to select the final design seen in Figure 1.1 below. With the final design selected, the team performed a cost analysis for the single prototype as well as a production run of the vehicle.

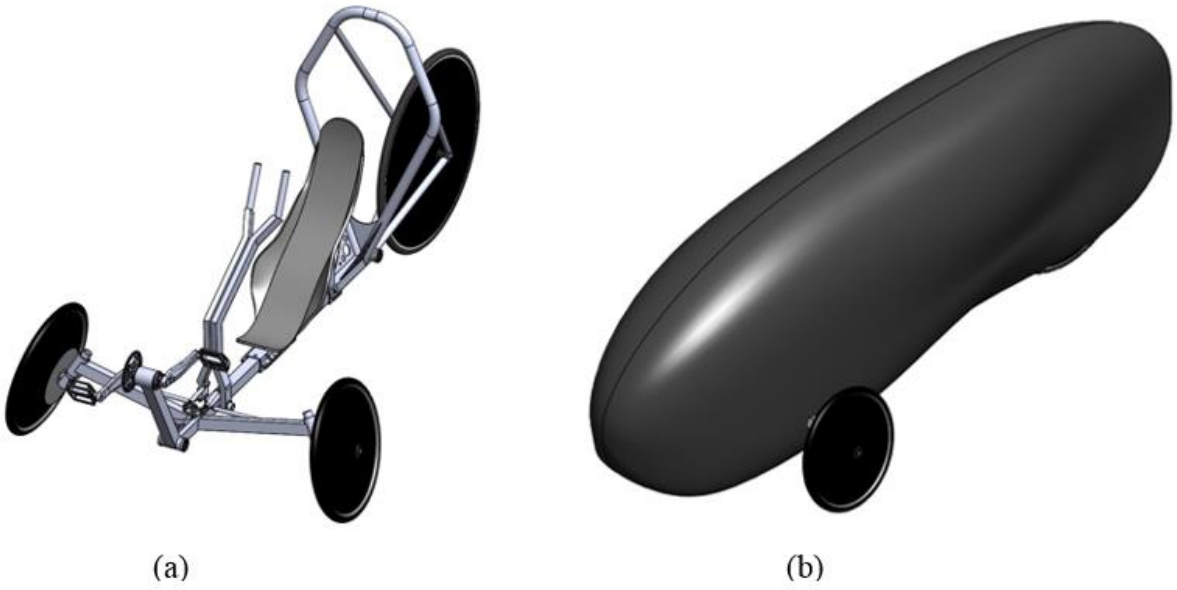

Figure 1.1-Final Design (a) Without Fairing, (b) With Fairing

1.1 CLIENT

The Human Powered Vehicle project has two major clients. These are the American Society of Mechanical Engineers, and the Northern Arizona University ASME Student Section Advisor Perry Wood. The Human Powered Vehicle Challenge is a worldwide competition through American Society of Mechanical Engineers. While ASME is a client for this project the main client is Perry Wood, a Mechanical Engineering lecturer at Northern Arizona University. Perry

Wood has been the section advisor for eight years and this will be his fifth year being the client for a capstone human powered vehicle project.

1.2 PROBLEM DESCRIPTION

The client, Perry Wood, presented a problem to the team that current forms of transportation do not meet the needs of society. Specifically, he expressed the lack of a completely human powered form of transportation that can travel at high speeds, operate in an urban environment, and protect the rider from various weather conditions and hazards.

1.3 IDENTIFICATION OF NEED

After the HPVC was assigned, the group met with the client, Perry Wood, and discussed what outcome he would like to see from this project. After the meeting, the team thoroughly reviewed the HPVC rules set forth by ASME. Multiple topics were deemed important, from which, the following need statement was formed:

"There is no current form of transportation that provides the benefits of bicycle commuting, while offering the practicality of automobiles."

The need statement exposes a noticeable gap between the two categories of bicycle commuting and automobile transportation. For instance, bicycle commuting includes less financial expenditures and traffic, ease of access to parking, and health benefits. Automobiles offer multiple benefits including weather protection, aerodynamics, operator comfort, safety, and cargo space.

1.4 PROJECT GOAL

From the need statement above, Team 9 created the following project goal:

"Design a human powered vehicle that can function as an alternative form of transportation."

With this project goal the team will have the ability to venture into territories that previous NAU teams have not in the past.

1.5 OBJECTIVES AND CONSTRAINTS

The design objectives for this project are based on the customer needs, as well as the desire for a successful performance at the ASME Human Powered Vehicle Challenge. The design objectives can be seen in Table 1.1.

Design constraints were established from the above objectives; these are displayed in Table 1.2. Additional constraints were taken from the HPVC rulebook [8], to make the vehicle suitable for competition.

Table 1.1-Objectives

Objective	**Measurement Bias**	**Units**
Vehicle can reach high speeds	Top speed on a flat surface	mph
Light weight	Total weight of vehicle	lbs
Highly maneuverable	Turning radius	ft
Contains cargo space	Volume of storage space	ft^3
Support cargo weight	Load storage space can hold	lbs
Large field of view	Total horizontal plane rider can see	degrees
Protects rider from roll over	Force roll bar can sustain	lbs
Aerodynamic	Drag force on vehicle	lbs
Production run manufacturability	Unit manufacturing cost for production run of 360	dollars
Fits diverse range of operators	Amount of seat adjustability	ft

Table 1.2-Constraints

Costumer Constraints	**ASME Competition Constraints**
Capable of exceeding 40 M/h (64.4 km/h)	Turning radius of ≤ 26.25 ft (8 m)
Vehicle weight of ≤ 80 lbf (36.3 kg)	Capable of completing 6.21 miles (10 km) in under 2.5 hours
Coefficient of drag less than that of a traditional cyclist	Roll protection system must handle 600lbf (2670N) at an angle of 12 degrees from vertical with less than 2 in (5.1 cm) deflection and 300 lbf (1330 N) side load with less than 1.5 in (3.8 cm) deflection
Development budget of $6500.00	Must have a seat belt
	Field of view must equal or exceed 180°
	Vehicle must be capable of traversing a 5% uphill or 7% downhill
	Carry a parcel of 15 X 13 X 7.9 in (38 X 33 X 20 cm) with a mass of 12.1lbf (5.5 kg)
	Come to a stop at a speed of 15.5 M/h (25 km/h) in a distance ≤ 19.7ft (6 m)
	Head lights, tail lights, side view mirrors, reflectors, and a horn

1.6 OPERATING ENVIORNMENT

In order for the team's human powered vehicle to meet the stated objectives, the vehicle must be tested within various operating environments. These environments include computer software, laboratories, field tests, and other miscellaneous environments.

In order to test the vehicle for the highest speed it is capable of reaching, the team members will each ride the vehicle down a long straight road as fast as they can. A GPS will be used to measure the max speed. Maneuverability will be tested by setting up cones in a parking lot at the desired radius and turning the vehicle within these cones.

The team will create a second roll bar identical to the roll bar that will be used on the vehicle to protect the rider and test it in a laboratory. A load will be applied to the roll bar using a Load Cell to determine the load required for failure. A laboratory will also be used when testing a 3-D printed model of the fairing in a wind tunnel. This test will tell the team if the goal of a low coefficient of drag can be achieved with the designed fairing. SolidWorks will also be useful for the same type of test on the computer generated fairing model.

Many tests can be conducted in various environments using a common tool, trial and error, or just the bike and team members. These tests will most likely occur in a machine shop where the bike is stored. A common tool such as a scale will be used to weigh the vehicle as well as the cargo that the vehicle will carry. The cargo space must be able to hold the given weight and fit a particular size of cargo, which can simply be placed in that space to ensure a perfect fit. Several tests can be conducted while a rider is sitting in the stationary vehicle. One of these tests, a visual test, includes the rider's field of view. One team member can hold an object and can pick various locations around the sides and front of the vehicle and ask the rider sitting inside the vehicle if he or she can see that object at each location. By doing this test, the team will know where there are blind spots and can make adjustments as necessary. Another test is the adjustability of the seat. Riders of various heights will adjust the seat as needed and verify that their required seat placement is available.

1.7 STATE OF THE ART RESEARCH

The team utilized a range of resources during the design of the human powered vehicle. These sources range from experts in specific fields, dedicated human powered vehicle literature, and text books.

Field experts were invaluable to the success of the team. Members consulted experts in the fields of composites manufacturing, rapid prototyping, human powered vehicle design, machining, and heat treatment processes. These experts provided information to team members through verbal and email communications. In most cases these experts were contacted by team members in an effort to find solutions to a specific problem. Often information contributed exceeded the original scope of contacting the person. The contributions of these individuals have impacted nearly

every component of the vehicle. These experts were identified through either previous personal contact with a team member or at recommendation of the project's faculty advisor Perry Wood.

Team members also referenced the large amounts of human powered vehicle specific knowledge contained within literature dedicated to the relatively small field. The International Human Powered Vehicle Association (IHPVA) published a human powered vehicle specific, technical journal from 1977 to 2004. This journal was referenced extensively during the design of both the drivetrain and low aerodynamic drag components. *Bicycling Science* [6], a book published by the MIT press details the application of traditional mechanics and exercise science concepts to the pursuit of efficient, human powered vehicles. This source has provided a wide range of information to team members, including background information and technical calculation formulas.

As with most engineering tasks the application of techniques learned in classrooms and from textbooks is adequate. The team has utilized knowledge accumulated throughout their time as undergraduate students. For more complicated design scenarios classroom text books were referenced for both calculation formulas and technical explanations. Texts detailing the fields of statics, dynamics, fluid mechanics, heat transfer, thermodynamics, biomechanics, aerodynamics, machine design, manufacturing, computer aided design, and composites design, were all referenced during the design phase of this project.

1.8 QFD

In order for the team to measure the vehicle's features with engineering standards, a Quality Function Deployment (QFD) was created. The QFD will guide the team in making difficult design decisions with consideration to competitive products. As seen in Figure 1.1, the relationship between engineering requirements, customer requirements, and bench marks from past vehicles will be used to make design decisions. The customer requirements listed are those deemed most important by the client.

		Engineering Requirements									Bench Marks	
		Yield Strength	Deformation	Cost	Velocity	Coefficient of Drag, Cd·A	Volume	Degree	Distance	Weight	The AXE (2012-2013)	Rose Hulman
Customer Requirements	Reach high speeds				x						x	x
	Light weight			x						x		x
	Maneuverable								x	x	x	
	Carry cargo						x			x	x	x
	Large field of view							x				
	Protect rider	x	x									x
	Aerodynamic				x	x					x	x
	Manufacturability			x								x
	Range of rider sizes						x			x	x	
	Units	psi (kpa)	in (m)	$	ft/s (m/s)	in^2 (m^2)	in^3 (m^3)	°	ft (m)	lbf (kg)		
		Engineering Targets										

Figure 1.2-Quality Function Deployment

2.0 CONCEPT GENERATION

After evaluating the objectives and constraints of the project the team generated design concepts for the vehicle. To simplify the design process the vehicle was broken into six subsections with a single team member in charge of each section. These sections include: frame, steering, ergonomics, drivetrain, fairing, and innovation. For each subsection, three design concepts were generated and evaluated to make the best selection. Each of these design concepts will be discussed in detail, as well as the method for which these concepts will be analyzed.

2.1 GENERAL VEHICLE CONFIGURATION

Team 9 began the concept generation stage by exploring options for a general vehicle type that would perform best during the rigors of competition and for our client, Perry Wood. After initial research, the team came to the conclusion that a successful vehicle would convert the majority of the limited power source into forward propulsion, while remaining easy to control during a variety of operating scenarios.

With a large number of factors contributing to the speed and handling of any one vehicle, team members had a challenging time identifying a clear winner from a list of potential configurations. Criteria are weighted with the use of a comparison chart, seen in Table 2.1.

Table 2.1-Derivation of Score Factors

	Low Speed Stability	Stop & Go Traffic	Top Speed	Cargo Capability	(Vehicle Weight)/Rider	Efficiency	Maintenance	Durability
Low Speed Stability		1	1	1	0	1	0	0
Stop & Go Traffic	0		1	0	0	1	0	0
Top Speed	0	1		0	0	1	1	1
Cargo Capability	0	1	1		1	1	0	1
(Vehicle Weight)/Rider	1	1	1	0		1	0	0
Efficiency	0	0	0	0	0		0	0
Maintenance	1	1	0	1	1	1		0
Durability	1	1	0	0	1	1	0	
Sub Total								
% Of Total (Score Factor)	0.107	0.214	0.143	0.071	0.107	0.250	0.036	0.071

The comparison chart allows the teams to specify an attribute's relative importance among the other attributes. Each "1" in a given column illustrates that the attribute defined in that column is of greater importance than the attribute defined in the corresponding row. Score factors are derived from a sum of each column divided by the total number of points earned from the relative importance assessment. When selecting a vehicle configuration the team evaluated six different types of vehicles, these configurations can be seen in Table 2.2 below. See Table 2.3 for the decision matrix that provided aid in selecting the vehicle configuration.

Table 2.2-Vehicle Type Description

Vehicle Type	Description
Recumbent Bicycle	2 wheeled vehicle with rider in a feet first and reclined position
4 Wheeled	4 wheeled vehicle with rider in a feet first and reclined position
Delta Trike	3 wheeled vehicle, 1 in front, 2 in rear, with rider in feet first and reclined position
Tadpole Trike	3 wheeled vehicle, 2 in front, 1 in rear, with rider in feet first and reclined position
Airplane	Airplane with thrust derived from human power
Multi Rider Vehicle	Any of the previous configurations with power derived from multiple riders

Table 2.3-Vehicle Configuration Decision Matrix

	Score Factor	Recumbent Bicycle	4 Wheeled	Delta Trike	Tadpole Trike	Airplane	Multiple Rider Vehicle
Low Speed stability	0.107	2	6	4	5	1	3
Stop & Go Traffic	0.214	2	6	4	5	1	3
Top Speed	0.143	6	3	4	5	1	2
Cargo Capability	0.071	3	6	4	5	1	2
Vehicle Weight/Rider	0.107	6	2	5	5	3	4
Efficiency	0.250	6	2	4	5	1	3
Maintenance	0.036	6	3	5	5	1	4
Durability	0.071	2	6	5	5	1	4
Scores	1.00	4.21	4.04	4.21		1.21	3.00

Design concepts are ranked from 1 to 6, with 6 representing a vehicle that would perform the best in the specified scenario, and 1 representing the vehicle that would perform the worst.

The information contained within the decision matrix indicates that a tadpole trike should be the vehicle configuration used for this project. Team members felt the decision matrix was accurate and truly indicated a vehicle that would perform best under our tests. The team subsequently chose to pursue the decision matrix suggestion.

The configuration described as a tadpole trike is shown in Figure 2.1. This arrangement consists of two front wheels mounted coaxially with roughly 1 meter in between them and 0.5 meters in front of the rider's hips. A third wheel is located along the vehicle centerline, directly behind the operator. The rider operates the vehicle from a recumbent position with propulsion power originating in the legs of the driver. Power input is usually located in the front of the vehicle, with the recumbent position being defined as a reclined, seated orientation.

Figure 2.1-Tadpole Trike

The team found that the tadpole trike was not the best performer in any of the design criteria. Instead, it was consistently second ranked in every category. The team discovered that the chosen configuration of a tadpole trike would not be the ideal choice if only intended for top speed attempts, or endurance competitions. However, the vehicle designers found this configuration provides the best all-around performance required to finish well in both the speed and endurance competitions at the ASME HPVC.

2.2 FRAME DESIGN

The frame design involves the main structure of the vehicle, as well as the roll protection system. The frame needs to be very strong and stiff to maximize power transfer and to protect the rider. Weight is also a key component of the frame design. Since the frame is going to make up a large portion of the overall weight of the vehicle, any methods to reduce weight will have a large impact to the overall weight of the system. The frame should also allow for the seat to be easily integrated into the system. For rider safety the roll protection system must keep any rider of the vehicle from coming into contact with the ground in the event of a rollover. For the competition this system is also required to support a 600lb top load and a 300lb side load, with minimal deflections in either case.

Three major designs were considered for the frame, each of which will be discussed in detail below. All of the designs share a few common points. Each frame incorporates a three wheel design, with two wheels in the front and a drive wheel in the back. Each design includes a single hoop roll bar that will extend to the top of the tallest rider's head, and will extend no further than to the edges of the widest shoulders. This will provide roll protection for all of the riders, while minimizing the cross sectional area of the vehicle to reduce drag.

The first frame design concept utilizes a single circular center tube as the main body of the frame, seen in Figure 2.2. Circular tubing has a very good strength to weight ratio, but allows for some bending and torsional deflections [2]. Circular tubing is also very common, so it would be

easy to obtain tubing in the exact dimensions required. Seat integration and overall fabrication will be more difficult since everything will have to be attached to a round surface.

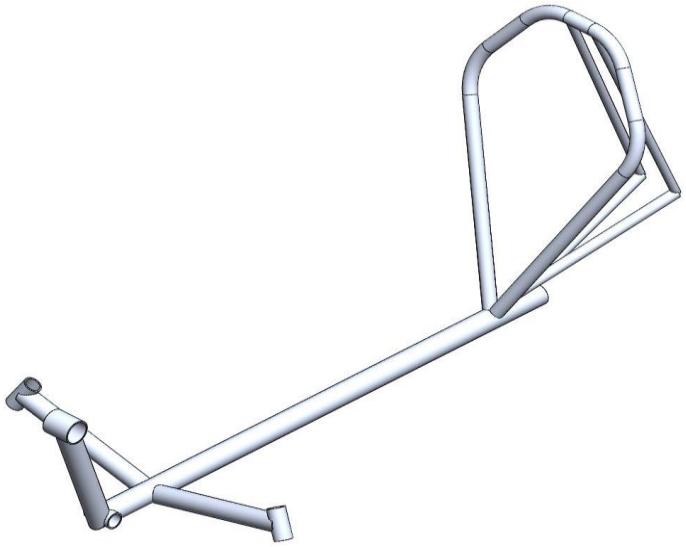

Figure 2.2-Single Center Tube Design

A second design considered, illustrated in Figure 2.3, uses a rectangular center tube. With a rectangular cross section it is possible to obtain a much higher moment of inertia and polar moment of inertia in a specific plane [1]. This will result in a very good resistance to both torsional and bending deflections. With the square flat surfaces, this design will allow for simplified seat integration and manufacturing. However, this design will have a slightly lower strength to weight ratio, and rectangular tubing is less common so finding the correct sizing may prove difficult.

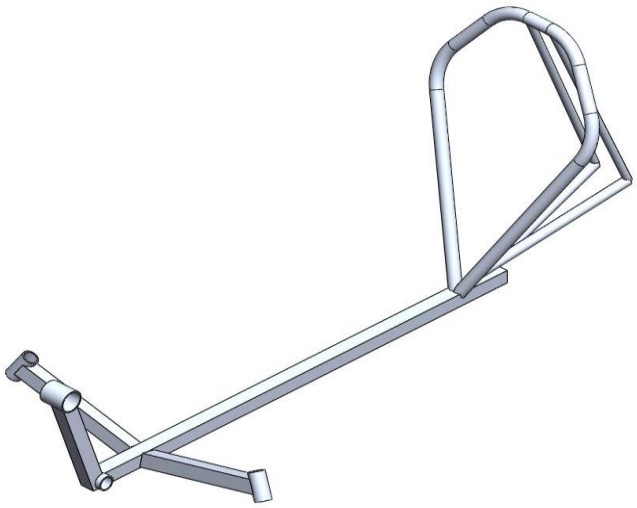

Figure 2.3- Rectangular Center Tube Design

The final design, seen in Figure 2.4, uses a system of two circular center tubes that run the length of the entire structure. This design will provide good resistance to deflections since it will be distributed over two bodies. With two separate attachment points seat integration will be simplified, and since this is composed of circular tube members, finding all of the correct sizes should not be a problem. This system will not have as great of a strength to weight ratio as the single circular tube design, and the fabrication time and complexity will be high.

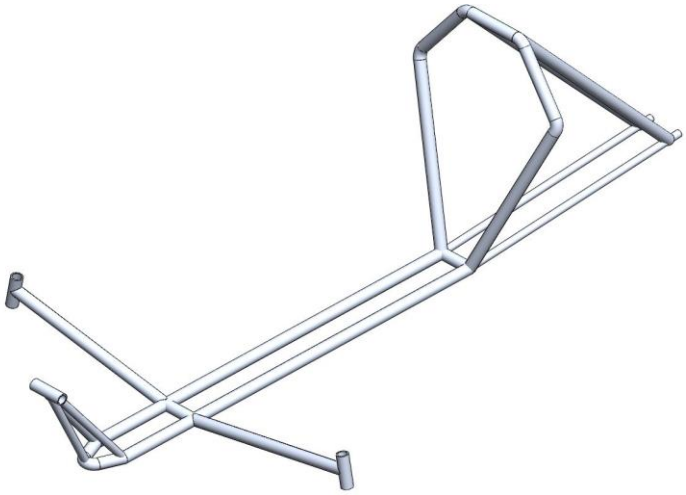

Figure 2.4- Double Circular Center Tube Design

To compare these three designs a criteria matrix was created, seen in Table 2.1. The four criteria that were compared were: weight, ease of seat integration, resistance to deflection, and fabrication time. From this matrix the resistance to deflection is the most important of the four criteria, receiving a weighting factor of 0.4. Using these factors and criteria, a decision matrix was created, it is displayed in Table 2.2. Each of the designs were ranked against each other for all of the criteria. The design that satisfied a specific criterion the best received the highest rank, of three. These ranks were then multiplied by the weighting factors from the criteria matrix, and then the sum of all the scores for each design was taken.

Table 2.1- Frame Criteria

	Weight	Ease Of Seat Integration	Resistance To Deflection	Fabrication Time
Weight		1	1	0
Ease Of Seat Integration	0		1	1
Resistance To Deflection	0	0		0
Fabrication Time	1	0	0	
Weighting Factor	**0.2**	**0.2**	**0.4**	**0.2**

The rectangular center tube design received the highest score in the decision matrix, and this will be the design the team is going to pursue. This design has the most resistance to deflection, the most simplified seat integration, and the flat surfaces will make the fabrication time the shortest of the three.

Table 2.2- Frame Decision Matrix

	Weight	Ease Of Seat Integration	Resistance To Deflection	Fabrication Time	**Score**
Score Factor	0.2	0.2	0.4	0.2	**1.0**
Circular	3	1	1	2	**1.6**
Rectangular	2	3	3	3	**2.8**
Double Circular	1	2	2	1	**1.6**

2.3 STEERING DESIGN

The steering for the human powered vehicle is a crucial component that will determine how well the vehicle will maneuver. The steering for the vehicle has constraints, given by the HPVC rule document. The rule document requires the vehicle to make a complete U-turn within an 8 meter radius [8]. The steering of the vehicle, however, cannot be too sensitive for the drag or speed trap portion of the competition. Therefore, the steering will likely have a sensitivity adjustment. The entire system must also be lightweight. Another requirement for the steering is to be responsive. This is defined as the lack of excess amount of play or movement in the input without response at the wheels. The steering also needs to be comfortable to use and not impede rider pedaling. Finally, the steering cannot require an excessive amount of force to operate, especially during tight maneuvering movements.

There are three different types of steering systems being considered for the vehicle; the first of which is a rack and pinion setup similar to that used in most cars. The next type is a Pittman arm, which is used in most solid front axle vehicle applications, such as trucks and jeeps. The final design being considered is a bell crank with a push-pull interface, similar to that found in a zero turn lawn mower.

The first design is the rack and pinion system with a typical steering wheel, as seen in Figure 2.5. This is the most common style for motorized cars. It uses a rack, which is generally a bar with gear teeth cut into it, and a meshing pinion gear that moves the rack left and right, which in turn moves the tie rods. The tie rods are adjustable linkages that transfer the linear motion to the knuckles, which are the parts that mount the wheels to the frame and allow them to pivot. A benefit of this design is that most parts to make this system are commercially available.

However, one of the limitations of the rack and pinion system is that commercially available systems require about two full rotations of the pinion, which is directly connected to the steering wheel. This will be difficult to do within the confined space of the fairing. The rack and pinion systems that do not require a full two rotations are excessively heavier and require roughly twice the force compared to the standard rack and pinion set. Lastly, rack and pinion systems interfere with the operator's ability to exit the vehicle because the steering wheel is between the rider's legs.

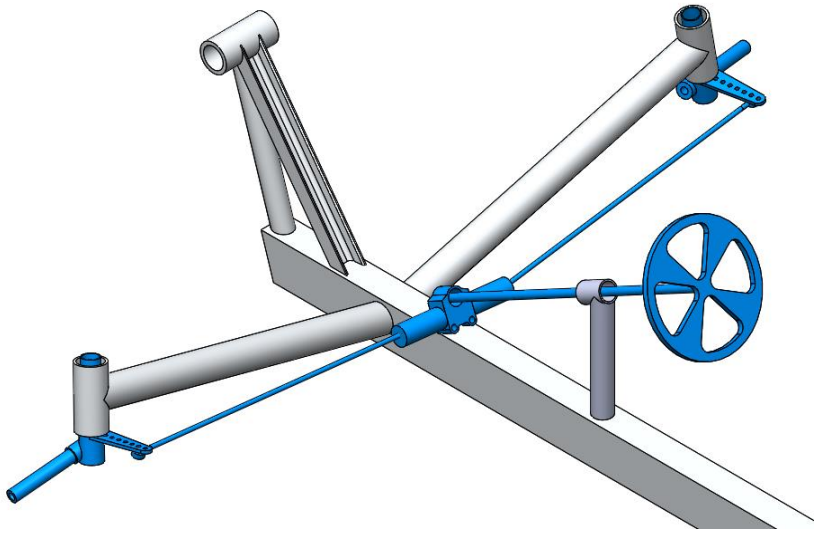

Figure 2.5-Rack and Pinion

The second design, shown in Figure 2.6, is a Pitman arm system that uses the same steering wheel as a rack and pinion system. Pitman arm steering systems are often used on go-carts, trucks, jeeps, and other heavy-duty applications. Pitman arm systems work by using the rotational motion of the steering wheel to turn a cantilever arm. At the end of the cantilever arm, two tie rods are attached that transfer motion to the wheels. The benefits of this of system are that it is lightweight. It will also require minimal fabrication and provide minimal play in the steering. One of the problems with this design is that it requires a large input force. Finally, the operator interface will be the same as with a rack and pinion and will have the same obstacles with exiting the vehicle.

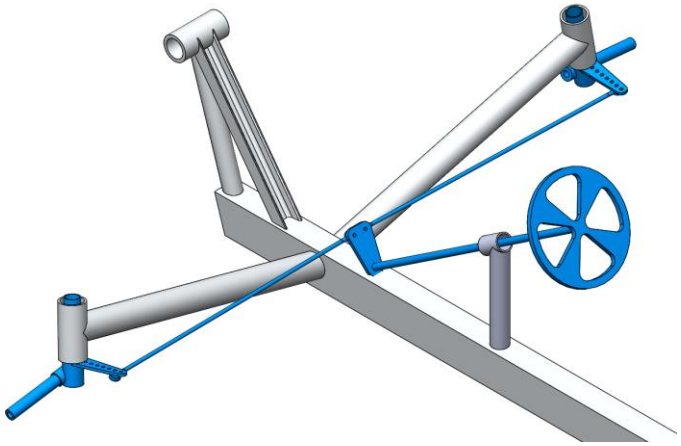

Figure 2.6-Pitman Arm

The final option is the bell crank push pull system, shown in Figure 2.7. This design is not directly used on any commercial vehicle the team is aware of. The input system is, however, very similar to that used in a zero turning radius lawn mowers. The operator would have two handles to interface with, where the user pulls right to turn right and pulls left to turn left. This system uses a set of adjustable linkages from the steering arms to turn a central bell crank. The bell crank is a part that is fixed to the frame, but is allowed to rotate about a vertical axis. The purpose of this is to transfer the horizontal rotational motion of the steering arms to a vertical axis. The tie rods are then connected to the bell crank, which are in turn connected to the knuckles in the same manner as the previous two systems. The benefits of this system include a wide range of adjustability, as well as large amounts of leverage for easy maneuvering. This system also offers the possibility of folding out of the way for rider egress. The down sides of this system, however, include increased play with an extra set of linkages and extra fabrication time.

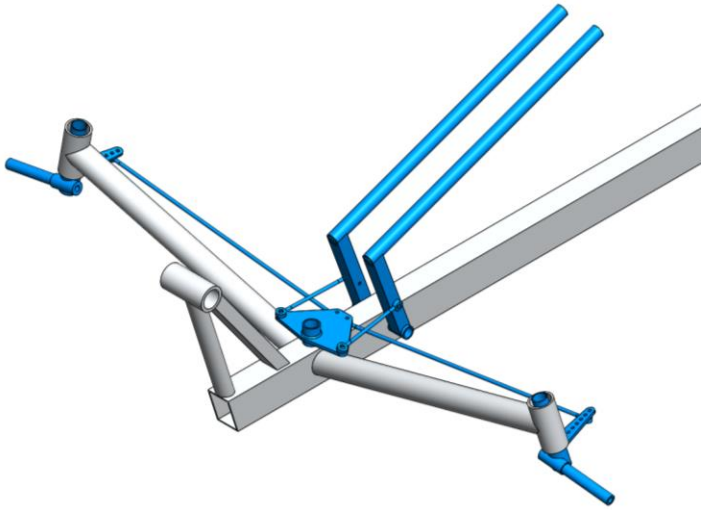

Figure 2.7-Bell Crank Push Pull

A criteria matrix was created to determine the importance of each section. This matrix is used to create a ranking system to weigh the different designs. The criteria used were: weight, cost, ease of use, ease of exiting the vehicle, fabrication, adjustability, and play. Each criterion was ranked against all of the other criteria on a scale of 0 to 1 with increments of 0.1. Table 2.4 shows ease of use was ranked highest with weight being of slightly less importance.

Table 2.4-Steering Criteria

Criteria	**Weight**	**Cost**	**Ease Of Use**	**Ease Of Exiting Vehicle**	**Fabrication Time**	**Adjustability**	**Play**
Weight		0.3	0.7	0.4	0.1	0.5	0.2
Cost	0.7		0.7	0.8	0.2	0.7	0.8
Ease Of Use	0.3	0.3		0.3	0.1	0.2	0.5
Ease Of Exiting Vehicle	0.6	0.2	0.7		0.1	0.2	0.3
Fabrication Time	0.9	0.8	0.9	0.9		0.8	0.9
Adjustability	0.5	0.3	0.8	0.8	0.2		0.2
Play	0.8	0.2	0.5	0.7	0.1	0.8	
Weight Of Criteria	3.8	2.1	4.3	3.9	0.8	3.2	2.9
Weight Factor	**0.18**	**0.1**	**0.2**	**0.19**	**0.04**	**0.15**	**0.14**

Table 2.5 compares each of the designs, where each design is given a rank from 1 to 10. The score for a given criteria is then multiplied by the corresponding weight each criterion received in Table 2.4. The weighted scores for each criterion are then summed to find the total score for each design.

Table 2.5-Steering Decision Matrix

	Weight	**Cost**	**Ease Of Use**	**Ease Of Exiting Vehicle**	**Fabrication Time**	**Adjustability**	**Play**	**Score**
RACK & PINION	2	2	4	2	9	3	4	
WEIGHTED SCORE	0.36	0.2	0.82	0.37	0.34	0.46	0.55	3.1
PITMAN ARM	8	3	3	2	7	3	8	
WEIGHTED SCORE	1.45	0.3	0.61	0.37	0.27	0.46	1.12	4.56
BELL CRANK PUSH PULL	6	8	7	8	3	6	3	
WEIGHTED SCORE	1.09	0.8	1.43	1.49	0.11	0.91	0.41	6.25

Based on the scores calculated in the matrix above, rack and pinion was determined to be the worst choice, pitman arm was the second best and the bell crank push/pull system was determined to be the best. Despite its weight, it was the best in ease of use and ease of exiting the vehicle.

2.4 ERGONOMICS DESIGN

Ergonomics for the human powered vehicle focuses on rider position and comfort. These design aspects are important because they allow the rider to get maximum efficiency with the vehicle while maintaining comfort. A key design aspect established by the team is seat adjustability. The team members vary in height from 5’4” to 6’3” and it is imperative that every member is able to operate the vehicle. With this in mind, the seat design must include a way to adjust the seat quickly to fit the appropriate operator. After brainstorming several designs, three concepts were chosen to be investigated more in depth. These concepts include the type of bracket needed to support the seat while sliding along the frame.

The first concept, as seen in Figure 2.8, includes rectangular lower brackets and one rectangular vertical tube connected to the mid back of the seat. The lower brackets will slide along the frame to adjust for rider height.

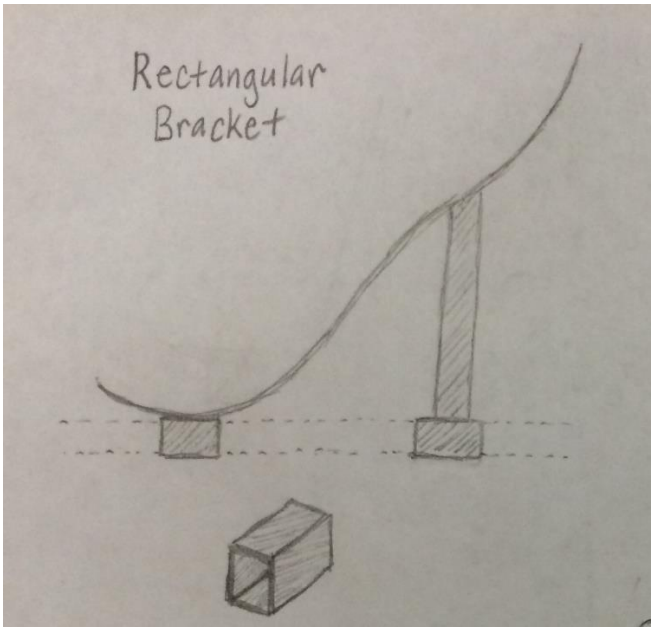

Figure 2.8 - Rectangular Bracket

The second concept, as seen in Figure 2.9, includes cylindrical lower brackets and one round vertical tube connected to the mid back of the seat. The cylindrical lower bracket provides minimal torsion support for the seat.

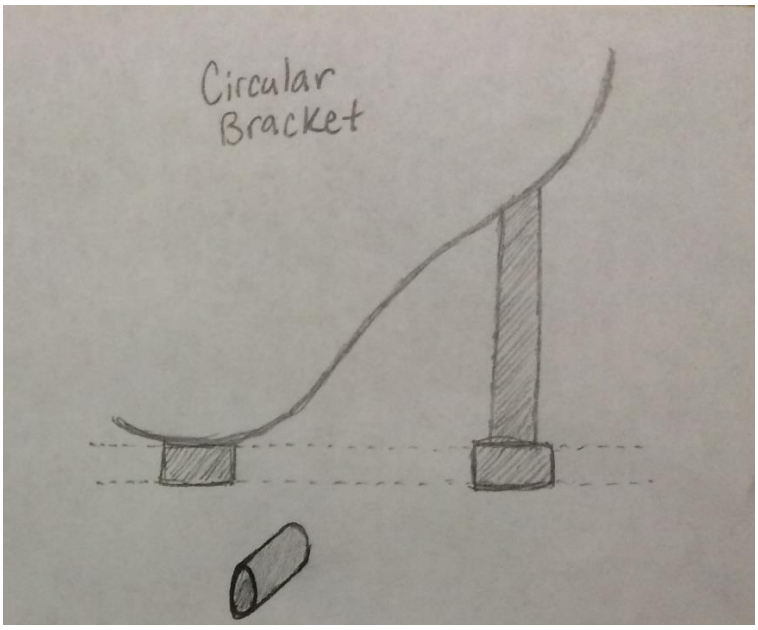

Figure 2.9 - Circular Bracket

The third concept, as seen in Figure 2.10, includes two side-by-side cylindrical lower brackets and a back support bar. This bracket layout provides greater torsional support. However, this design weighs significantly more.

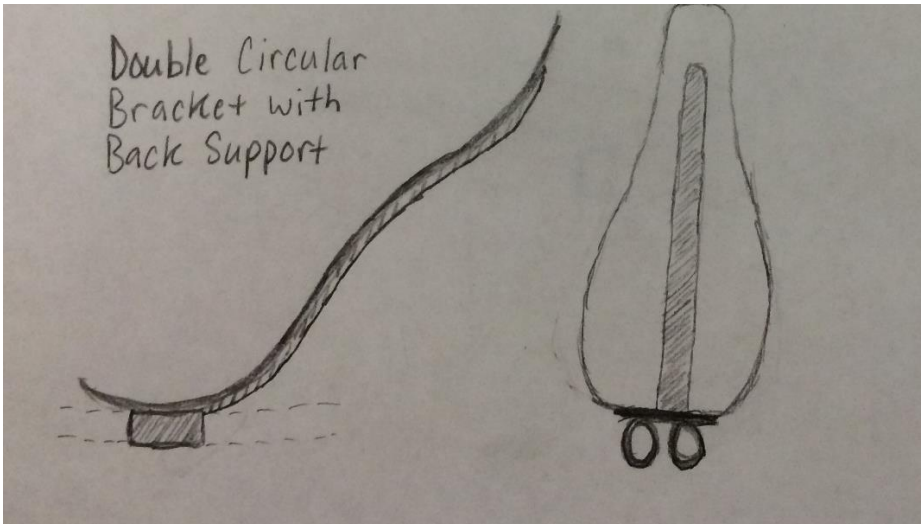

Figure 2.10-Double Circular Bracket

Due to the dependence of the design for the bottom bracket with the frame design, the rectangular bracket was selected.

One of the most important aspects of ergonomics is the rider position. This pertains to the angle between the rider's back and center tubing of the frame, the rider's chest and center of the cranks, and the center of the cranks and center tube of the frame. The maximum power output

from the operator depends on these angles because different muscles are used at different angles. The angle between the rider's back and center tube of the frame will be determined first, as it relates to the rider's visibility. The rider's eye level should be slightly higher than the top of the rider's foot on the pedals. Currently, the team is conducting a test using a trainer bike in the recumbent position that can be adjusted in multiple ways to determine the position that allows for maximum power output. A sketch of this trainer can be seen in Figure 2.11.

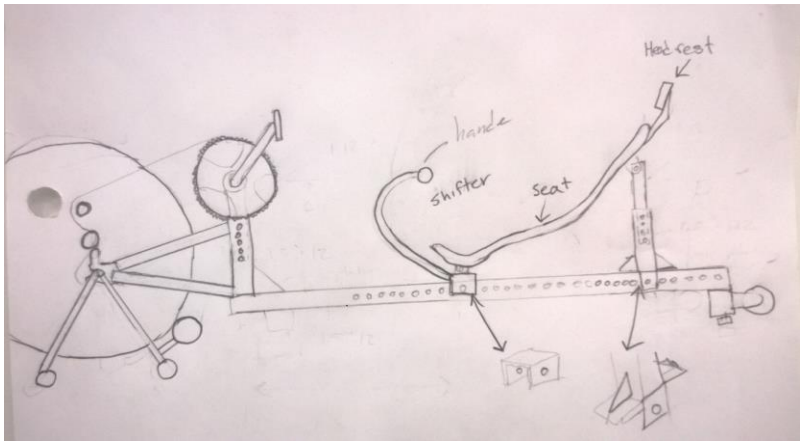

Figure 2.11-Power Testing Trainer

2.5 DRIVETRAIN DESIGN

The drivetrain subsection of the vehicle design encompasses the component selection and configuration of the vehicle's drive mechanisms. Due to the competition's requirement of the drive mechanism being powered solely by a human operator, the drivetrain will have a configuration similar to a bicycle. This involves the rider pedaling a crank system, as well as having the ability to shift gears to attain higher speeds. Figure 2.12 below, shows the location of the drivetrain with respect to the overall vehicle.

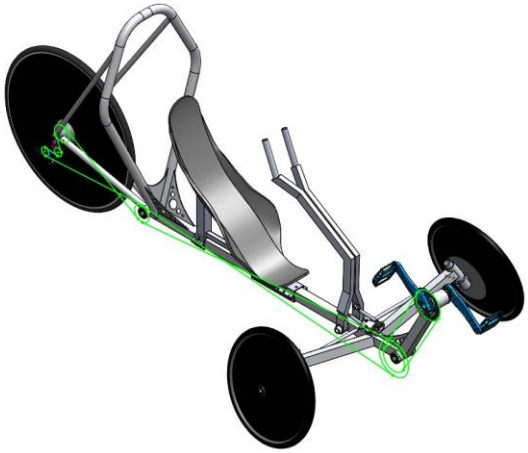

Figure 2.12-Drivetrain Location on Vehicle

Through the concept generation phase, three key drivetrain designs were researched and evaluated for application within the vehicle. These designs include an internally geared hub, step up gear, and a step up gear with the inclusion of a reverse gear. Figure 2.13 shows the general configuration of the drivetrain for the vehicle with the difference between each concept involving component selection. For each design considered, location 1 in the figure refers to the crank set and the dotted lines represent the chain line.

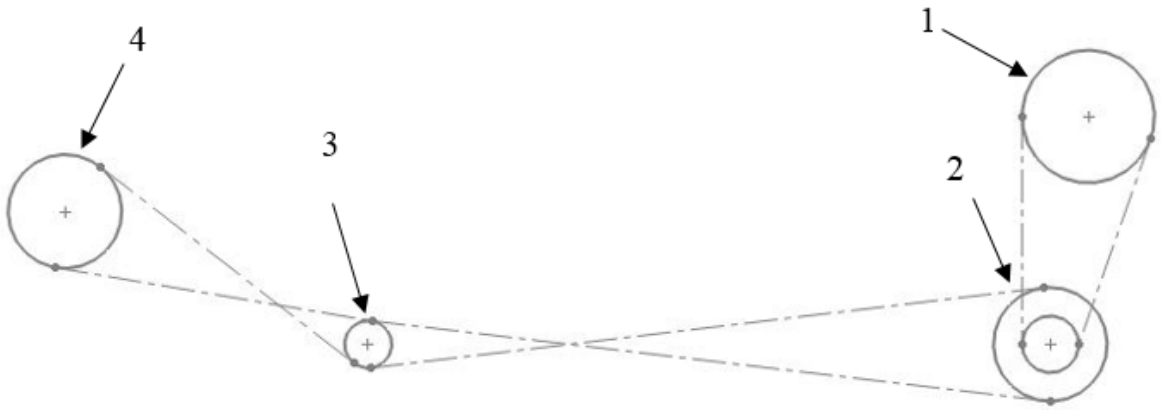

Figure 2.13-Drivetrain Layout

The first design concept considered was an internally geared hub. This design uses the configuration seen in Figure 2.13, with location 4 designating the internal hub. This design has the advantages of a constant chain length and protection of gears from the elements. The disadvantages include increased weight, and a drop in efficiency when compared to a standard rear cassette. The efficiency of an internal hub at a given gear is 90.8% compared to 93.1% of a standard rear cassette and derailleur at the same gear [7].

The next design considered was a step up gear configuration, with a standard cassette in the rear. This design focuses on the use of different sized gears in location 2 for improved gear ratios. The advantages of this design include a lower weight, easy bike repair, and the ability to fine tune the gear ratio. The disadvantages include a varying length chain line, and exposure to the elements.

The last design generated was a step up gear configuration with the inclusion of a reverse gear. The layout of this setup would be identical to the step up gear configuration displayed above, except for at location 3, where a clutch system would engage a reverse gear. This design, as seen in Figure 2.14, allows the idler gear at location 3 to spin freely when not engaged. When engaged through the use of a cable, the shaft would lock and allow direct drive of the rear wheel. This design combines the benefits of the step up gear with the ability to go in reverse.

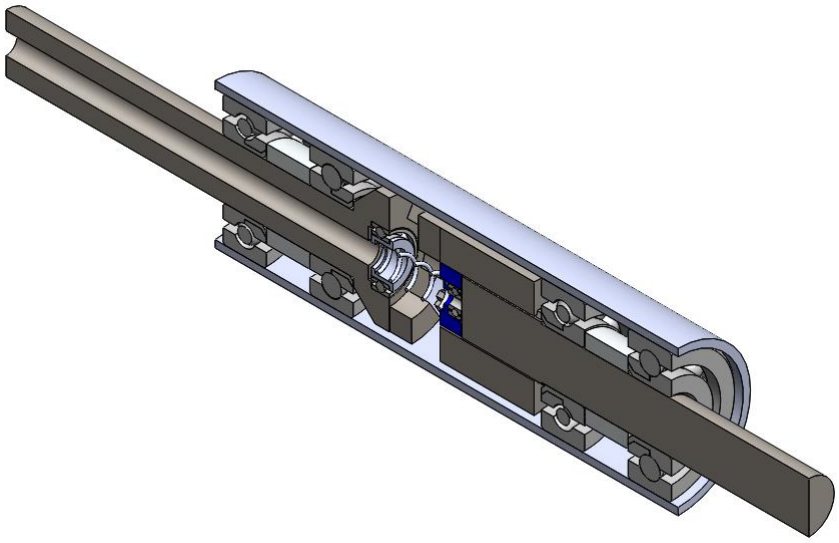

Figure 2.14- Reverse Clutch

After evaluation of the design concepts, the third design, a step up gear configuration with the inclusion of a reverse gear, was selected. This was chosen due to the added advantage provided by the reverse gear with the benefits of the step up gear. This design will allow a fine tuned gear ratio for maximum speed and maneuverability.

2.6 FAIRING DESIGN

Within the competition rules, it states “Each Vehicle shall include components, devices, or systems engineered specifically to reduce aerodynamic drag [8].” To complete these requirements, the team will be designing and creating a composite based fairing. A composite is a mixture of at least two materials, where one must be strong and stiff while the other, in ratio, is less strong but surrounds the strong material with an intimate bond [5]. Some examples of a composite include fiber reinforced polymers, concrete, and wood. While material has not been selected at this stage of the project, the overall design will be discussed and compared. Basic designs include: a front fairing, a tail fairing, and a full fairing. All three designs will be evaluated and matched to one another to see the differences. From this, the results will lead to a final decision and the beginning of the analysis.

The front fairing is a simple design that is used to help organize the fluid at the front of the vehicle to allow laminar flow to begin. Once the flow is smooth, the goal is to then have the flow pass over the operator and the tail of the vehicle. For this to happen, the nose would have to have a large cross sectional area to insure the rider and vehicle components were within that area. From Equation 1, if you were to increase the cross sectional area normal to the flow, the force would increase linearly, assuming the coefficient of drag, density of the fluid, and velocity stay constant. With a larger force, it would take more energy for the rider to reach top speeds or

maintain cruising speeds. For a simple example, the fairing would have a coefficient of drag equal to that of a half sphere. Another issue with this design, is that once the flow passes over the edge of the fairing, turbulence would then be produced, leading to more drag forces against the rider. As seen in Figure 2.15, the nose would be a smooth surface with no sharp angles, while only covering a small section of the vehicle. The benefits include low weight, ease of manufacturing, wide range of view, and ease of access.

$$F_d = \frac{1}{2} C_d \rho V^2 A \tag{2.1}$$

Where:

C_d= Coefficient of drag
F_d= Drag Force [lbs]
ρ= Density [slug/in^3]
A=Area [in^2]
V= Velocity [in/s]

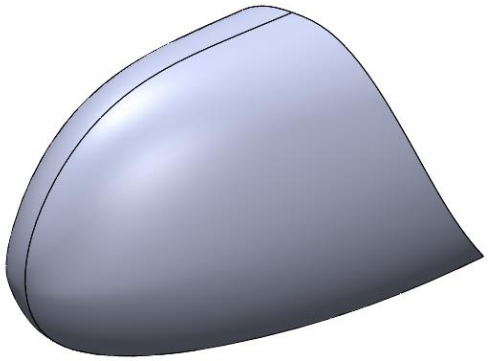

Figure 2.15-Front Fairing

Similar to the front faring, a tail faring would produce nearly the same results. While riding, assuming the riders body would fit in the hole seen in Figure 2.16, the air would hit the rider like that of a flat vertical plate. Upon diffusing around the rider, the air would follow the smooth curves of the fairing and stay in a streamline flow till the air left the tail. This would only happen at certain speeds, until turbulent flow would take effect from hitting the rider's body, thus causing more drag. With this design, there would be a similar coefficient of drag to that of a half sphere, where the flow is perpendicular to the flat surface. Its benefits, like the front fairing, are low weight, manufacturability, wide range of view, and accessibility to the bike.

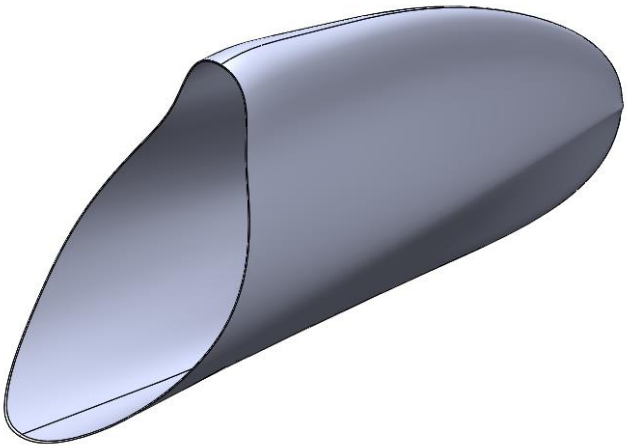

Figure 2.16-Rear Fairing

The final design concept, as seen in Figure 2.17, is a fully enclosed fairing. This would provide the benefits of being weather proof, rider protection, security, and decrease in drag forces. Although the weight of the piece will be higher than that of the partial faring, the coefficient of drag will decrease, helping the rider overcome the extra weight. For instance, once the air makes contact with the front of the fairing, it will follow the curves of the body until the air reaches the tail of the fairing. The coefficient of drag is similar to that of a streamlined body, which is around .04 [3]. Manufacturing the part will also be time extensive and complicated due to multiple layups for doors, window, removable nose cone, as well as a removable tail section.

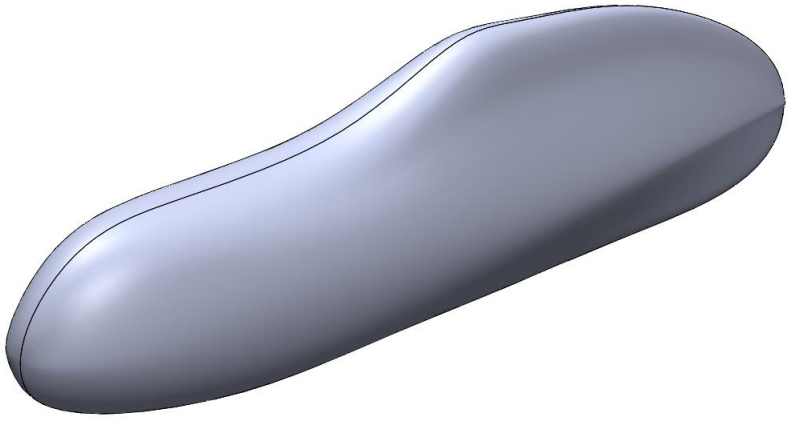

Figure 2.17-Full Fairing

From the three designs above, the fairing section came to a conclusion that the full fairing, although heavier than the other two, will have a better coefficient of drag compared to the partial fairings. It will also keep the rider out of the elements and allow the rider to have a sense of security. The fairing shown in Figure 2.17 is a conceptual model and in no way dictates the final design shape. From this step forward, many changes will be made to the shape including: the length, height, and width. These variables will be changed either independently or dependently,

thus creating numerous designs. These designs will be placed under computation fluid dynamics and their results, compared and evaluated. In conclusion, the team will be designing a full fairing to allow for better aerodynamics and weather proofing.

2.7 INNOVATION DESIGN

Each year, ASME judges set three topics of interest for teams to focus on for the design of a HPVC entry. In 2014, ASME has placed emphasis on: weather proofing, rider safety, and sustainable manufacturing. The members of the 2014 design team have chosen to pursue each of these topics in the design and fabrication of their entry to the HPVC. Of the three options, a single topic of innovation will be selected for presentation to the judges at competition as our innovative solution to the problem they have identified.

While none of the designs conceived under the innovation subsection are critical to the basic operation of the vehicle, these concepts will work to further improve human powered vehicles as a viable, safe, and comfortable replacement for traditional automobiles. The team will be drawing much of its inspiration from the automotive industry, while still remaining loyal to the environmentally friendly, health conscious culture associated with human powered vehicles.

ASME has intentionally allowed teams to interpret the term weatherproofing openly, leaving no constraints on which direction teams may pursue. This year the team chose to focus their weather proofing solutions towards high temperatures and rainy operation.

During research, the team identified how critical it is to adequately cool the operator if high power output is desired. A ducting system that allows external air to enter the fairing volume was devised. However, this concept alone would not prove beneficial in hot operating environments. Furthermore, open ducts could allow moderate amounts of precipitation to enter the fairing.

Subsequently a servo operated, closing vent design was developed. This will allow the vent to shut during cold or wet operating environments. The ability of the duct to close also gives the rider the option to close off the system when lower aerodynamic drag is of greater benefit than increased cooling.

For operation on days that are excessively warm, the team considered methods for cooling the incoming air to a temperature below that of the ambient, surrounding air. This temperature decrease would increase heat transfer between the operator’s skin and surrounding air. While the incoming wind velocity will improve the evaporation of sweat, further cooling the operator.

A finned cold block and evaporative cooling solution will be explored as methods for cooling the incoming air. However, neither solution may be viable if further analysis determines that, for the system to be effective, either its size or mass is unreasonably large for the application. A preliminary model of the proposed duct and finned cold block can be seen in Figures 2.18 and 2.19.

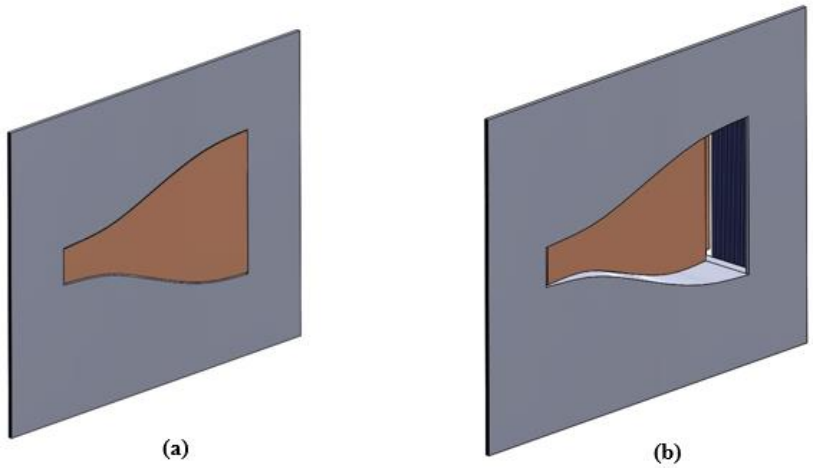

Figure 2.18-(a) Exterior Vent Open, (b) Exterior Vent Closed

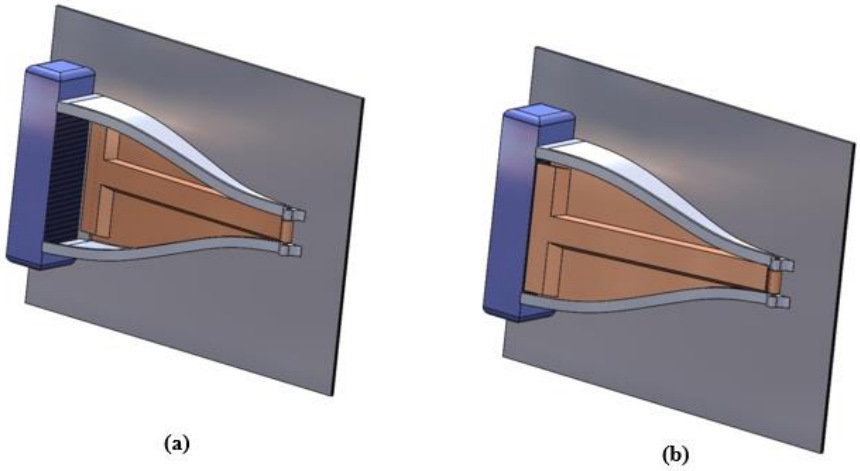

Figure 2.19-(a) Interior Vent Open, (b) Interior Vent Closed

One of the most beneficial aspects of automobiles is their ability to keep their operators relatively comfortable under adverse conditions; meanwhile bicycles perform poorly in this area. Team members will attempt to design a vehicle that will be completely watertight while operating during rainy weather. This will require any openings to the outside to be closed and sealed during a rain storm.

Another feature seen in automobiles that the team wishes to incorporate is the ability to communicate driver intentions. For optimal safety, the team has chosen to outfit the vehicle with a fully functional light communication system, including: headlights, taillights, brake lights, and turning signals. Low drag side view mirrors will also be installed to further increase driver awareness.

Sustainable manufacturing refers to the team's ability to construct the vehicle with a minimal impact on the environment. Because incorporating all contemporary methods of sustainable manufacturing is out of the scope of this project, the team chose to focus its efforts on one popular aspect of this methodology, waste. Specifically, team members will focus on the minimization of waste and the recycling of materials previously deemed unusable. This methodology will extend through all aspects of the design and construction of the vehicle.

Team members have identified abundant sources of useful materials in non-ideal states. These include: metal shavings, metal scraps, various plastics, graphite and fiberglass scraps. The team will explore the viability of combining these materials to form a new composite material that has improved properties relative to the raw forms of the source materials. In the event such a combination is identified, it will be utilized on the vehicle when appropriate. Figure 2.20, shows a mold that has been fabricated for testing of material combinations.

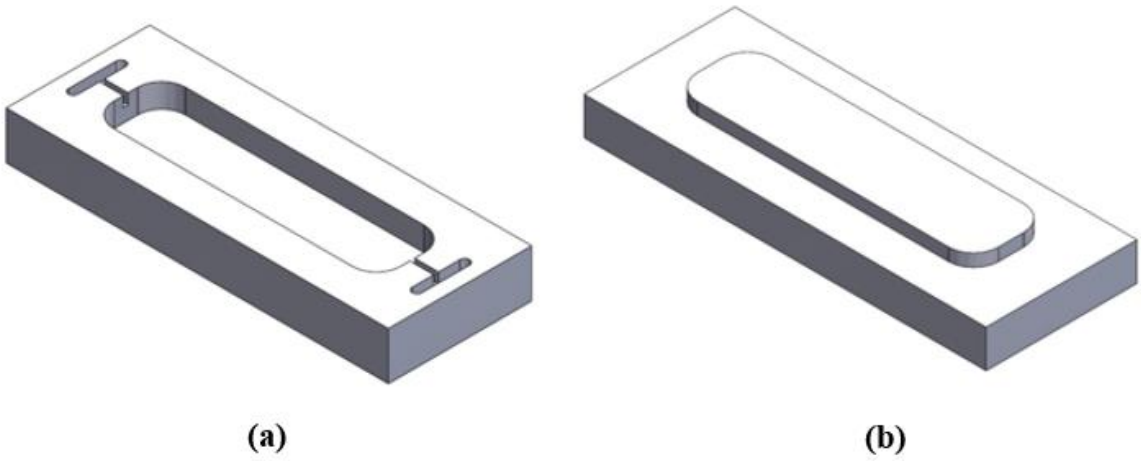

Figure 2.20-(a) Test Mold Bottom, (b) Test Mold Top

Aluminum castings fabricated from scrap metal chips are also under consideration. Vehicle parts that require machining produce considerable amounts of waste that is generally discarded. The team is evaluating the possibility of collecting this machining waste and recasting this material into new parts.

3.0 ENGINEERING ANALYSIS

After producing several design concepts, the team conducted analysis on the chosen design for each subsection. The analysis was completed using hand calculations, MATLAB, Finite Element Analysis (FEA) in SolidWorks, and flow analysis in SolidWorks. The frame design required several tests to determine the deflection in the roll bar and stress in the outriggers. Similar tests were done for steering on the knuckles. For the ergonomics section, a rider position study was conducted to determine the angle at which the rider would be reclined in the recumbent position. Gear ratios were calculated for the drivetrain analysis and reverse gear concept. The full fairing

needed various analysis calculations, such as fluid flow. Finally, for the innovation aspect of the bike, heat transfer was used for the venting system, and a tipping analysis was performed to confirm the safety of the vehicle. Each of these analyses are presented in full detail along with the final design for each subsection.

3.1 FRAME

The frame section of the analysis was broken into three separate sections: the main center tube, the outriggers, and the roll bar. Bending resistances were examined for the center tube because they were deemed important. The outriggers and the roll bar were both analyzed for stresses and deflections. Along with the above analysis, all the weights were compared to find the most optimal strength to weight ratio for each part.

Initially five different configurations were analyzed by hand. These configurations include: 2" diameter aluminum with 0.125" thickness, 1.75" diameter aluminum with 0.125" thickness, 1.5"x1.5" square aluminum with 0.125" thickness, 2"x1" rectangular aluminum with 0.125" thickness, and 1.5" diameter steel with 0.058" thickness, which was used as a baseline comparison because it was used on NAU's Human Powered Vehicle in the past. All of the aluminum being analyzed is 6061 T6 and the steel is 4130.

The first analysis task was to find resistance to deflection for the center tube for each configuration. The frame was simplified to a simply supported beam with an applied load to the top. From this, a free body diagram was constructed, as seen in Figure 3.1. The deflection for this case can be found using the following equation [1]:

$$y = \frac{Fbx}{6EIL}(x^2 + b^2 - l^2) \tag{3.1}$$

Where:

F= applied force [lb]
b= distance from B to force [in]
x= distance from A to force [in]
L= length of beam [in]
E= modulus of elasticity [ksi]
I= moment of inertia [in^4]

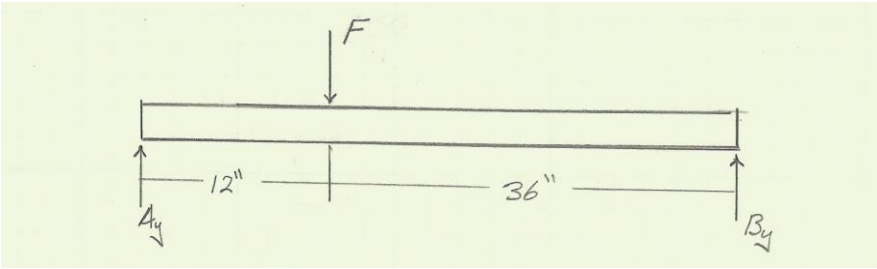

Figure 3.1-Frame Free Body Diagram

The modulus of elasticity for 6061 T6 aluminum is 10,400 ksi, and for 4130, the modulus of elasticity is 29,000 ksi [2]. The moment of inertia was found for the rectangular and square cross sections using the following equation:

$$I_{rec} = \frac{b_1 h_1^3 - b_2 h_3^3}{12} \tag{3.2}$$

Where:

b_1= outside base [in]
b_2= inner base [in]
h_1= outer height [in]
h_2= inner height [in]

To find the moment of inertia for the circular cross sections the following equation was used:

$$I_{cir} = \pi \frac{d_o^4 - d_i^4}{64} \tag{3.3}$$

Where:

d_o= outer diameter [in]
d_i= inner diameter [in]

The same deflection calculations were performed on the outriggers. These were simplified into a cantilever beam with an applied load to the end. The free body diagram for this can be seen below:

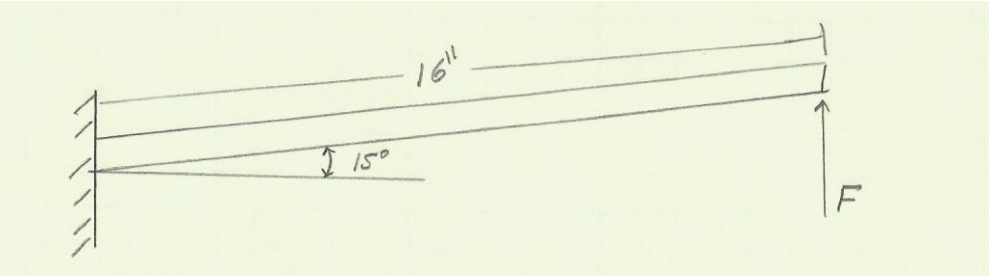

Figure 3.2-Outrigger Free Body Diagram

The deflection for this scenario is given by the following equation:

$$y = \frac{PL^3}{3EI} \tag{3.4}$$

Where:

P= Fcos(15°) [lbs]

In addition to this, the bending stresses on the outriggers also needed to be calculated. To accomplish this, the following equation was used:

$$\sigma = \frac{Mc}{I} \tag{3.5}$$

Where:

c= distance from neutral axis to extreme fiber [in]
M= moment [lb-in]

Stress concentrations were also taken into account for the outrigger connection to the frame. To find the stress concentration the following equations were used:

$$K_f \approx 1 + q(k_t - 1) \tag{3.6}$$

Where:

q= notch sensitivity
k_t= theoretical stress concentration factor

$$\sigma_{max} = K_f \sigma_{nom} \tag{3.7}$$

K_t and q were approximated for aluminum using tables [2]. K_f was found to be 1.54 for the square geometry and 1.45 for the round geometry.

The results from these calculations are given in Table 3.1 below. The force applied on the main tube was 600lb, and the force on the edge of the outriggers was 275lb, measured from accelerometer tests, seen in Appendix C. The deflections were also calculated for a lateral load applied in the z-direction of the material. The lateral load for the main tube was 300lb and the lateral load for the outriggers was 100lb.

Table 3.1-Hand Calculation Results

Configuration	**1.5”OD x0.058”ST**	**2”OD x0.125”AL**	**1.5” x1.5”X0.125”AL**	**1.75”OD x0.125”AL**	**2”x1” x0.125”AL**
Main Tube Deflection [in]	0.392	0.230	0.342	0.353	0.225
Outrigger Deflection [in]	0.183	0.107	0.159	0.165	0.105
Main Tube Lateral Deflection [in]	0.196	0.115	0.171	0.176	0.356
Outrigger Lateral Deflection [in]	0.069	0.040	0.060	0.062	0.125
Weight [lb/in]	0.075	0.071	0.066	0.061	0.066
Outrigger Stress [psi]	46598	13077	14593	17551	12813
Outrigger Stress Max [psi]	55917	18961	22473	25448	19732

With aluminum having a yield strength of 40,000 psi [2], none of the configurations failed, but from this data it was clear that the 1.5”x1.5”x0.125” square tube, 2”x0.125” circular tube, and the 1.75”x0.125” circular tube were the best choices to continue analysis with. SolidWorks models were constructed for the three configurations and finite element analysis was used on each configuration to compare to the hand calculations.

The results of the outrigger calculations for the 1.5”x1.5” square tubing is displayed in Figures 3.3 and 3.4. The max stress on the outrigger was 16,309 psi, and the max deflection was calculated to be 0.159”. The stress number is in between the nominal and max calculated by hand, and the deflection is exactly the number calculated by hand. Therefore, these numbers appear to be valid.

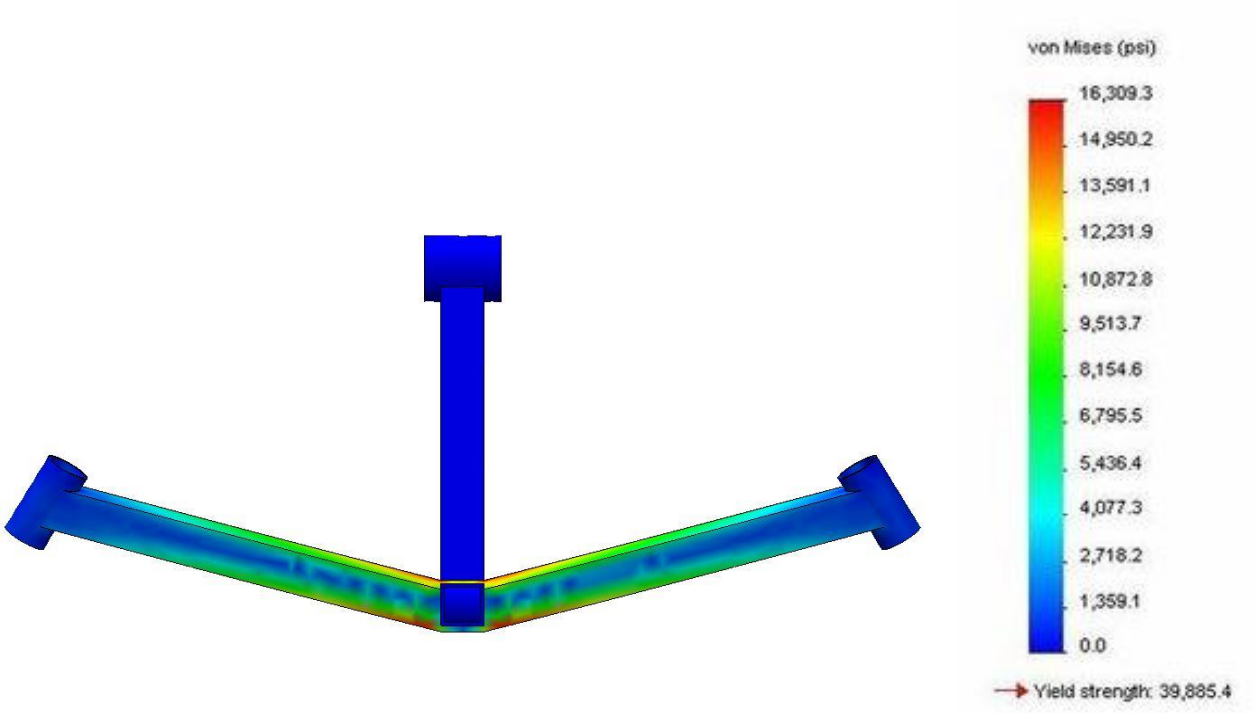

Figure 3.3-Square Outrigger Stress

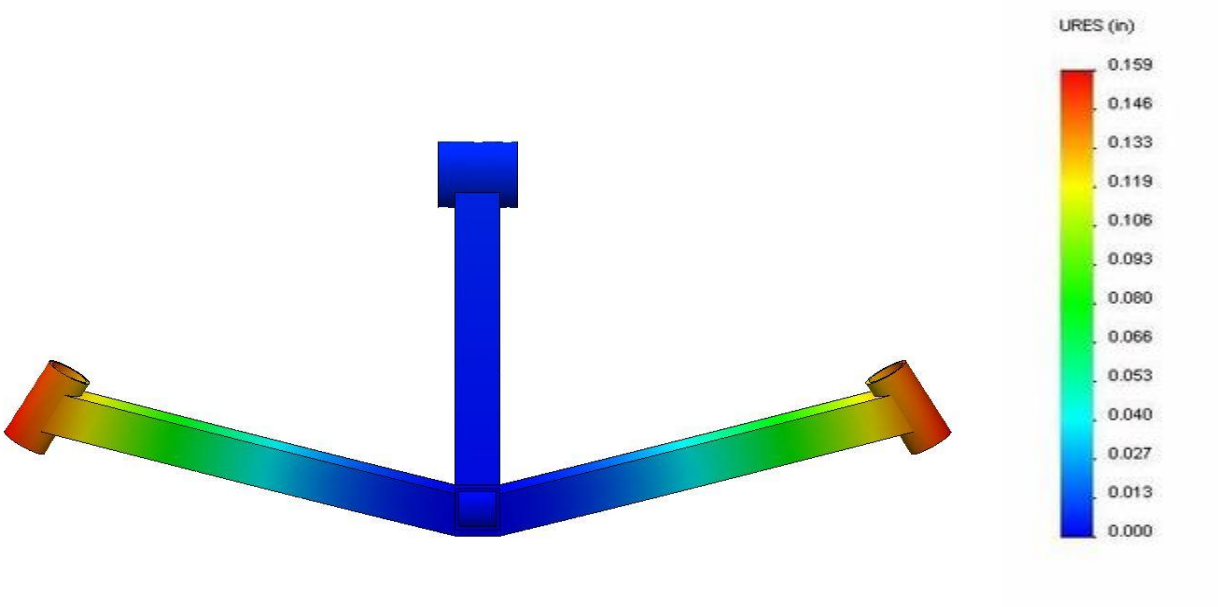

Figure 3.4-Square Outrigger Deflection

The finite element analysis results for the 1.75” circular tubing outriggers is displayed in Figures 3.5 and 3.6. The max stress the outrigger experienced in this test was 21,897 psi, and the maximum deflection was 0.139”. The stress, again, fell between the nominal and maximum calculated values, and the deflection was slightly less than the value calculated by hand.

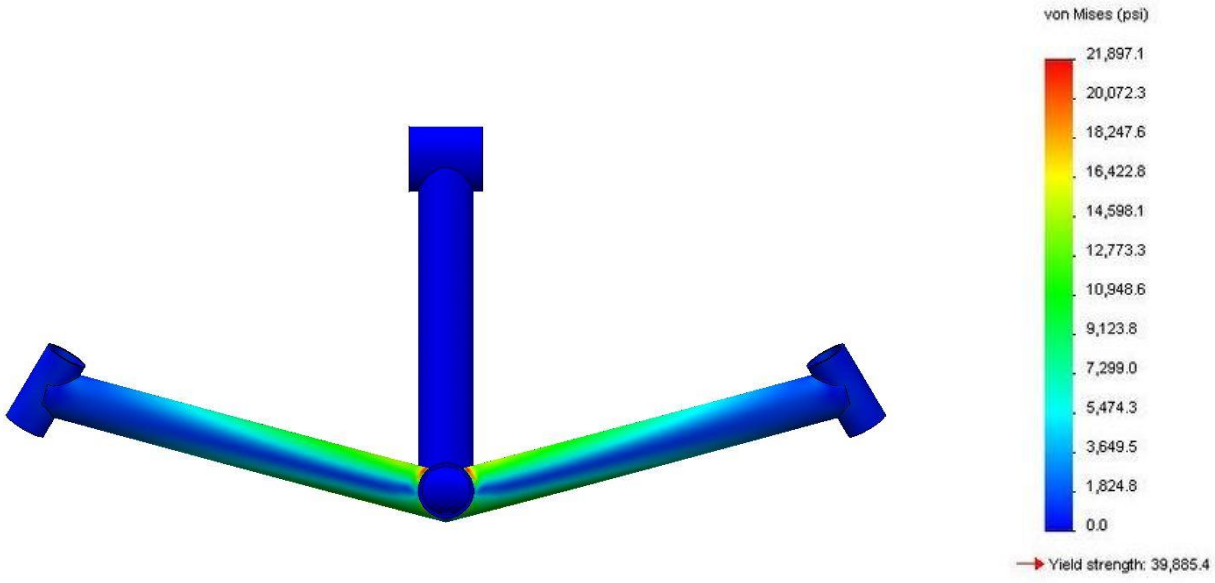

Figure 3.5-Circular Outrigger Stress

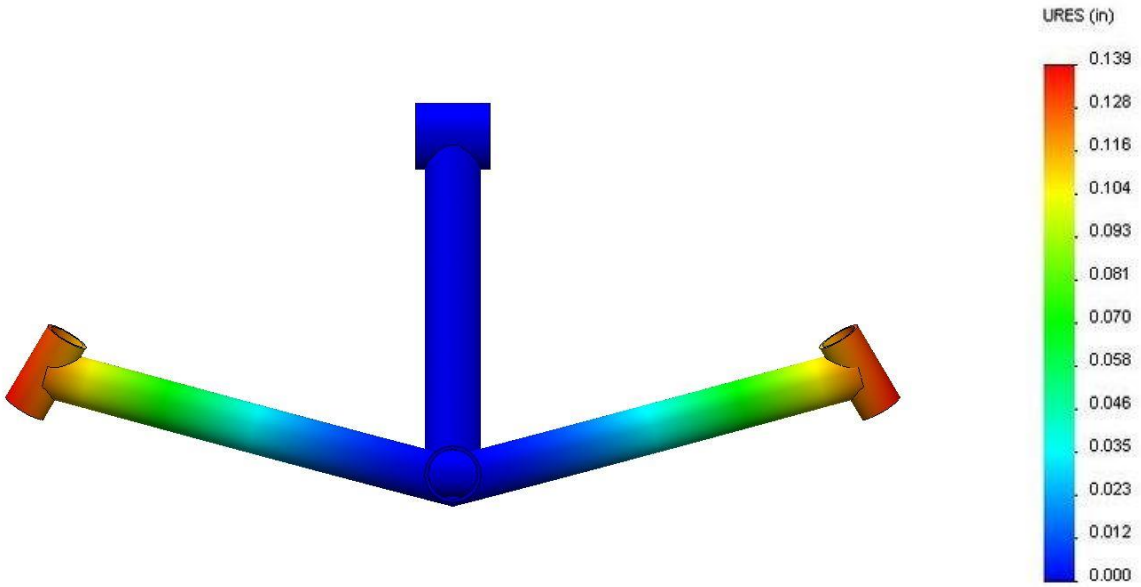

Figure 3.6-Circular Outrigger Deflection

The roll bar was also tested in three separate loading configurations: the max driving load of 225lb at the wheel from the accelerometer readings, 600lb top load, and 300lb side load as per the competition requirements.

The 225lb load at the wheel test can be seen in Figure 3.7. This test resulted in a maximum stress of 13,600 psi.

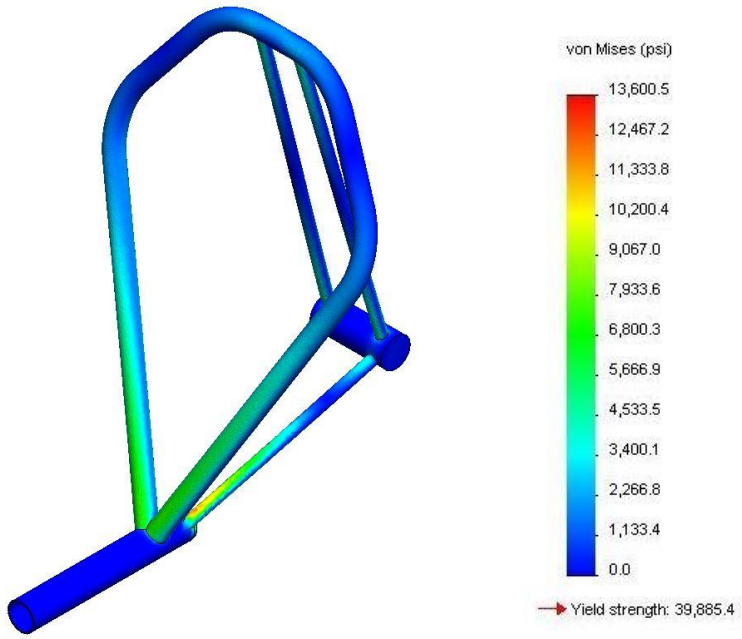

Figure 3.7-Driving Load Roll Bar Stress

The next test was the 600lb top load applied at an angle of 12° from vertical. The maximum stress experienced was 25,926psi, and the overall deformation was 0.607”, which is well below the competition requirements of 2”. This deflection can be seen in Figure 3.8 below:

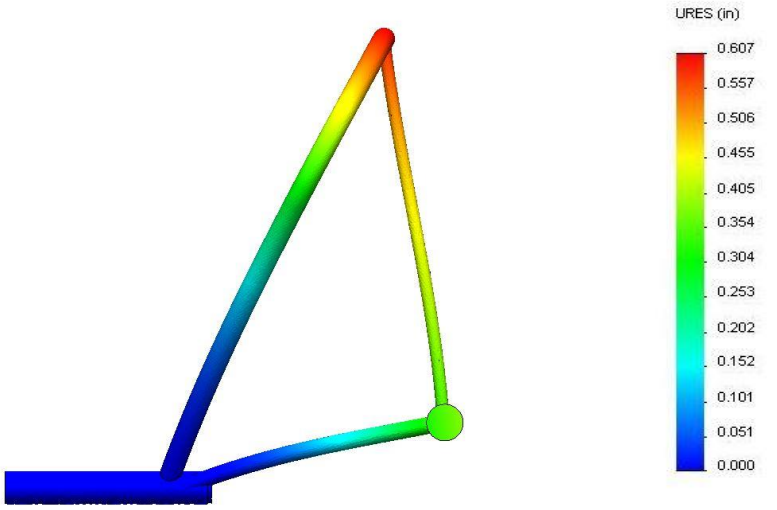

Figure 3.8-Top Load Roll Bar Deflection

With the 300lb load applied at shoulder height, the roll bar experienced a maximum stress of 20,171 psi and a maximum deflection of 0.511”, again below the competition requirement of less than 1.5”. This deflection can be seen in the Figure 3.9 below:

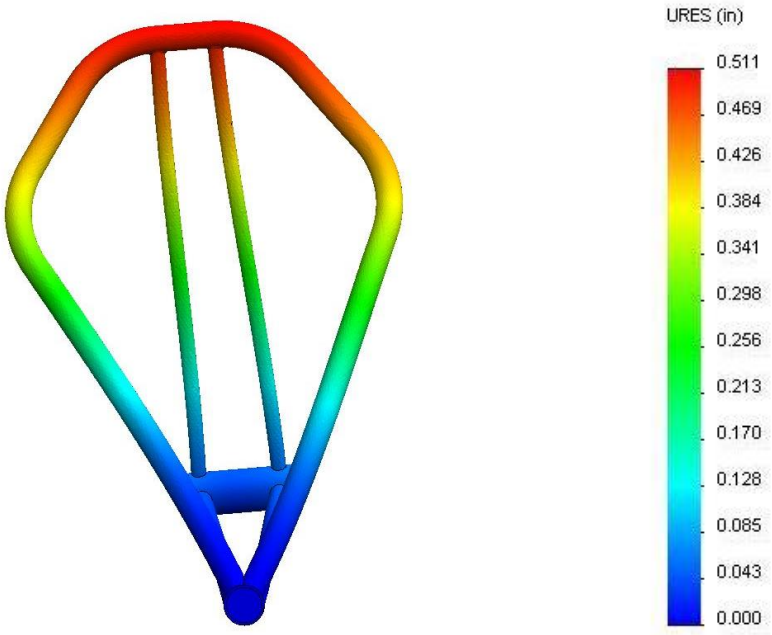

Figure 3.9-Side Load Roll Bar Deflection

A summary of the comparisons between the finite element analysis and the hand calculations is given below in Table 3.2. Since several assumptions were made to perform the calculations, and all of these results are close to what was calculated, these results appear to be accurate.

Table 3.2-FEA vs. Calculated Results

Configuration	**1.5x1.5X0.125AL**	**1.75ODx0.125AL**
Calculated Deflection [in]	0.159	0.165
FEA Deflection [in]	0.159	0.139
Calculated Nominal Stress [psi]	14593	17551
Calculated Max Stress [psi]	22473	25448
FEA Stress [psi]	16309	21897

Based on the above results the team will be selecting the square, 1.5”x1.5”x0.125” aluminum configuration. The square configuration provides better resistances to deflections than the baseline 1.5” diameter steel circular tube, and it has less stress on the outriggers than the circular outrigger. The square shape also simplifies the manufacturing and seat integration considerably. The square configuration center tube will also be lighter than the circular configuration. The selected configuration for the frame can be seen in the figure below:

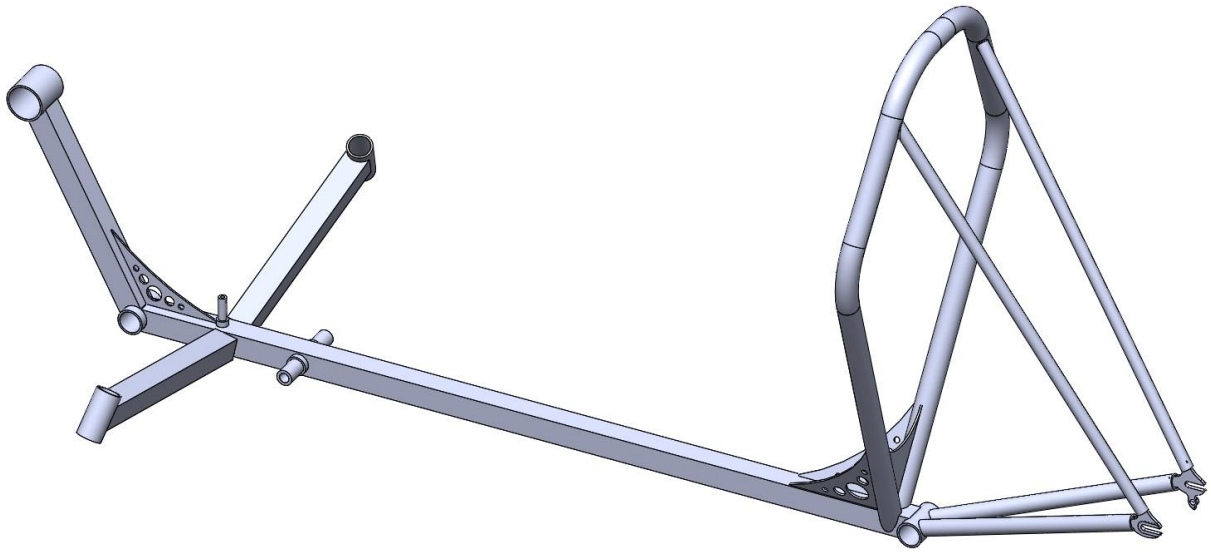

Figure 3.10-Frame Final Configuration

3.2 STEERING

There are several key steering geometries for a two front-wheeled Trike. These include: a caster, camber, kingpin and axle offset. For this system a custom knuckle will be made, which will pivot in a tube and be connected to the frame using a standard 1-1/8 in headset. This is the part on a typical bicycle that attaches the fork to the frame and allows it to pivot using a pair of bearings. The knuckle and position can be seen in Figure 3.11 and 3.12 and, combined with the frame, incorporates all of the steering geometries.

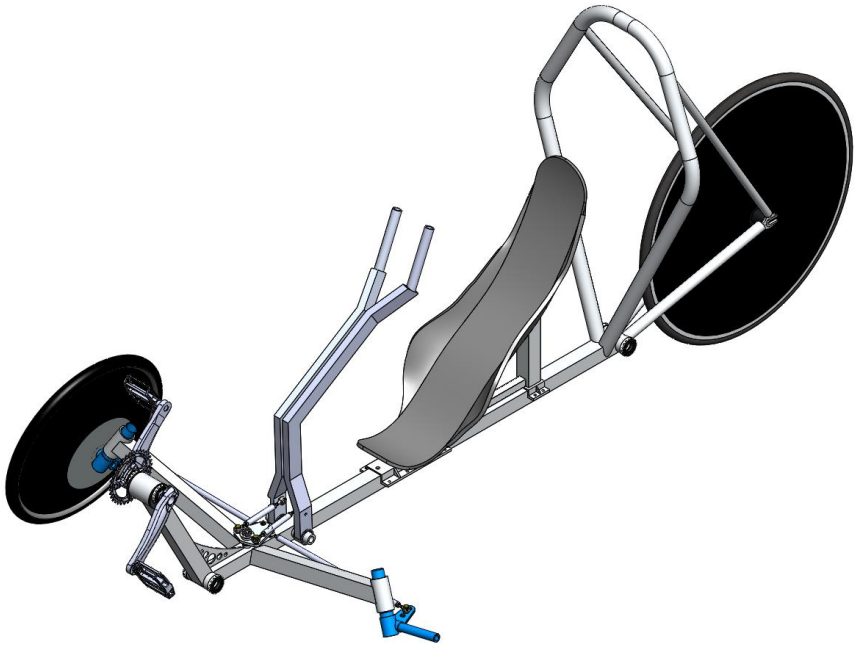

Figure 3.11-Knuckle Position

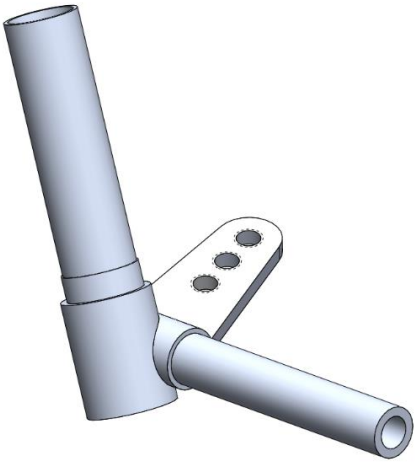

Figure 3.12-Steering Knuckle

The first steering geometry is the caster angle. Caster is the degree of the pivot angle tilted forward, as shown in Figure 3.13 below. The caster angle is critical because it causes the wheels to automatically return to a straight position after turning. This geometry is not exclusive to human powered vehicles, and is used in almost all vehicles with two front steering wheels. Most automobiles use a 4-5 degree caster angle while go carts and racing vehicles generally use a much more aggressive angle [9]. The team selected to use, roughly, a 13 degree caster angle due to research and past experience. Horwitz used a 12 degree angle and an old NAU HPVC bike used a 12.5 degree angle and handled extremely well [9].

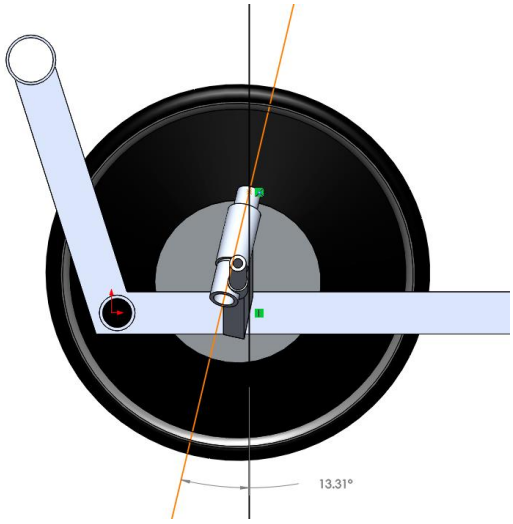

Figure 3.13-Caster Angle

The next important steering angle is the camber. This is the angle from the wheels to vertical, which can be seen in Figure 3.14. If the tops of the wheels are closer than the bottoms, the vehicle is said to have negative camber. If the bottoms of the wheels are closer, then the vehicle has a positive camber. Most vehicles have a negative or neutral camber [9]. The team decided to go with a 12 degree negative camber for several reasons. These reasons include improved stability and loading on the wheels. Bicycle wheels are designed to be loaded vertically because the loading stays vertical in relation to the wheel, while a typical bicycle leans into a turn. This application, however, will have very high side loading on the wheels. Therefore, having a drastic negative camber helps keep more of the force in the vertical axis of the wheel. Another reason is past experience with similar caster angle.

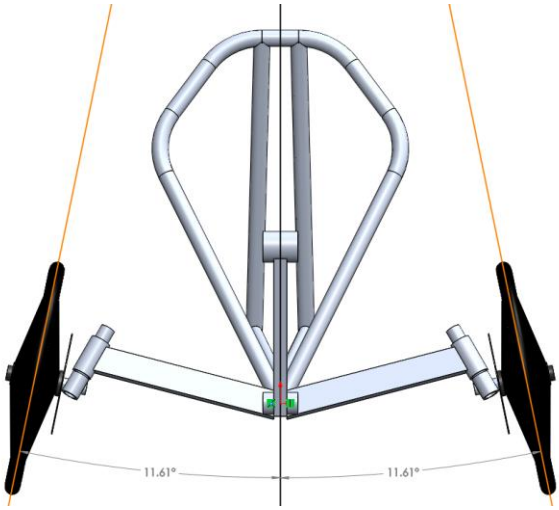

Figure 3.14-Camber Angle

The next geometry is the kingpin angle. This is the angle of the pivot axis from vertical viewing from the front as can be seen in Figure 3.15 below. Some vehicles implement center point steering, in which the tire pivots about the tire patch, where the tire contacts the ground. Center point steering is desirable because it allows for more precise and efficient steering [9]. The efficiency comes from helping eliminate tire scrubbing, which is unnecessary friction when the tires turn. With the geometry given, the kingpin angle becomes 30 degrees to achieve center point turning.

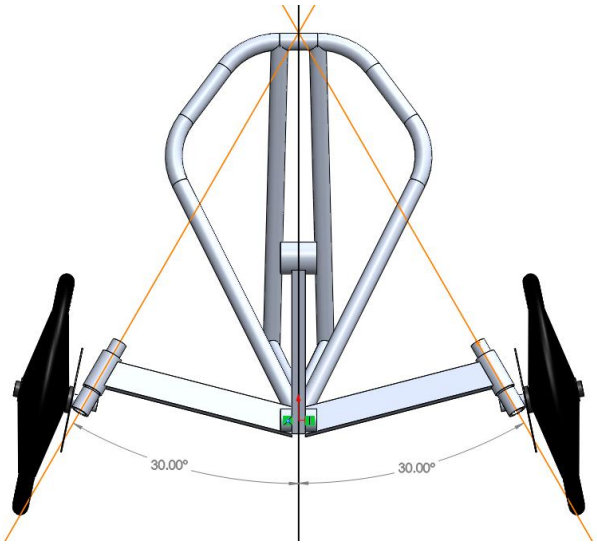

Figure 3.15-Kingpin Angle

The final critical geometry is the axle offset. This offset helps drastically with steering stability. If the axle of the wheel is in front of or in line with the pivot axis, the caster angle is negated. This can also cause undesirable steering motions. The most stable position is for the axle to be

behind the pivot axis [9]. The team has chosen to put the axle 0.5 inches behind the pivot axis because of research and past experience with old NAU HPVC vehicles.

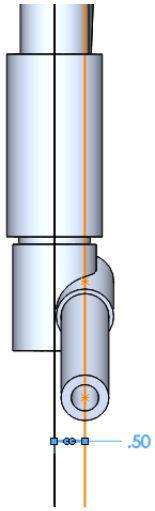

Figure 3.16-Axle Offset

After determining all of the geometries for steering, the final outside dimensions of the steering knuckle were finalized. Weight is a large factor for this vehicle and the knuckles are an easy part to optimize to try and reduce weight. The knuckles used in past NAU HPVC vehicles have both been steel and aluminum. Analysis was done using different configurations of aluminum and steel. The FEA testing analysis was set up with two fixture points, one at the top and one at the bottom, to simulate the two bearings in the headset to apply the force correctly. A distributed force was then applied to the axle using the kingpin and caster angles to simulate the force that would be on the axle with the wheel; this can be seen in Figure 3.17 below. This force was determined using accelerometer data, as shown in Appendix C. The force was then multiplied by a factor to account for issues with the test as well as accelerometer location.

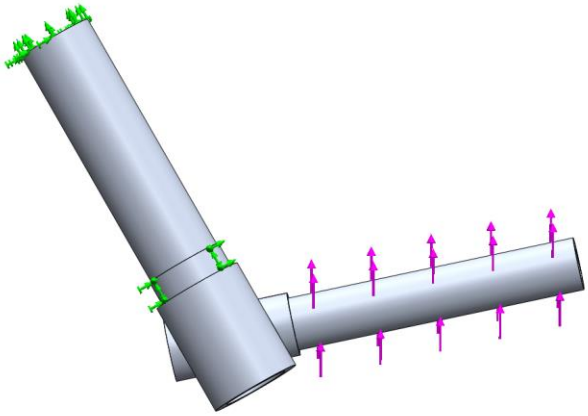

Figure 3.17-FEA Setup

The first configuration tested was 6061 T6 heat treated aluminum, seen in Figure 3.18. Both the steer tube and axle are hollow and are somewhat thin-walled. The force applied was 353 lbf. The yield strength of the aluminum is 40,000 psi and a max stress of 20,000 psi resulted in a factor of safety of 2 before yield. The weight of this configuration is 0.43 lbs.

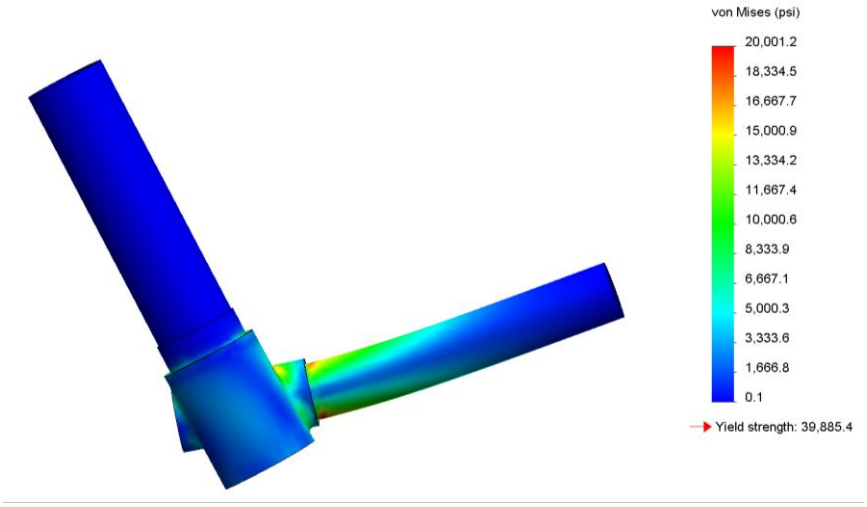

Figure 3.18-Aluminum FEA

The next configuration is 4130 chromoly, seen in Figure 3.19. This configuration was optimized to make the tubes as thin as possible while minimizing stresses. The force and fixtures applied were the same as the previous configuration. The outside dimensions of this setup are also identical to the previous configuration. Only the inside diameters changed to reduce material and weight. The yield strength of the chromoly is 67,000 psi and a max stress calculated was 34,000 psi, leaving the factor of safety at 2 for yielding. The weight of this setup is 0.73 lbs, despite having the same factor of safety as the aluminum.

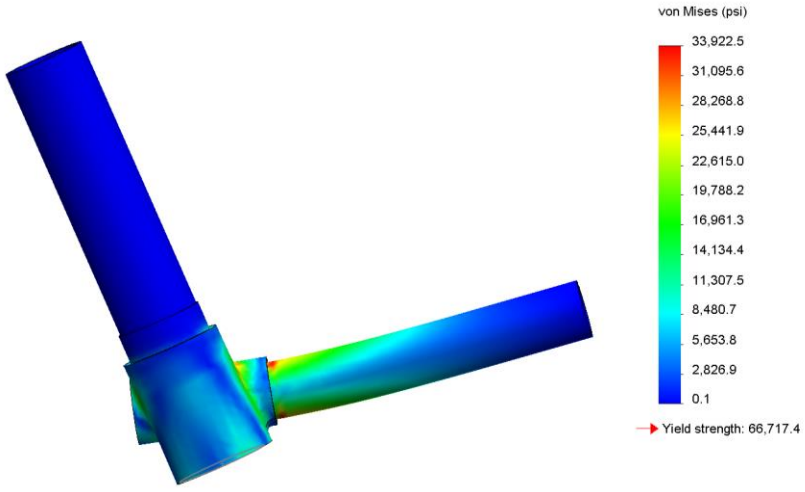

Figure 3.19-Chromoly FEA

3.3 ERGONOMICS

Ergonomics for the human powered vehicle focuses on rider position and comfort. These design aspects are important because they allow the rider to get maximum efficiency with the vehicle while maintaining comfort. In order to determine the position of the rider in the vehicle, the team conducted several tests using a stationary recumbent bicycle. The tests were done on a Monday, Wednesday, and Friday of one week and each team member was positioned at a different angle (shown in Figure 3.20) each day. These angles were 115°, 122°, and 130°. Each rider had to complete a ten-minute warm-up, followed by a one-minute sprint and a three-minute endurance test. The tests allowed the team to measure max and average power, max and average cadence, average heart rate, and energy expended. The data collected in these tests can be seen in Appendix C.

Figure 3.20-Rider Position Angle

Figure 3.21 shows the max power of each team member's three tests for the one-minute sprint. The results show that an angle of 130° was the most common for having the highest max power among the team members. Since the riders vary significantly in weight, the power to weight ratio was calculated. The 130° angle had the highest average ratio.

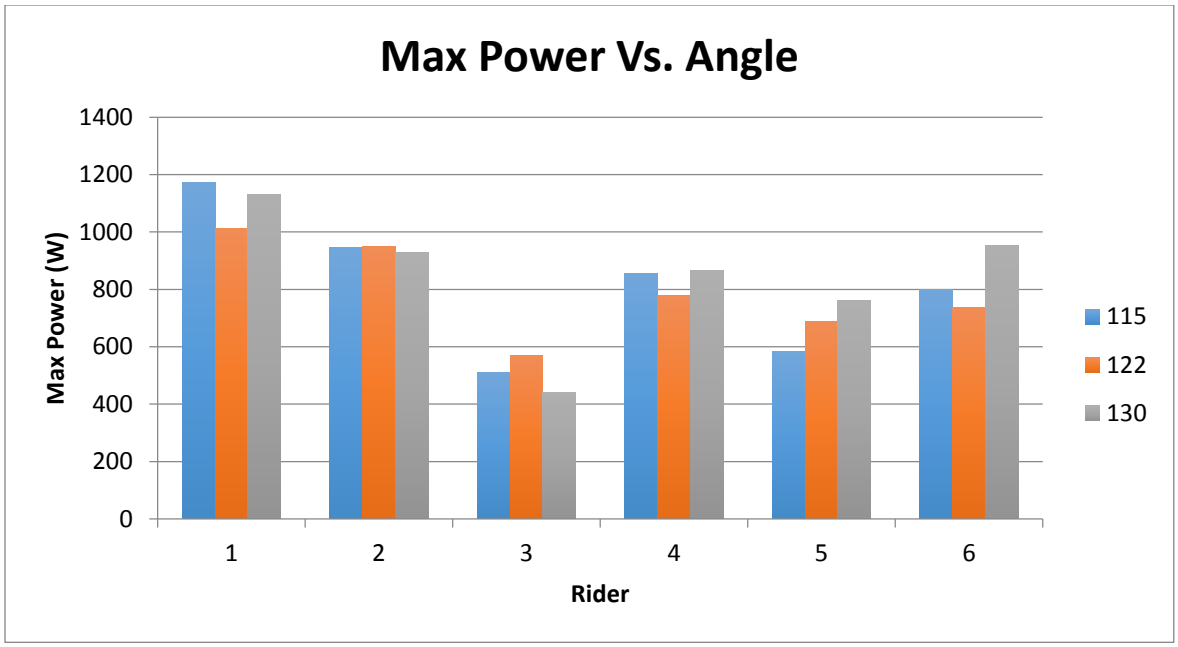

Figure 3.21-Max Power at Various Angles

Figure 3.22 shows the average power of each team member's three tests for the three-minute endurance test. These results show that an angle of 122° was the most common for having the highest average power among the team members. An angle of 122° also had the highest average for the power to weight ratio.

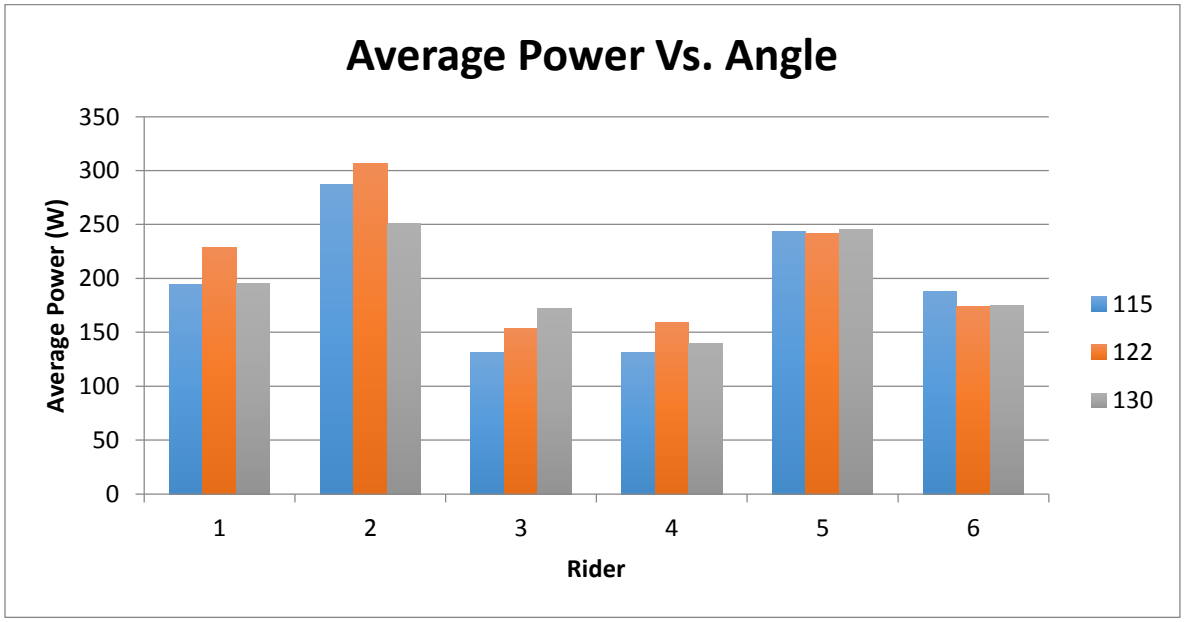

Figure 3.22-Average Power at Various Angles

There are several factors that could have affected the tests, such as the energy level, food and sleep. These could affect the amount of effort the rider strives to put forth during the test. The

team did their best to keep each test as controlled as possible. The team has concluded that many more tests would need to be done to obtain a more accurate result, but these tests give the team a general range of seat positions that can be chosen for optimal power output.

After discussion, the team chose an angle of 122° for the final rider position. It was decided that the endurance test was more important than the sprint test because the vehicle is meant to be used in urban environments, which includes farther distances than a typical sprint. Visibility is also an important factor. By choosing a less steep angle, the rider will be able to see over the pedals and therefore, creates a safer vehicle.

After confirming that the chosen position angle for the rider would be 122°, the final focus for ergonomics was how seat can be adjusted for various riders. The team members vary in height from 5'4" to 6'3" and it is imperative that every member is able to operate the vehicle. With this in mind, the seat design must include a way to adjust the seat quickly to fit the appropriate operator. Through brainstorming, the team concluded that the easiest way to secure the seat in position would be with a quick-release pin. For easy pin access, the hole would be through the bottom bracket and through the top surface of the square center tubing. It will be placed directly in front of the edge of the seat, between the rider's legs. Delrin plastic, known for its low coefficient of friction, will be used inside the bracket and along the center tube so the seat will slide forward and backward easily. The assembly of the pin system, bottom bracket, and back support bracket can be seen in Figure 3.23.

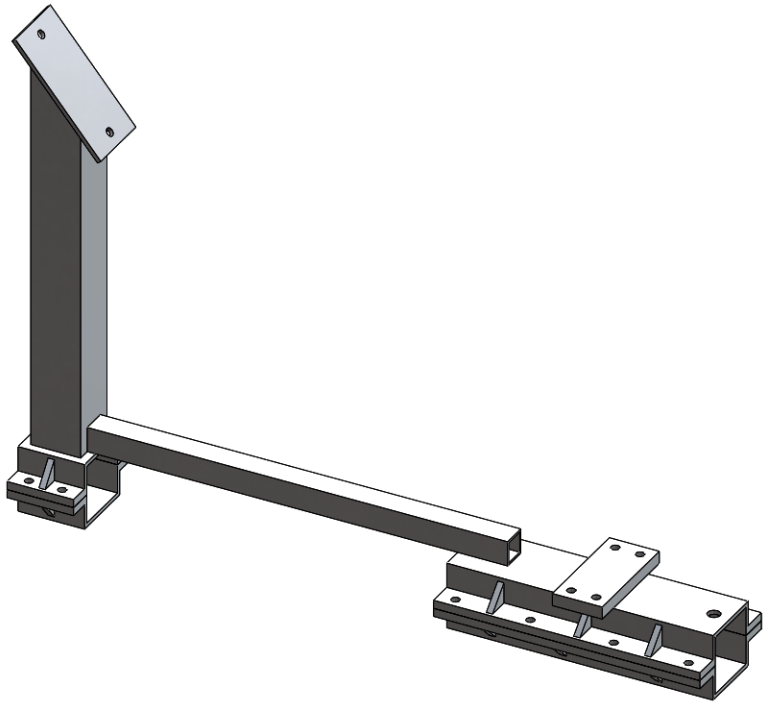

Figure 3.23-Seat Bracket

3.4 DRIVETRAIN

To analyze the drivetrain of the vehicle a MATLAB code was used to select the optimal gear ratios to achieve a maximum velocity with minimal rider effort. These two aspects of the drivetrain were analyzed as the project had a client given requirement of reaching a speed of 40 mph as well as a competition based requirement of navigating a course with sections of high and low speeds.

To begin the analysis an average and maximum rider cadence was found from a rider position study. The results of the rider position study for average power can be seen in Figure 3.22 in the ergonomics analysis section. From this rider position study the instantaneous maximum and average cadences were collected and are displayed in Table 3.3 below.

Table 3.3-Rider Cadence

	Average Cadence (RPM)	**Max Cadence (RPM)**
Rider 1	70	149
Rider 2	101	133
Rider 3	91	149
Rider 4	93	141
Rider 5	91	135
Rider 6	90	143
Average	**89.33**	**141.67**
Rounded Average	**90**	**140**

The results presented in the table allowed the team to select two cadence values to be used in analysis. These included an average cadence of 90 rpm for extended periods of time and a maximum cadence of 110 rpm when a top speed is desired. The value of 110 rpm was selected by viewing the maximum instantaneous cadences displayed in the table, 140 rpm, and selecting a cadence that was 20% lower than the lowest achieved maximum in order to better represent an achievable maximum.

After establishing the two rider cadences to be analyzed, the team used a MATLAB code to calculate the gear ratios and respective speeds for the vehicle. In order to achieve the client requirement of reaching 40 mph the team chose to select a gear ratio that provided a max speed 5% over the requirement, a maximum speed of 42.25 mph. The vehicle needed to reach this speed while attaining the lowest gear ratio on the easiest gears. Table 3.4 below displays the gear ratio and speed at each of the positions on the rear cassette.

Table 3.4-Gear Ratios and Speeds

Gear Ratio	Speed at 90 RPM (MPH)	Speed at 110 RPM (MPH)
1.50	10.56	12.91
1.69	11.88	14.52
1.93	13.58	16.60
2.25	15.84	19.36
2.57	18.11	22.13
3.00	21.13	25.82
3.38	23.77	29.05
3.86	27.16	33.20
4.50	31.69	38.73
4.91	34.57	**42.25**

As seen in the table, the vehicle has a gear ratio of reaching 42.25 mph while having a gear ratio of 1.5 in the lowest possible gear. By selecting a configuration with a low gear ratio the vehicle will be capable of the start and stop motion on the course as well as reaching a max speed.

3.5 FAIRING

To ensure that the team will have a fast vehicle, the fairing must move the air around it in such a way that the minimum amount of force is applied to the vehicle. The possibilities are endless towards designing a fairing, but the team has decided to look at The Axe's fairing from last year, and create a design stemmed from that. The length, width, and height are all important in designing a fairing and those variables will be changed to see the relationships between them. While the fairing model has other components in the design, like the airfoil 2415 seen below, they will be kept constant [11]. For the length of the vehicle, a starting length of 96 inches was chosen from the dimensions of the test rig used in the rider position study. From there, the size was increased from 96 inches to 108 inches with six inch increments. The minimum width was based on the largest shoulder width of a team mate. The smallest width started at 18 inches, increasing to 24 inches, with increments of two inches. Finally, the height was based on the angles mentioned previously in the ergonomics section with the tallest team member's geometry. The angles were converted to the different heights of 33, 37, and 39 inches. The variables were applied and created thirty six different fairing designs to be analyzed.

$$y_t = \frac{tC}{0.2}\left[.2969\left(\sqrt{\frac{x}{C}}\right) - .1260\left(\frac{x}{C}\right) - .3516\left(\frac{x}{C}\right)^2 + .2843\left(\frac{x}{C}\right)^3 - .1015\left(\frac{x}{C}\right)^4\right] \qquad (3.8)$$

Where:

y_t = Y coordinate of air foil [in]
t = thickness coefficient
x = X coordinate of airfoil [in]
C = airfoil length [in]

When setting up the computational fluid dynamics, CDF, in SolidWorks, assumptions had to be made to retrieve results. To begin, the fluid was air at a temperature of 68° Fahrenheit and was assumed to have laminar flow. The velocity was equal to 704 inches per second, which equates to forty miles per hour, same as the team's goal. The body had a roughness of .012 microns, which is equivalent to the surface of aluminum. This can be assumed because the epoxy matrix in the carbon fiber composite takes on the surface characteristics of its mold. Lastly, the boundaries for the fluid analysis were 300 inches in length, 68 inches in width, and 96 inches in height.

Prior to completing the analysis the team had hypothesized that a fairing with the smallest width, height, and length would produce the lowest coefficient of drag, C_d. In the equation seen below, it does seem intuitive for the C_d to be low if the area is low.

$$C_d = \frac{2F_d}{\rho A V^2} \tag{3.9}$$

Analysis began with the length being changed at every width and height combination. To change the length of the fairing, the "c" variable as well as the "t" variable in the air foil equation had to be changed. The "t" variable had to be changed because it is a function of "c". Once completed, the results favored a fairing with a length of 102 inches with 50% of the data points having the lowest C_d, in each category. A length of 108 inches came in second with 42%, while the length of 96 inches had only 8% with the lowest C_d. From these results it is noted that the general fairing design has a lower C_d at longer lengths. See Appendix C for the data results.

Next, the width was changed at every length and height combination. Like the length, the airfoil equation constant, "t", had to be changed to modify the width along the body of the fairing. From the results of the CFD analysis, the width of 22 inches had 44% of the data points with the lowest C_d in each category. The widths of 20 and 18 inches had the same percent of 22%, while the widest width of 24 inches had 11% of the lowest C_d data points. As mentioned before, the team had hypothesized that the smallest width would produce the smallest C_d. The results from the CFD show that the fairing with one of the largest widths produces the lowest C_d. See Appendix C for the data results.

Lastly, the height was changed at every length and width combination. Unlike the previous two dimensions, the upper and lower splines were changed to modify the height. The height of 33 inches produced the most results with the lowest C_d. It scored better than the heights of 37 and 39 inches ten out of the twelve scenarios. The heights of 37 and 39 inches both had 8% of the data points below the C_d. In conclusion, a shorter fairing results in a lower C_d.

As mentioned above, the angle of the rider was chosen to be 122°, which correlates to the height of 37 inches. Table 3.5, shown below, consists of all of the options relating to the height of 37 inches. The shape with the lowest coefficient of drag is that of the size 108L, 22W, and 37H. The closet option after that would be a fairing of the size 102L, 18W, and 37H.

Table 3.5-Coefficient of Drag Comparison

Length (in)	Width (in)	Height (in)	Speed (in/s)	Force (lbs)	Area (in^2)	Cd
96	18	37	704	0.5995	681.54	0.038
96	20	37	704	0.5132	716.58	0.031
96	22	37	704	0.5417	760.07	0.031
96	24	37	704	0.6170	803.72	0.033
102	18	37	704	0.4110	670.37	0.026
102	20	37	704	0.4957	702.1	0.030
102	22	37	704	0.5659	753.55	0.032
102	24	37	704	0.5126	790.64	0.028
108	18	37	704	0.5400	670.51	0.035
108	20	37	704	0.4895	701.49	0.030
108	22	37	704	0.4376	740.06	0.025
108	24	37	704	0.5767	788.48	0.032

In conclusion, the team's hypothesis was incorrect. Although having the smallest height proved to be true, the smallest length and width didn't result in the smallest C_d. From this point forward the sizes of 108L, 22W, and 37H will be used to create a fairing that will be modified in multiple aspects, thus leading to a printed model for physical testing.

With the results from the generic testing completed and the final model of the assembly nearly complete, the next step was to create a fairing that would fit the frame and the rider. To complete this task, multiple dimensions had to be found. For example the cylindrical volume that the feet encompass, the linear movement of the steering arms, the derailleur linear route, and other component's linear or radial paths. Once these constraints were determined, imitation drawings were placed into the model to see the constraints for the fairing design.

To create the fairing, the NACA equation shown in Figure 3.24 was used as a side profile guide curve. This curve designated the fairings length and one of the widest points. In the figure it shows the NACA profile with respect to a person looking from the top of the vehicle towards the ground.

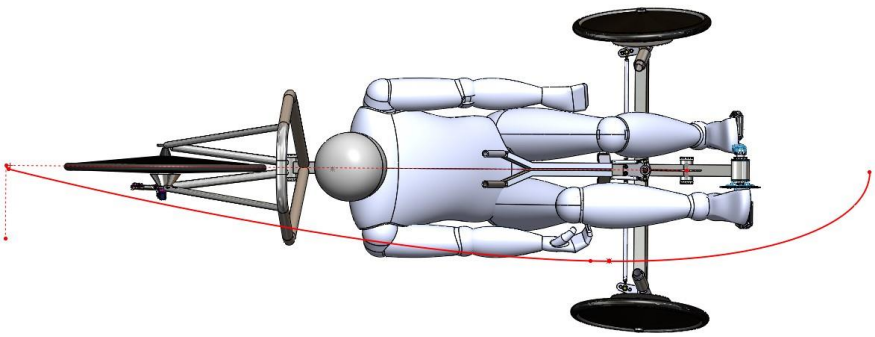

Figure 3.24-Top Profile of NACA Airfoil

From there, a bottom and top profile were created with the constraints of the cylindrical volume that the riders feet would encompass while pedaling. In Figure 3.25 the top profile and bottom profile can be viewed.

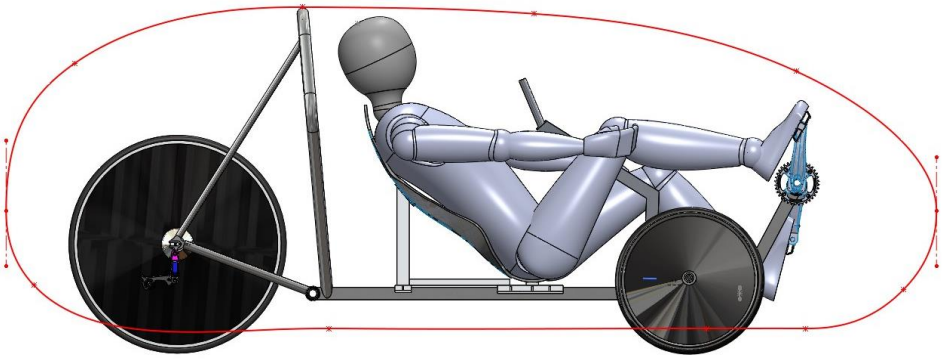

Figure 3.25-Top and Bottom Profile

Lastly, multiple side profiles were created to ensure that the faring would not interfere with the cylindrical volume that the rider's feet would encompass, the roll bar, the steering arms, and the riders head. Figure 3.26 shows the side profile that follows the roll bar.

Figure 3.26-Front Roll Bar Profile

Upon analyzing over fifteen different fairing designs which ranged in profile edits, length changes, and bottom and top profile changes, a final design was created that resulted in a drag force of 2.09 lbs. When placed into the coefficient of drag equation, Equation 3.9, the coefficient of drag for the vehicle was .09. Figure 3.27 shows the simulated model under SolidWorks flow simulation. The stream line's discoloration shows the velocity change along the body as air flows around it. As seen, the velocity of the air behind the wheels is causing the most intrusion to the boundary layer on the surface of the fairing, thus resulting in a higher force then what was shown in the generic testing data.

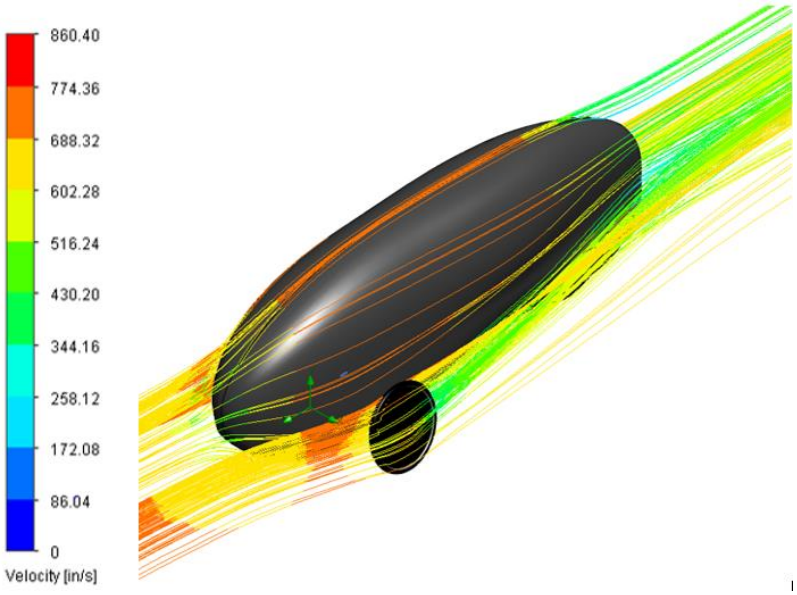

Figure 3.27-SolidWorks CFD Simulation

One of the team's goals, as stated earlier, was to have a lower coefficient of drag times area then that of a cyclist. In the *Bicycling Science* [6] text, the coefficient of drag for a racing bike with a rider in tight clothing in the crouched position is 0.88. The frontal area for said cyclist is 558 in^2 [6]. Those number equate to a C_dA equal to 491 in^2. With the completion of CFD analysis and fairing design, the fairings total frontal area was equal to 977 in^2. When the values of 977 in^2 and 0.09 are multiplied together, a C_dA of 90.2in^2 is achieved. Comparing the C_dA of the fairing covered vehicle to that of the cyclist, the fairing has one-fifth the C_dA than that of a cyclist. With this information it is shown that the fairing covered vehicle has a more efficient design that will help utilize the rider energy to reach high speeds.

Although a low drag force was found to be applied to the vehicle at the 40 miles per hour, the equation shown below uses the drag force, the velocity, and other factors to calculate what wattage the rider would have to expend to achieve said speed.

$$W = \frac{V\left[\frac{F_d}{V^2}(V + V_w) + mg(s + C_R)\right]}{\eta} \tag{3.10}$$

Where:

W= Power [watts]
V= Velocity [m/s]
V_w= Wind Velocity [m/s]
m = Mass [kg]
g = Acceleration due to Gravity [m/s^2]
s = Slope of a hill [º]
C_R = Coefficient of Rolling Resistance
η = Drive Train Efficiency

With the assumptions of no slope, C_r equals 0.0045, V_w equals zero, mass equals 127 kg, η is equal to 0.8, gravity equals 9.81 meters per second squared, velocity equals 17.9 meters per second, and drag force equals 9.3 Newtons. With these numbers, the rider would need to output 333.5 watts to reach a speed of 17.9 meters per second or 40 miles per hour. This wattage was easily achieved by all of our riders at some point during the sprint tests detailed in the ergonomics section.

The final design of the fairing can be seen in Figure 3.28. It produces a low coefficient of drag of 0.09 with a force of 2.09 pounds at 40 miles per hour. With these low numbers and the team's ability to produce the wattage needed to reach 40mph, the team's goal of achieving high speeds will be met.

Figure 3.28-Final Fairing Design

3.6 INNOVATION

The team intends to design a vehicle that is operable in a range of climate conditions. Of upmost concern was comfort of the rider in warm conditions. Even mildly warm ambient air temperatures can make the interior vehicle a harsh environment for physical activity. With this in mind, the team is designing a method for circulating ambient air through the shell during operation in typical weather. This system will be passive, lightweight, and removable to condition the incoming air in more adverse environments.

The first design placed a cold, finned block in line with incoming circulation air, with the intention that it would remove energy, thus cooling the air before it flows over the operator. The block itself would be machined out of aluminum, with a sealed hollow cavity filled with water. An ice core would allow the block to remain cold for longer periods of time. As the ice undergoes phase transition to water, the fin base temperature will remain semi constant. The large amount of energy required to force the phase transition, as represented by the Heat of Fusion, will allow for more energy absorption. A vehicle owner would place the finned block in their freezer for an adequate amount of time prior to driving the vehicle, at which time, the block would be mounted in its location inside the vehicle shell. As warm air passes over the fins, its energy is transferred to the aluminum fins and ice core, eventually melting the internal ice and raising it to ambient temperature. A concept model of this system can be seen in Figure 3.29, with the blue mass representing the cold block.

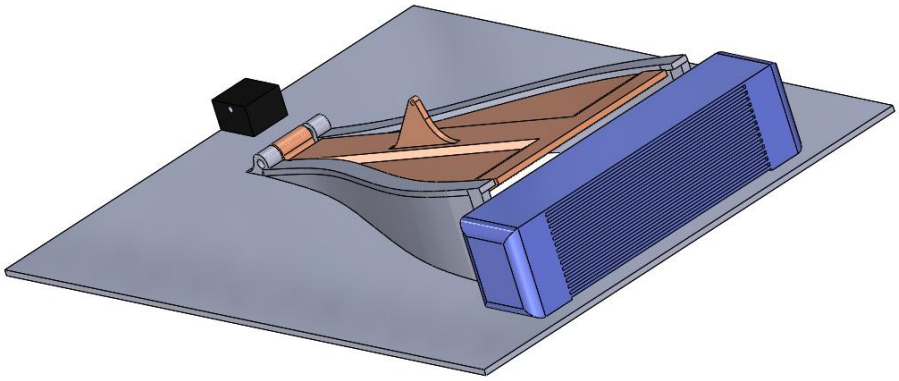

Figure 3.29-Vent Design

With internal vehicle dimensions unavailable, a generous model was developed to represent a plausible outcome for finned surface area with favorable material properties. An assumption of 6 fins with .1m by .05 m dimensions was made, with their thickness small enough to be negligible. The thermal resistance of the aluminum block shell was also assumed negligible, effectively modeling the fins and base as made from ice itself. A convection coefficient, h, was calculated using from Equation 10 for mixed boundary layer conditions.

$$\bar{h}_l = \frac{\overline{Nu}_l k}{l} \tag{3.11}$$

$$\overline{Nu}_l = \left(.037 Re_l^{\frac{4}{5}} - A \right) Pr^{\frac{1}{3}} \tag{3.12}$$

$$A = .037 Re_{l,c}^{4/5} - .664 Re_{l,c}^{1/2} \tag{3.13}$$

Where:

$\bar{h}_l$= Average convection coefficient
$\overline{Nu}_l$= Average Nusselt Number
Re_l = Reynolds Number at the end of a flat plate
$Re_{l,c}$= Critical Reynolds number for boundary layer transition
Pr = Pradtl Number [Ns/m^2]

Equations 3.11, 3.12, and 3.13 result in a convection coefficient of 31 $\frac{w}{m^2 \cdot K}$ at a velocity off 9 m/s (20 mph). Assuming an ambient air temperature, a surface area, and a flow rate of 26°C, .0625

m^2, and 9 m/s respectively, the ice will remain within 12° of its initial temperature for roughly 46 minutes. 46 minutes is a sufficient period of time for a cooling system to operate, however this design is limited by quality of performance rather than longevity of performance. The system is limited by its small size and weight constraints which simply do not allow for amount of surface area required to produce the desired cooling of incoming air. With the current assumptions, only a 1°C temperature drop is achieved.

The team also considered the viability of a small scale passive evaporative cooling system that would utilized air flowing though the duct to evaporate water from a wet fabric, thus causing a temperature drop to the incoming air. However, 2014 HPVC events are held in San Jose, California and Orlando, Florida, both of which have average April relative humidity's in the range of 65 to 75% [12]. Meanwhile, their average daily temperatures are roughly 63°F and 75°F respectively. Wet bulb temperatures for these climates indicate that the achievable temperature drop from an ideal evaporative cooling system will be roughly 8°F. Upon considering inevitable inefficiencies of a passive system, Team 9 decided further pursuit of a passive cooling system was not an effective use of time. However, the vehicle will incorporate the remotely operated vent system to aid in air ventilation.

The air for the system will enter the vehicle interior through a servo operated, closable duct embedded into the composite fairing. This duct is operated by the vehicle rider through the use of a button in the cockpit. The ability to close the duct serves two purposes. First, as daytime high temperatures drop, the rider may find that they wish for a warmer environment to travel in. Closing the duct will reduce air circulation and begin to increase the interior temperature as the rider's body puts out heat. Secondly, these ducts will introduce a measureable amount of aerodynamic drag on the vehicle; the ability to seal off this port will give the rider the option to temporarily sacrifice internal temperature for a higher vehicle velocity.

As previously stated, this duct will be actuated by a servo with a 90° operating range. The linkage that transfers rotation from the servo to the duct flap is designed so that lockout occurs at the closed extreme of the flap position, requiring a minimal amount of battery power to hold the flap shut. This is achieved with the usage of a 4:1 lever arm ratio. This part will be fabricated using a fused deposition modeling additive manufacturing process. A detailed view of the vent electromechanical system can be seen in Figure 3.30. This system will be imbedded into the fairing during its manufacturing process.

Figure 3.30-Servo Driven Vent Assembly

Lighting systems are the competition standard for roadway communication. Brake lights, tail lights, headlights, and turn signals are required for maximum competition ranking. However, the quality and visibility of such lights is not regulated.

After evaluating the visibility of lights of automobiles the team found it necessary for any light on a vehicle to be visible from a minimum of 180° horizontally. This requirement is flexible in that it allows either the hardware of the light itself to be visible or a clear, unquestionable view of the light emitted by the hardware.

It was also determined that successful turn signals must be visible from behind, to the side, and in front of the vehicle. Rather than placing two turn signal light sets on the human powered vehicle like those of an automobile, the team will include a continuous LED strip around the circumference of the front wheel fairings. The arrangement of the light safety and communication systems and their ranges of visibility can be seen in Figure 3.31.

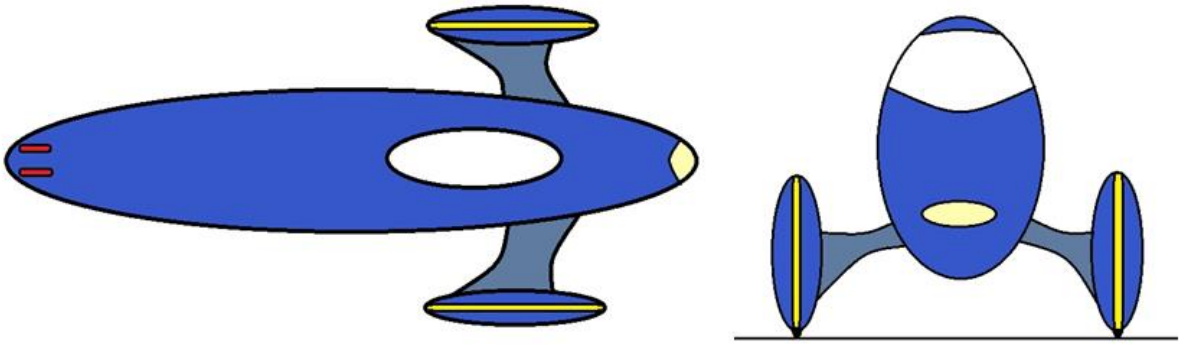

Figure 3.31-Vehicle Lighting Arrangement

The team wanted to ensure that the vehicle would resist roll over during aggressive driving. To accomplish this, the width of the vehicle was designed so that the tires would lose traction before the vehicle initiated a tip.

Analysis was performed to determine the minimum front wheel width that would avoid tipping conditions. First a total vehicle and rider weight of 240lbs was assumed to be distributed evenly over all three wheels during static scenarios. However, for tipping conditions to occur, all the system's mass would be carried by the rear and one front wheel. This creates a new distribution of 80lbs per tire in contact with the ground. The static friction coefficient, μ_s, of rubber on asphalt was assumed to be 0.8. The total system center of gravity was assumed at the mid plane of the vehicle, 50% of the way between the front and back wheels, and 14in above the ground.

For tipping to occur during an aggressive turn, the lateral inertial force, F, acting at the center of gravity must be so great that the moment it creates about the tire contact patches must be greater than the moment created by the vehicle weight W about the same contact patch. However, the lateral inertial force F must also be lower in magnitude than the maximum frictional force, f, before movement begins, where:

$$f = \mu_s N \tag{3.14}$$

Or in this case

$$f = 0.8 * 120 = 96\ lbs \tag{3.15}$$

Where:

f= Force due to friction [lbs]
μ_s= Coefficient of static friction
N= Normal force [lbs]

Finally, slipping at both wheels in contact with the ground is not required to avoid a tip. One wheel breaking loose will cause a shift in the vehicle's direction of travel and weight distribution to adequately avoid a tip.

If slipping is to occur before tipping, the lateral inertial force F required to overcome the weight of the vehicle must be significantly greater than the maximum frictional force f at either of the two tires carrying the load of the vehicle. See Figure 3.32 for a diagram of the force relationship.

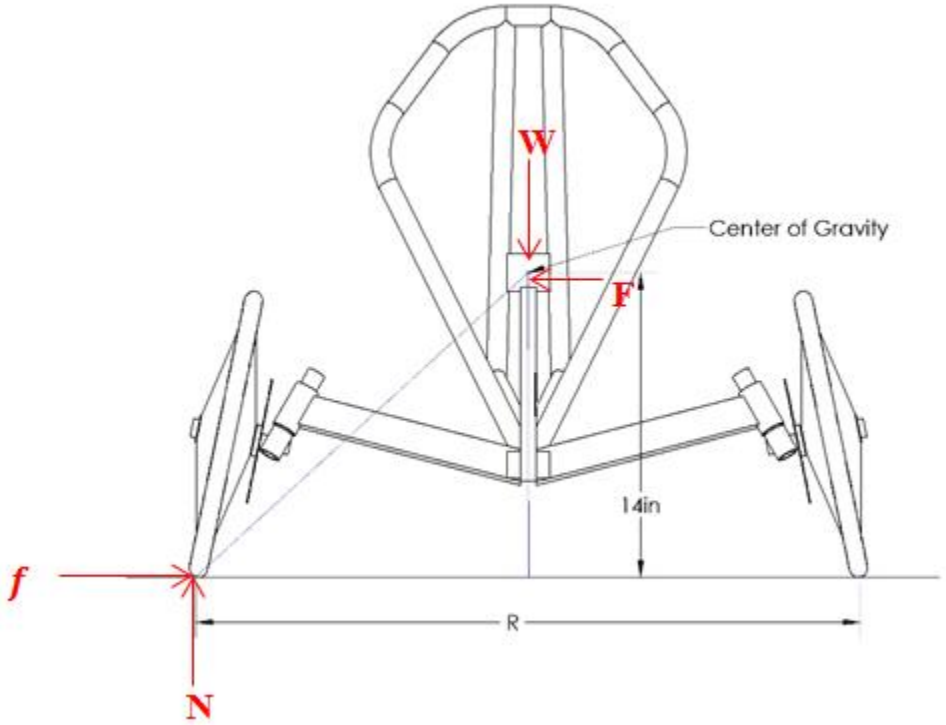

Figure 3.32-Tipping Analysis FBD

For a three wheeled vehicle, lateral tipping occurs about an axis drawn from the contact patch of either of the two front wheels to the contact patch of the rear wheel, also shown in Figure 24. Because of this, the distance A from the center of gravity to the tipping axis is not simply half the vehicle width. Instead, the distance to the tipping axis can be defined by the geometry in Figure 3.33**.**

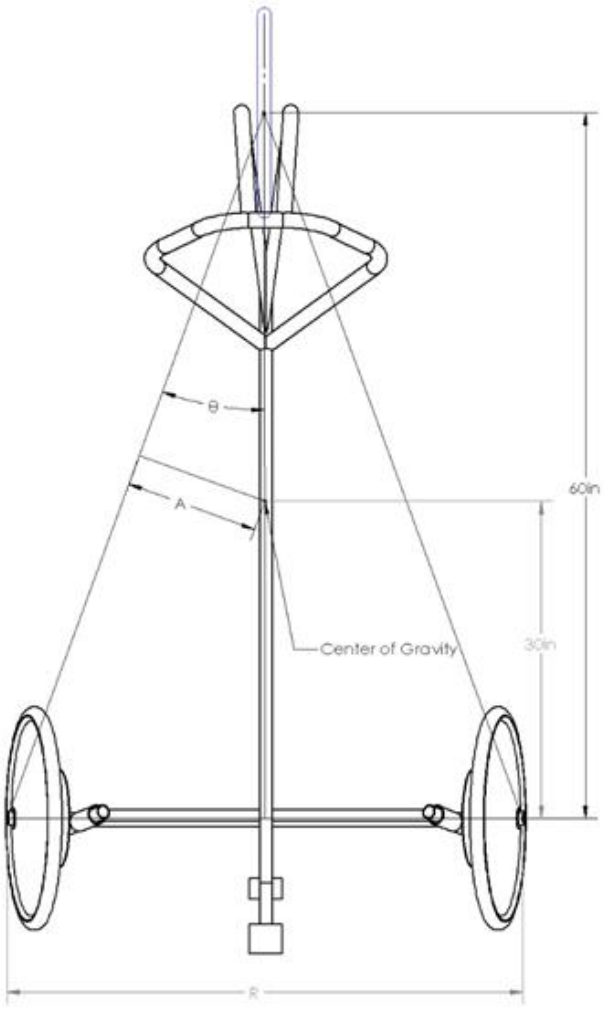

Figure 3.33-Tipping Axis Location

Solving for the minimum required distance A to avoid tipping requires setting $F \Rightarrow f$ and can be seen below:

$$W * A = F * 14\ in \tag{3.16}$$

Substituting in the assumptions and solving for A gives

$$A \geq\ 5.6\ in \tag{3.17}$$

Back solving for the minimum front wheel width R gives

$$\theta = \sin^{-1}\frac{5.6}{30} = 10.76° \tag{3.18}$$

$$R = 2L\tan\theta = 23\ in \tag{3.19}$$

Where:

W= Weight of the vehicle acting at center of gravity [lbs]
A= length from CG to tipping axis [in]
F= Inertial force causing tipping [lbs]
θ= angle from tipping axis to vehicle centerline [^{o}]

The minimum critical width was determined to be 23 in to avoid tipping during aggressive turning. However, bicycle lanes are usually a minimum of 48 inches in width. Subsequently, the width of the vehicle front wheels was chosen to be 42 in, which will allow for a stable vehicle on all types of terrain, yet still capable of traveling within bicycle specific lanes with space on either side.

ASME continually pushes entrants to be innovative in the design and manufacturing of their vehicles. Human powered vehicles are often one-off mobiles fabricated from exotic, costly materials, especially when their main purpose is to be used as a competition entry. It was felt that an effective way to offset these costs yet still have a vehicle that performs competitively was to seek out alternative, recycled materials. More specifically, we will attempt to recycle scrap materials from our own manufacturing of the vehicle. Tables 3.6 and 3.7 show a list of waste materials traditionally produced during the fabrication of a human powered vehicle.

Table 3.6-Possible Recyclable Reinforcement Materials

Reinforcement Materials	**Source**
Aluminum chips as collected or powered	Machining of components
Wood Fibers	Fixtures and shipping
Powdered previously laid up carbon fiber	Last year's vehicle, research projects
Cardboard	Shipping supplies
Scrap carbon fiber and fiberglass clippings	Local composite product manufactures

Table 3.7-Possible Recyclable Matrix Materials

Matrix Materials	**Source**
Epoxy Resin	Left over from previous and current builds
High density polyethylene	Discarded water bottles and shipping materials
Nylon	Dupont material samples
Delrin	Dupont material samples
ABS	Contaminated FDM materials

Combinations of these materials will be attempted, with the desire of creating a composite material with properties that can be utilized on the vehicle. Currently the team is continuing to collect these materials. However, a few material combinations have already been tested. In Figure 3.34, an array of successful recycled materials can be seen. All materials will have their properties and machinability evaluated.

Figure 3.34-left to right: Recycled High Density Polyethylene (HDPE), (HDPE), Recycled Carbon Fiber and Epoxy resin composite, Lathe turnings and epoxy resin composite

4.0 COST ANALYSIS

For a cost analysis of the vehicle, the team analyzed the costs associated with the prototype vehicle to be built this spring as well as a production run of the vehicle. This relates to the design objective of creating a design ready for production run manufacturability. For the competition, the team must show the costs related to a production run of ten vehicles a month for three years. To best accomplish this analysis, the team created a detailed bill of materials and calculated the capital costs, overhead costs, and labor costs associated with a production run.

4.1 BILL OF MATERIALS

To provide an accurate representation of the components and materials needed for vehicle construction the team created a bill of materials (BOM) for each subsection of the design. Each of these includes the application on the vehicle, the specific part, its manufacturer's suggested retail price (MSRP), the cost to the team, and the source of purchase.

Table 4.1-Frame BOM

Application	Product	Qty	MSRP	Actual Cost	Projected Total	Source
Center Tube	1.5"x1.5"x0.125" 6061-T6 Tube	6'	$22.91	$22.91	$22.91	Online Metals
Outriggers	1.5"x1.5"x0.125" 6061-T6 Tube	4'	$16.52	$16.52	$16.52	Online Metals
Roll bar	1.375"ODx0.125" 6061-T6 Tube	16'	$145.00	$145.00	$145.00	Online Metals
Roll bar	1"ODx0.125" 6061-T6 Tube	4'	$24.80	$24.80	$24.80	Online Metals
Roll bar	0.75"ODx0.125" 6061-T6 Tube	7'	$40.55	$40.55	$40.55	Online Metals
Gusset	0.25" Thick 6061-T6 Plate	2'	$28.54	$28.54	$28.54	Online Metals
Dropouts	Rear dropout with hanger	1	$55.89	$55.89	$55.89	Paragon Machine Works
Head Tubes	Front wheel head tubes	2	$15.00	$15.00	$30.00	Absolute Bikes
Bottom Bracket	Drivetrain bottom brackets	3	$20.00	$20.00	$60.00	Absolute Bikes
Overall	T6 Heat Treatment	1	$1,000.00	$0.00	$0.00	Phoenix Heat Treating
Roll bar	Computer bending	2	$300.00	$0.00	$0.00	Di-Matrix
	Totals				**$424.21**	

Table 4.2-Steering BOM

Application	Product	Qty	MSRP	Actual Cost	Projected Total	Source
Knuckle Stock	1.5"x 12" round stock 6061	4	$14.05	$14.05	$56.20	McMaster-Carr
Axle/Spindle Stock	7/8" x36" round stock	1	$15.54	$15.54	$15.54	McMaster-Carr
Bell Crank	.25"x12"x12"	1	$30.39	$30.39	$30.39	McMaster-Carr
Hiem Joints	hiem joints 1/4-28	8	$10.62	$10.62	$84.96	McMaster-Carr
Spacer Stock	3/8" x 12" round 4130 stock	1	$3.21	$3.21	$3.21	McMaster-Carr
Threaded inserts	1/4"-28 threaded insert x10	1	$8.75	$8.75	$8.75	McMaster-Carr
1/4" bolts	1/4" 28 1" grade 8 x50	1	$8.35	$8.35	$8.35	McMaster-Carr
Damper	steering damper	1	$24.45	$24.45	$24.45	McMaster-Carr
Bushing Stock	bearing grade bronze 1" x 6.5"	1	$26.29	$26.29	$26.29	McMaster-Carr
Tierod Material	.5" x.065" thick x72"	1	$28.44	$28.44	$28.44	McMaster-Carr
Bushing Bolts	1/2 20 castle nut x10	1	$7.98	$7.98	$7.98	McMaster-Carr
Steering Arms	1 sq yard 3k 2x2	1	$59.95	$59.95	$59.95	fibre glast
Knuckle Pivot	Headsets	2	$30.00	$30.00	$60.00	Absolute Bikes
Brakes	bb7 w/ 160mm rotors set of 2	1	$106.65	$106.65	$106.65	Absolute Bikes
Brake Handle	avid fr-5	1	$11.60	$11.60	$11.60	Absolute Bikes
Brake Splitter	brake splitter br3341	1	$39.60	$39.60	$39.60	Absolute Bikes
Tubes	20 inch tubes	4	$8.00	$5.00	$20.00	Absolute Bikes
Tire	20 inch tire	2	$60.00	$35.00	$70.00	Absolute Bikes
Hub Bearings	Kris King Hub Bearings	2	$45.00	$45.00	$90.00	Absolute Bikes
Assorted tools	Assorted tools	1	$50.00	$50.00	$50.00	
	Totals				**$802.36**	

Table 4.3-Ergonomics BOM

Application	Product	Qty	MSRP	Actual Cost	Projected Total	Source
Seat	Fiberglass recumbent seat	1	$165.00	$145.00	$145.00	Power On Cycling
Seat Cushion	Foam pad	1	$40.00	$30.00	$30.00	Power On Cycling
Back Support Beam	1.5" x 0.125" 6061 TS Square Tube - 1'	1	$5.16	$5.16	$5.16	Online Metals
Connection Beam	0.75" x 0.062" 6061 T6 Square Tube - 2'	1	$2.40	$2.40	$2.40	Online Metals
Bottom Bracket	1" x 4" 6061 Bar - 1'	2	$30.11	$30.11	$60.22	McMaster-Carr
Sliding Material	Black Delrin 0.062" x 12" x 12" Sheet	1	$11.86	$11.86	$11.86	Plastics International
Pin	3/8" dia., 1" Grip Lg., QR Lock Pin	1	$14.09	$14.09	$14.09	Reid Supply Company
Headrest	Stuffing	1	$5.00	$5.00	$5.00	Walmart
Headrest	Fabric	1	$5.00	$5.00	$5.00	Walmart
Seatbelt	Lap Belt (2 Point Seat Belt)	1	$17.95	$17.95	$17.95	SeatBeltsPlus.com
	Totals				**$278.73**	

Table 4.4-Drivetrain BOM

Application	Product	Qty	MSRP	Actual Cost	Projected Total	Source
Crank	SRAM Red 22 53-39	1	$620.00	$307.00	$307.00	Absolute Bikes
Cassette	SRAM xg1099	1	$510.00	$260.00	$260.00	Absolute Bikes
Step up	SRAM x7 26-39	1	$226.00	$113.00	$113.00	Absolute Bikes
Deruiler	SRAM X9 Type 2 Medium Cage	1	$150.00	$73.00	$73.00	Absolute Bikes
Shifter	SRAM X0 10 speed Trigger*	1	$180.00	$89.00	$89.00	Absolute Bikes
Chain	SRAM PC 1051	3	$40.00	$20.00	$60.00	Absolute Bikes
Gear	36 tooth 120 BPD	1	$40.00	$20.00	$20.00	Absolute Bikes
Rear Wheel	Stans ZTR Alpha 340 disk	1	$400.00	$200.00	$200.00	Absolute Bikes
Rear Tire	700c rear tire	2	$70.00	$35.00	$70.00	Absolute Bikes
Rear Tube	700c tube	2	$20.00	$10.00	$20.00	Absolute Bikes
Inner Bearing	Ball Bearing, 1/2" ID 1-1/8" OD	2	$9.51	$9.51	$19.02	McMaster-Carr
Cable Bearing	Ball Bearing, 2mm ID 6mm OD	1	$6.05	$6.05	$6.05	McMaster-Carr
Spring Bearing	Ball Bearing, 5/16" ID 1/2" OD	2	$6.20	$6.20	$12.40	McMaster-Carr
Spring	0.25 OD pack of 12	1	$9.80	$9.80	$9.80	McMaster-Carr
Tube	Aluminum 1.120" ID 1-1/4" OD	1	$10.62	$10.62	$10.62	McMaster-Carr
Spline	1 ft w/cut fee	2	$17.05	$8.53	$17.05	Grob
Spline Sleeve	Matching spline sleeve	2	$8.60	$4.30	$8.60	Grob
Bottom Bracket	External bottom bracket	1	$40.00	$20.00	$20.00	Absolute Bikes
Brake Cable	Shimano brake cable	1	$3.50	$3.50	$3.50	Absolute Bikes
Gear	Rear wheel	1	$40.00	$20.00	$20.00	Absolute Bikes
Idler Gear	Small gears on reverse shaft	2	$10.00	$5.00	$10.00	Absolute Bikes
	Total				**$1,349.04**	

Table 4.5-Fairing BOM

Application	Product	Qty	MSRP	Actual Cost	Projected Total	Source
Male Mold	Foam	19	$50.50	$50.50	$959.50	Homco
Male Mold	Fiberglass per yard 50"	18	$6.60	$6.60	$118.80	Aircraft Spruce
Male Mold	Bondo	2	$17.99	$17.99	$35.98	Homco
Male Mold	Wood 48X96X1/4	4	$17.99	$17.99	$71.96	Homco
Female Mold	Fiberglass per yard 50"	36	$6.60	$6.60	$237.60	Aircraft Spruce
Female Mold	Bleader Cloth	8	$7.95	$7.95	$63.60	Fibre Glast
Female Mold	Peel Ply	8	$8.95	$8.95	$71.60	Fibre Glast
Female Mold	Vaccum Bagging	8	$4.95	$4.95	$39.60	Fibre Glast
Female Mold	Sealant	1	$7.95	$7.95	$7.95	Fibre Glast
Fairing	Carbon Fiber 2x2 twill 50", per yard	18	$20.50	$20.50	$369.00	Soller Composites
Fairing	Bleader Cloth	8	$7.95	$7.95	$63.60	Fibre Glast
Fairing	Peel Ply	8	$8.95	$8.95	$71.60	Fibre Glast
Fairing	Vaccum Bagging	8	$4.95	$4.95	$39.60	Fibre Glast
Fairing	Sealant	1	$7.95	$7.95	$7.95	Fibre Glast
All	Resin 5.25 Gallons	1	$568.00	$568.00	$568.00	Aircraft Spruce
All	General: brushes, gloves, etc	1	$200.00	$200.00	$200.00	
	Totals				**$2,926.34**	

Table 4.6-Innovation BOM

Application	Product	Qty	MSRP	Actual Cost	Projected Total	Source
Closing Ducts	Driving servos	2	$20.00	$20.00	$40.00	servocity.com
Closing Ducts	Carbon composite flap	2	$20.00	$0.00	$0.00	Soller Composites
Closing Ducts	Resin for flaps	2	$5.00	$0.00	$0.00	NAU Machine Shop
Closing Ducts	FDM material	1	$100.00	$0.00	$0.00	Dr. Tester
Anti Fog Duct	FDM material	1	$20.00	$0.00	$0.00	Dr. Tester
Turn Signals	LED Strips	2	$20.00	$0.00	$0.00	sbLED.com (sponsor)
Brake Lights	LED Strips	2	$15.00	$0.00	$0.00	sbLED.com (sponsor)
Interior Light	LED Strip	1	$15.00	$0.00	$0.00	sbLED.com (sponsor)
Turn Signals	Button	2	$4.00	$4.00	$8.00	Radioshack
Brake lights	Switch	1	$1.00	$1.00	$1.00	Radioshack
Interior Light	Button	1	$1.00	$1.00	$1.00	Radioshack
Head Light	Lumia 500 light	1	$110.00	$0.00	$0.00	Niterider (sponsor)
Seat Belt Light	LED	1	$0.10	$0.10	$0.10	Radioshack
Sustainable Manf.	Test molds	1	$50.00	$0.00	$0.00	NAU Machine Shop
Sustainable Manf.	Test mold resins	1	$40.00	$0.00	$0.00	NAU Machine Shop
Onboard Electronics	Control panel	1	$15.00	$0.00	$0.00	Soller Composites
Onboard Electronics	Battery	1	$50.00	$50.00	$50.00	Radioshack
Onboard Electronics	Wiring (50ft)	1	$10.00	$10.00	$10.00	Radioshack
Onboard Electronics	Master control switch	1	$2.00	$2.00	$2.00	Radioshack
Onboard Electronics	Various connectors	1	$30.00	$30.00	$30.00	Radioshack
Onboard Electronics	Wire routing	1	$20.00	$20.00	$20.00	Radioshack
Onboard Electronics	Battery charger	1	$30.00	$30.00	$30.00	Radioshack
Onboard Electronics	Battery box/holder FDM material	1	$50.00	$0.00	$0.00	Dr. Tester
	Totals				**$192.10**	

To calculate the overall cost of the vehicle, the sum of each subsection was calculated and placed into Table 4.7 below.

Table 4.7-Overall Costs

Subsection	**Projected Total**
Frame	$424.21
Fairing	$2,926.34
Steering	$802.36
Drivetrain	$1,349.04
Ergonomics	$278.73
Innovation	$192.10
Vehicle Total	**$5,972.78**

The total cost of the vehicle comes to $5,972.78. This is well below the team's client given constraint of a $6,500 starting budget.

4.2 MANUFACTURING COSTS

To analyze the costs associated with a production run of ten vehicles a month for three years, the team first considered the labor costs required for vehicle construction. The labor costs for the vehicle include the positions of a machinist/welder, composite tech, general labor, and a manager. These labor costs can be seen in Table 4.8 below.

Table 4.8-Labor Costs

Title	**Number of People**	**Cost per person per hr**	**Hours per Vehicle**	**Total Cost per vehicle**	**Total Cost**
Machinist/Welder	3	$16.00	90	$1,440.00	$518,400.00
Composite Tech	2	$14.00	20	$280.00	$100,800.00
General Labor	4	$10.00	20	$200.00	$72,000.00
Manager	1	$20.00	30	$600.00	$216,000.00
Totals	**10**	**$60.00**	**160**	**$2,520.00**	**$907,200.00**

The team then considered the capital costs for machinery and tooling required for vehicle construction. These capital costs cover the initial cost of each piece of machinery needed as well as tooling costs to represent consumables needed for construction. The detailed breakdown of costs can be seen below in Table 4.9.

Table 4.9-Capital Costs

Tools	**Price**	**Quantity**	**Total**
Milling Machine	$9,999.00	2	$19,998.00
Lathe	$6,999.00	2	$13,998.00
CNC 4 Axis Machine	$26,789.99	1	$26,789.99
Sander	$399.99	2	$799.98
Drill Press	$569.99	2	$1,139.98
Grinders	$199.99	4	$799.96
Tig Welder	$7,837.00	2	$15,674.00
Sheet Metal Shear	$2,195.99	1	$2,195.99
Sheet Metal Break	$799.99	1	$799.99
Welding Tanks	$230.00	2	$460.00
Power Notcher	$2,995.99	1	$2,995.99
Powered Pipe Bender	$4,959.00	1	$4,959.00
Hydraulic Press	$399.99	1	$399.99
Horizontal Band Saw	$1,229.90	1	$1,229.90
Vertical Band saw	$1,999.99	1	$1,999.99
Bench	$549.99	4	$2,199.96
Welding Bench	$6,999.99	1	$6,999.99
Vacuum Pump	$1,219.95	2	$2,439.90
Fittings and Hoses	$500.00	1	$500.00
Air Compressor	$1,299.99	1	$1,299.99
3D printer	$57,899.99	1	$57,899.99
Tool Box	$2,103.97	2	$4,207.94
General Tooling	$20,000.00	1	$20,000.00
		Overall Total	**$189,788.53**

4.3 TOTAL COST OF PRODUCTION

Along with the manufacturing costs, the team also calculated the overhead costs needed for the vehicle's production. These included the rental of a building with appropriate capabilities and the utility costs for running the machines. These costs can be seen in Table 4.10 below.

Table 4.10-Overhead Costs

Overhead	**Cost per month**	**Yearly Cost**	**Overall Cost**
Building Rental	$1,000.00	$12,000.00	$36,000.00
Utilities	$500.00	$6,000.00	$18,000.00
Total	**$1,500.00**	**$18,000.00**	**$54,000.00**

Using the bill of materials costs created for this vehicle design, the capital costs of equipment and tooling, as well as labor and overhead costs, the team was able to predict the cost of a production run for the design. The cost to produce ten vehicles a month for three years, 360 vehicles total, was $3,305,566.93. The details can be seen below in Table 4.11.

Table 4.11-Total Costs

Costs	**Total**
Capital	$189,788.53
Labor	$907,200.00
Overhead	$54,000.00
Materials	$2,154,578.40
Total	**$3,305,566.93**

5.0 CONCLUSIONS

Team 9 was tasked with designing a human powered vehicle that can function as an alternative form of transportation that provides the benefits of bicycle commuting while maintaining the practicality of an automobile. This project was commissioned by the faculty advisor of NAU's ASME student chapter, Perry Wood, who has been involved in numerous human powered vehicle projects throughout his time as an engineer.

Vehicles of various forms and structures were considered, ultimately Team 9 chose to move forward with a recumbent position tadpole trike; a three wheeled design with two wheels in the front and one in the rear. Tadpole trikes are propelled with the use of a drivetrain that transfers rotational energy from the human operator's legs to forward movement at the ground. A drivetrain of traditional bicycle components makes the vehicle easily serviceable and minimizes the requirement of proprietary parts. An aluminum alloy frame was developed to carry the load of the occupant and protect the rider in the event of a rollover. This frame and drivetrain, in combination with an adjustable steering system, allow the vehicle to be safely operated from zero to 40 MPH, with skilled drivers capable of even higher speeds. In order to achieve these maximum speeds with a human power source, a streamlined, low drag fairing was designed to

encompass the entire vehicle and operator. This shell is the result of over 15 iterations evaluated and optimized with computational fluid dynamics. The inclusion of this low drag shell will give this human powered vehicle aerodynamic forces one-fifth of those experienced on a traditional bicycle. A remote controlled air circulation system is integrated into the shell to keep operators comfortable in a variety of climate conditions. The reclined position of the operator was optimized through data collection experiments with the intention of placing occupants in a comfortable orientation without sacrificing power output. This was achieved with the use of a stationary power output monitoring fixture developed by Team 9. The prototype vehicle's total cost of development is estimated to be $6000. However, projections for a multiyear production run were also calculated at 3.3 million dollars for a run of 360 vehicles during a three year span.

The vehicle's construction will begin in January of 2014 and will continue through March of 2014. The performance of this vehicle will be evaluated at the Human Powered Vehicle Challenge (HPVC) hosted by the American Society of Mechanical Engineers (ASME) in April 2014.

6.0 REFERENCES

[1] R.C. Hibbeler, *Structural Analysis,* New Jersey, Pearson Prentice Hall, 2012

[2] R. G. Budynas and J. K. Nisbett, *Shigley's Mechanical Engineering Design,* New York, McGraw-Hill, 2011

[3] Philip J. Pritchard and John C. Leylegian, *Introduction to Fluid Mechanics*, Manhattan College: John Wiley & Sons, Inc., 2011.

[4] R.C. Hibbeler, *Engineering Mechanics – Statics,* Pearson Prentice Hall, 2010

[5] Zeke Smith, *Advanced Composite Techniques*, Napa, CA: Aeronaut Press, 2005.

[6] D.G. Wilson, *Bicycling Science*, Cambridge, MA: The MIT Press, 2004

[7] C. R. Kyle, Ph.D. and Frank Berto, "The mechanical efficiency of bicycle derailleur and hub-gear transmissions," Technical Journal of the IHPVA, vol. 52, pp. 3-11, 2001

[8] American Society of Mechanical Engineers, Rules for the 2014 Human Powered Vehicle Challenge (2014) [Online]. Available: https://community.asme.org/hpvc/m/default.aspx

[9] R. Horwitz, The Recumbent Trike Design Primer (8.0) (2010) [Online]. Available: http://hellbentcycles.com/trike_projects/Recumbent%20Trike%20Design%20Primer.pdf

[10] Atomic Zombie, Another Canadian Warrior tadpole trike, (2012) [Online] http://atomiczombie.wordpress.com/2012/03/21/another-canadian-warrior-tadpole-trike/

[11] Stanford, The NACA Airfoil Series, (2012) [Online] http://www.stanford.edu/~cantwell/AA200_Course_Material/The%20NACA%20airfoil%20series.pdf

[12] WeatherSpark, Average Weather For San Jose, California, USA, (2012) [Online] http://weatherspark.com/averages/31616/San-Jose-California-United-States

APPENDIX A – ENGINEERING DRAWINGS

List of Drawings

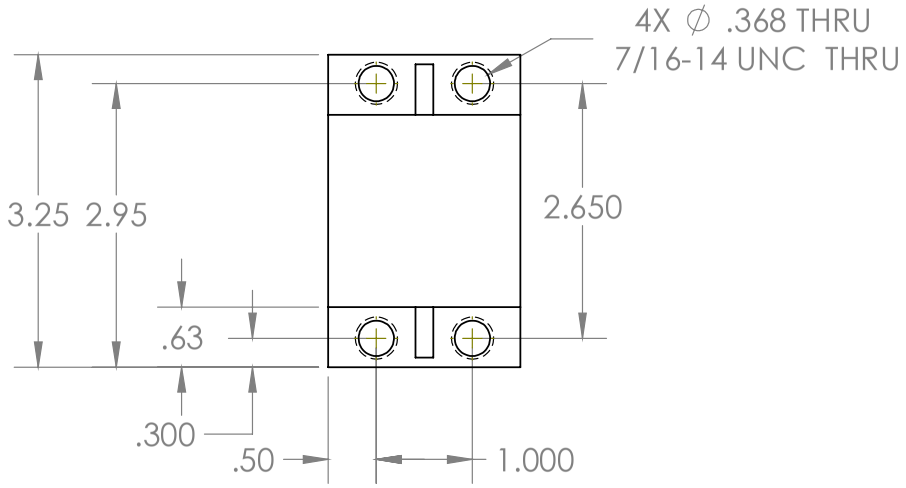

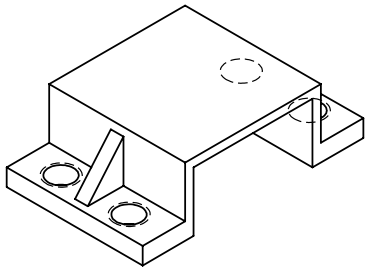

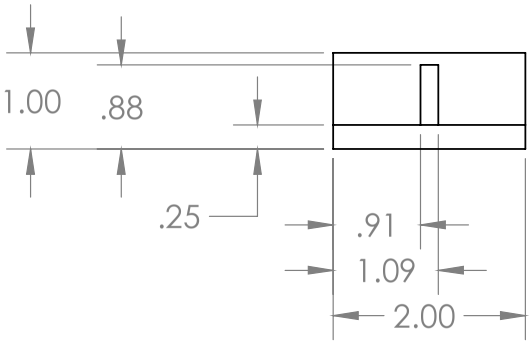

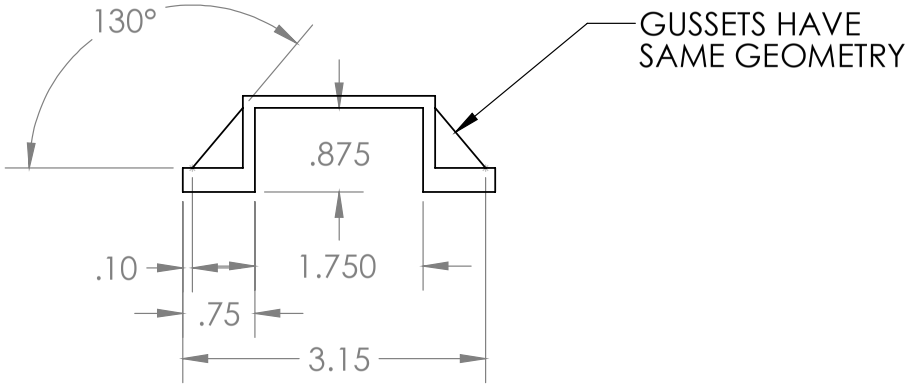

TEAM 9 HUMAN POWERED VEHICLE CHALLENGE

UNLESS OTHERWISE SPECIFIED:
DIMENSIONS ARE IN INCHES
GENERAL SURFACE FINISH 125
TOLERANCES:
FRACTIONAL ±1/16
ANGULAR: ± 0.5°
TWO PLACE DECIMAL ± .03
THREE PLACE DECIMAL ± .005

MATERIAL
6061-T6 (SS)

FINISH

COMMENTS:

DO NOT SCALE DRAWING

DRAWN BY:
KEVIN MONTOYA

TITLE:
BOTTOM BRACKET BACK

SIZE
A

DATE DRAWN
12/12/2013

SCALE: 1:2 | WEIGHT: 0.15 lbs | SHEET 1 OF 1

5 4 3 2 1

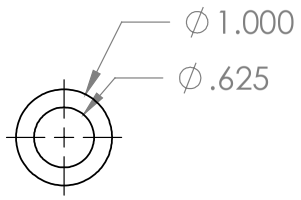

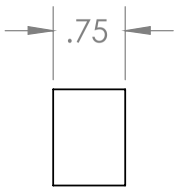

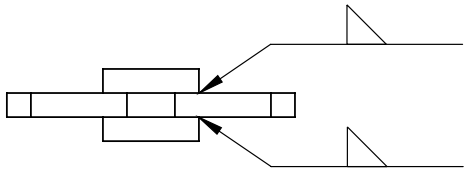

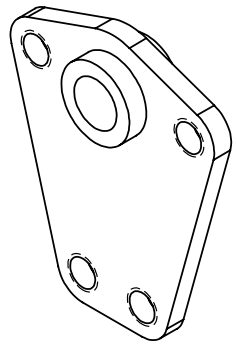

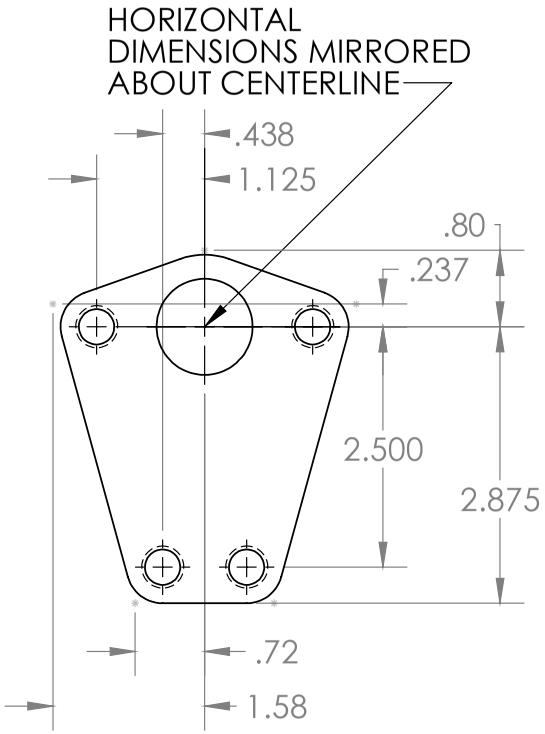

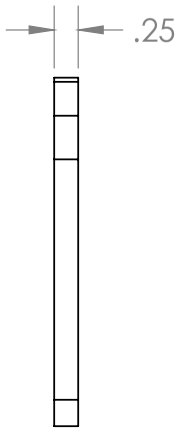

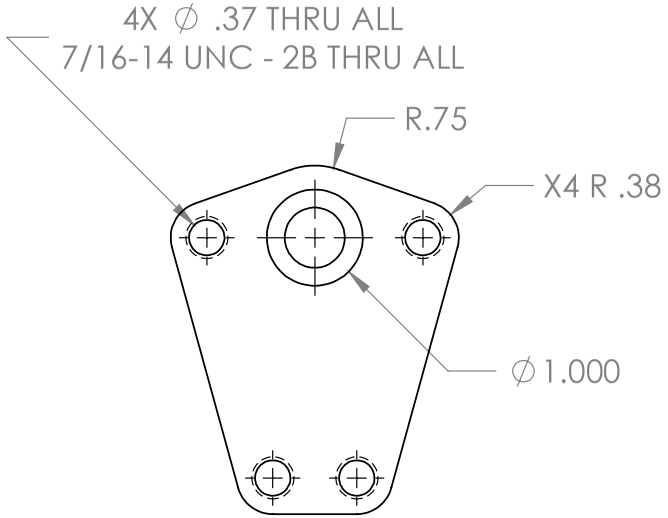

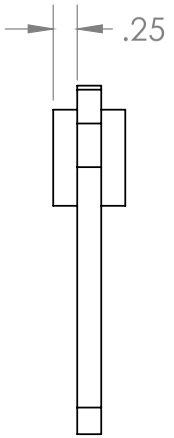

TEAM 9 HUMAN POWERED VEHICLE CHALLENGE

UNLESS OTHERWISE SPECIFIED:
DIMENSIONS ARE IN INCHES
GENERAL SURFACE FINISH 125
TOLERANCES:
FRACTIONAL ±1/16
ANGULAR: ± 0.5°
TWO PLACE DECIMAL ± .03
THREE PLACE DECIMAL ± .005

MATERIAL
6061-T6 (SS)

FINISH

COMMENTS:
MAIN BODY WILL BE INPUT INTO CAMWORKS FOR G-CODE GENERATION

DO NOT SCALE DRAWING

DRAWN BY:
ALEX HAWLEY

TITLE:
Bell Crank

SIZE
A

DATE DRAWN
12/10/2013

SCALE: 1:2 | WEIGHT: 0.20 | SHEET 1 OF 1

5 4 3 2 1

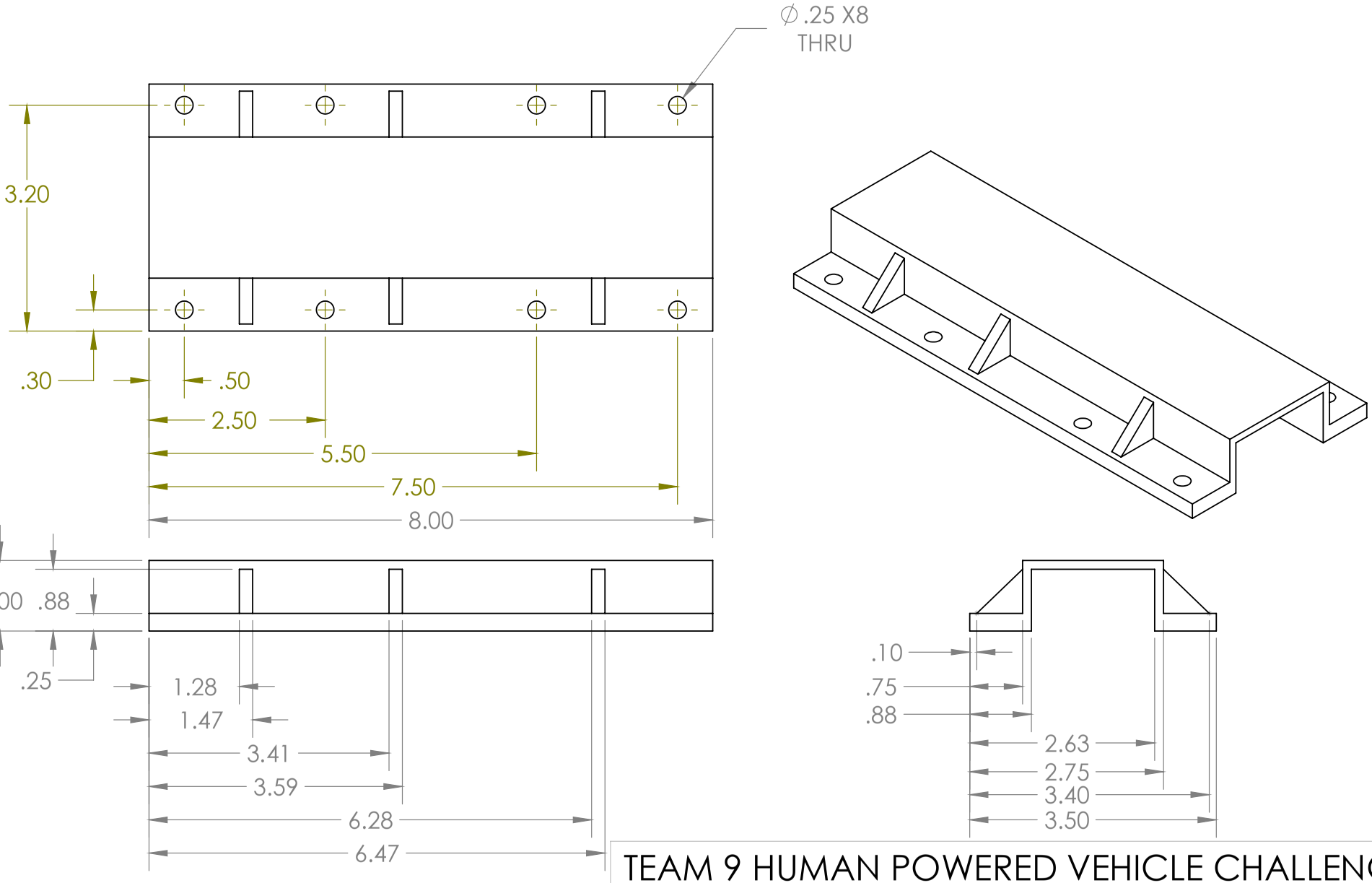

TEAM 9 HUMAN POWERED VEHICLE CHALLENGE

UNLESS OTHERWISE SPECIFIED:
DIMENSIONS ARE IN INCHES
GENERAL SURFACE FINISH 125
TOLERANCES:
FRACTIONAL ±1/16
ANGULAR: ± 0.5°
TWO PLACE DECIMAL ± .03
THREE PLACE DECIMAL ± .005

COMMENTS:

DRAWN BY: KEVIN MONTOYA

TITLE: BOTTOM BRACKET FRONT

SIZE A

DATE DRAWN 12/12/2013

MATERIAL 6061-T6 (SS)

FINISH

DO NOT SCALE DRAWING

SCALE: 1:2 | WEIGHT: 0.67 lbs | SHEET 1 OF 1

77

5 4 3 2 1

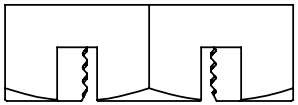

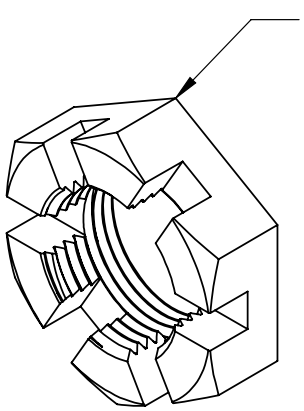

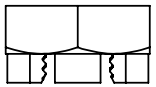

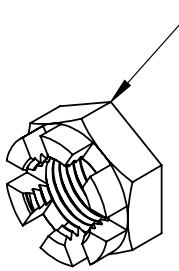

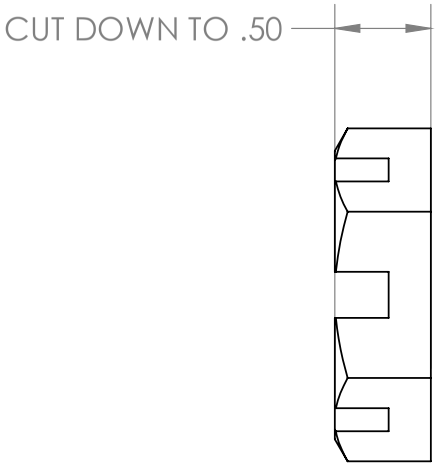

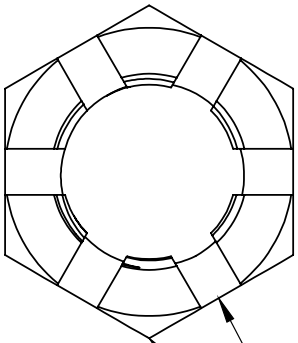

McMaster-Carr
Part# 95030A320

WEIGHT: 0.14lbs
EACH

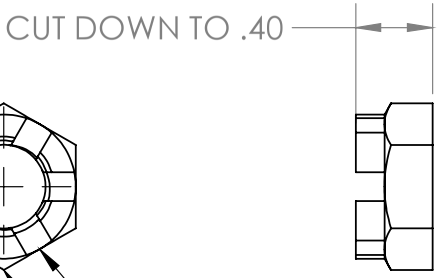

McMaster-Carr
Part# 95030A210

WEIGHT: 0.03 lbs
EACH

TEAM 9 HUMAN POWERED VEHICLE CHALLENGE

UNLESS OTHERWISE SPECIFIED:
DIMENSIONS ARE IN INCHES
GENERAL SURFACE FINISH 125
TOLERANCES:
FRACTIONAL ±1/16
ANGULAR: ± 0.5°
TWO PLACE DECIMAL ± .03
THREE PLACE DECIMAL ± .005

MATERIAL
Zinc-Plated Grade 2 Steel

FINISH

COMMENTS:

DO NOT SCALE DRAWING

DRAWN BY:
KEVIN MONTOYA

TITLE:
CASTLE NUTS

SIZE
A

DATE DRAWN
12/12/2013

SCALE: 1:1

WEIGHT: 0.17 lbs

SHEET 1 OF 1

78

5 4 3 2 1

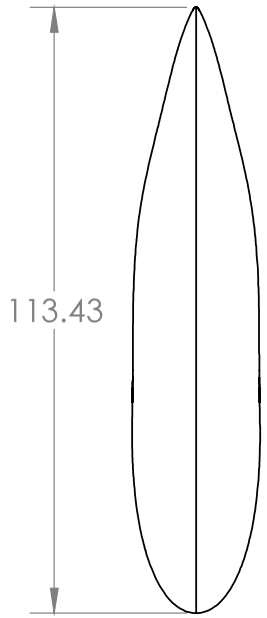

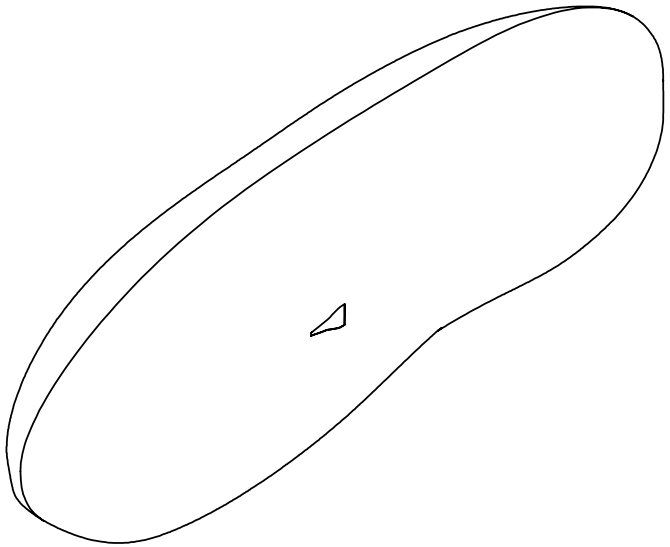

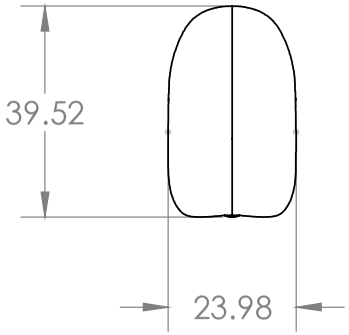

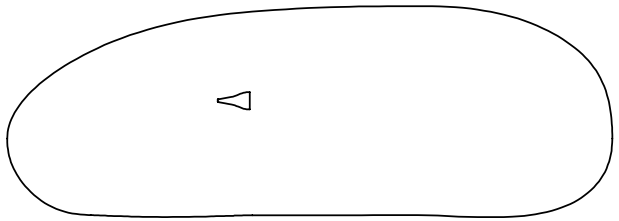

TEAM 9 HUMAN POWERED VEHICLE CHALLENGE

UNLESS OTHERWISE SPECIFIED:
DIMENSIONS ARE IN INCHES
GENERAL SURFACE FINISH 125
TOLERANCES:
FRACTIONAL ±1/16
ANGULAR: ± 0.5°
TWO PLACE DECIMAL ± .03
THREE PLACE DECIMAL ± .005

MATERIAL
Carbon Fiber 2X2 3K

FINISH

COMMENTS:

DO NOT SCALE DRAWING

DRAWN BY:
KEVIN MONTOYA

TITLE:
FAIRING

SIZE
A

DATE DRAWN
12/12/2013

SCALE: 1:36 | WEIGHT: 17.75 lbs | SHEET 1 OF 1

79

5 4 3 2 1

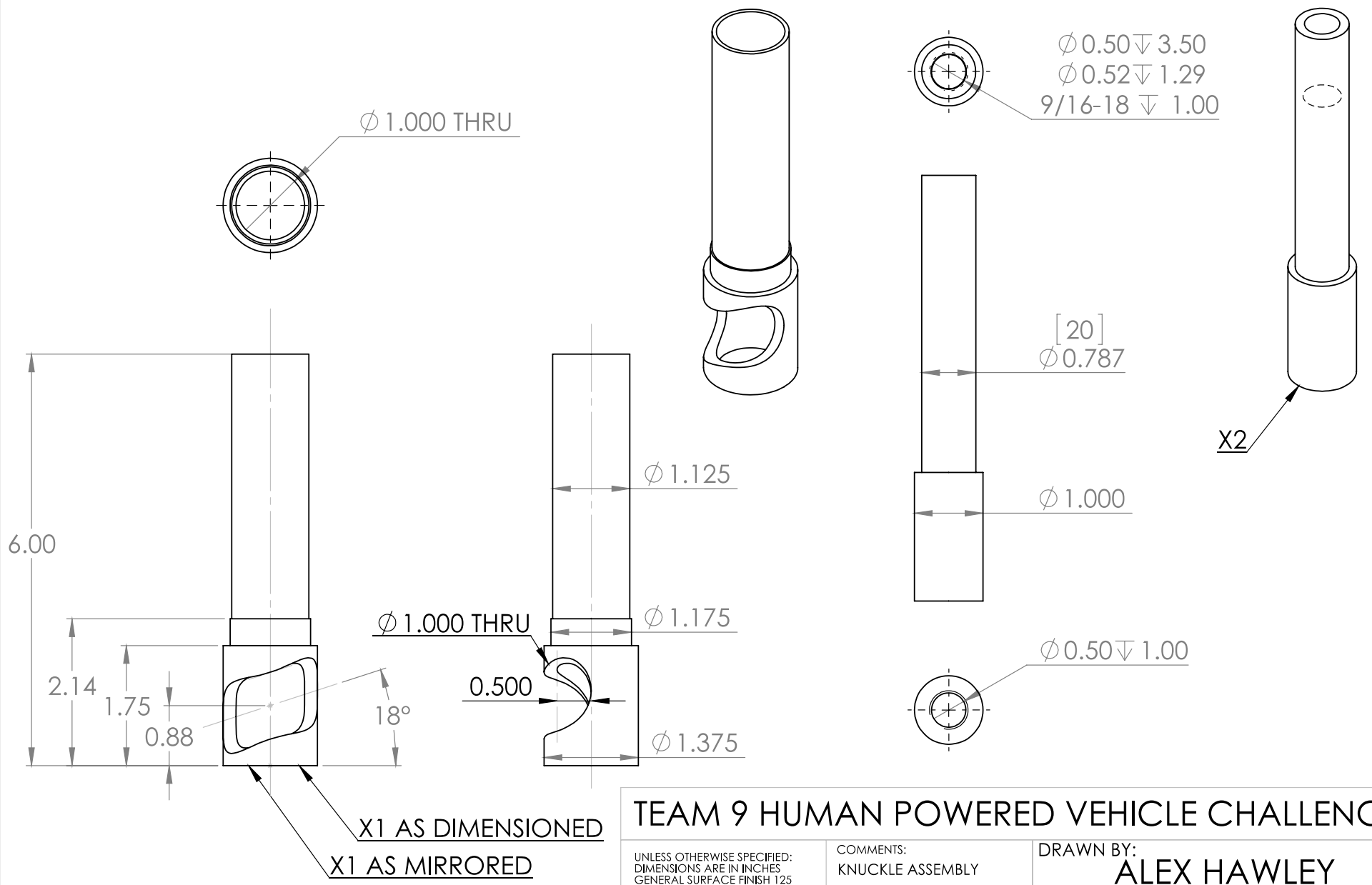

TEAM 9 HUMAN POWERED VEHICLE CHALLENGE

UNLESS OTHERWISE SPECIFIED:
DIMENSIONS ARE IN INCHES
GENERAL SURFACE FINISH 125
TOLERANCES:
FRACTIONAL ±1/16
ANGULAR: ± 0.5°
TWO PLACE DECIMAL ± .03
THREE PLACE DECIMAL ± .005

MATERIAL
6061-T6 (SS)

FINISH

COMMENTS:
KNUCKLE ASSEMBLY

DO NOT SCALE DRAWING

DRAWN BY:
ALEX HAWLEY

TITLE:
KNUCKLES

SIZE
A

DATE DRAWN
12/12/2013

SCALE: 1:2

WEIGHT: 0.62

SHEET 1 OF 3

80

5 4 3 2 1

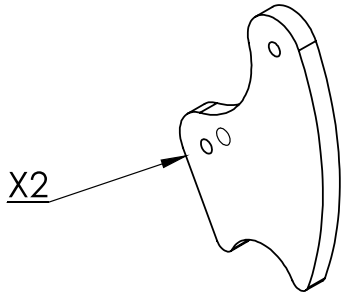

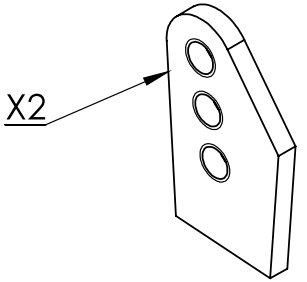

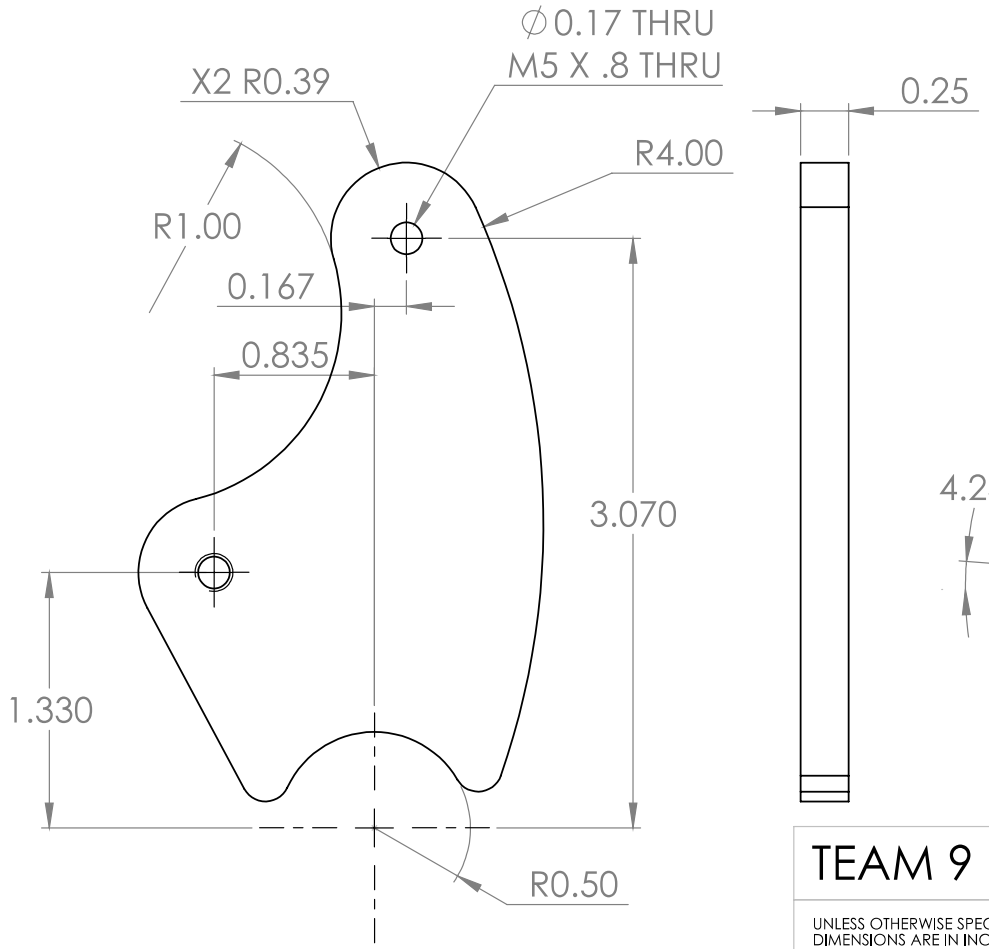

TEAM 9 HUMAN POWERED VEHICLE CHALLENGE

UNLESS OTHERWISE SPECIFIED:
DIMENSIONS ARE IN INCHES
GENERAL SURFACE FINISH 125
TOLERANCES:
FRACTIONAL ±1/16
ANGULAR: ± 0.5°
TWO PLACE DECIMAL ± .03
THREE PLACE DECIMAL ± .005

MATERIAL
6061-T6 (SS)

FINISH

COMMENTS:
KNUCKLE ASSEMBLY

DO NOT SCALE DRAWING

DRAWN BY:
ALEX HAWLEY

TITLE:
KNUCKLES

SIZE
A

DATE DRAWN
12/12/2013

SCALE: 1:1 | WEIGHT: 0.62 | SHEET 2 OF 3

81

5 4 3 2 1

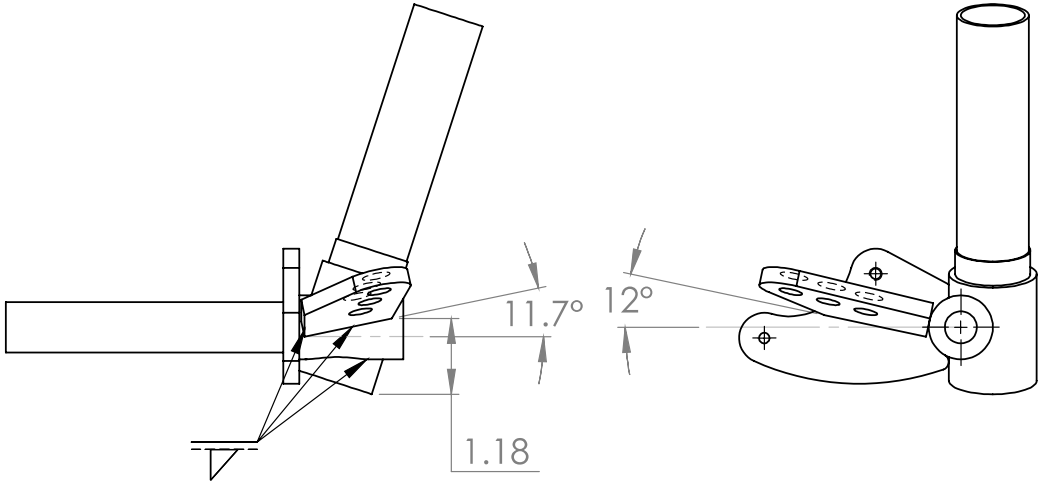

RIGHT CONFIGURATION

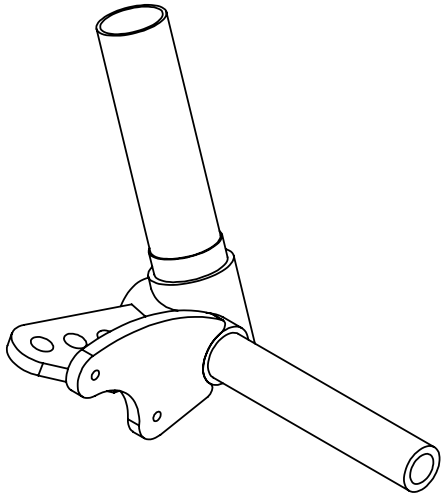

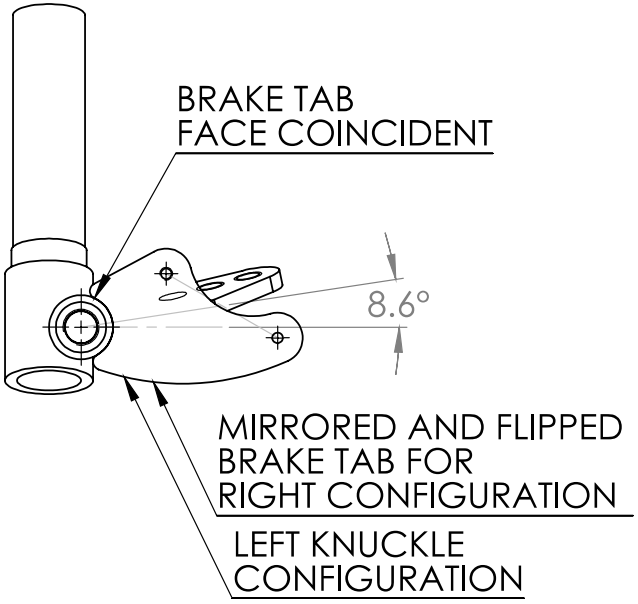

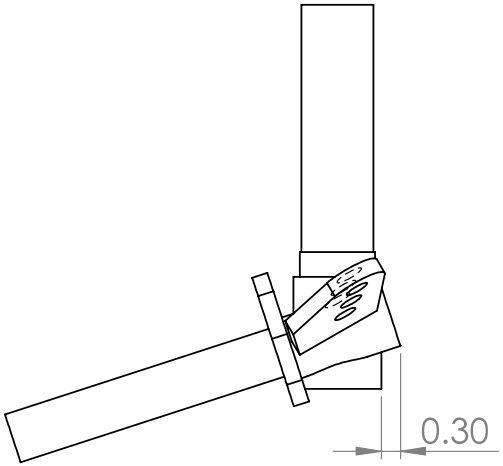

LEFT CONFIGURATION

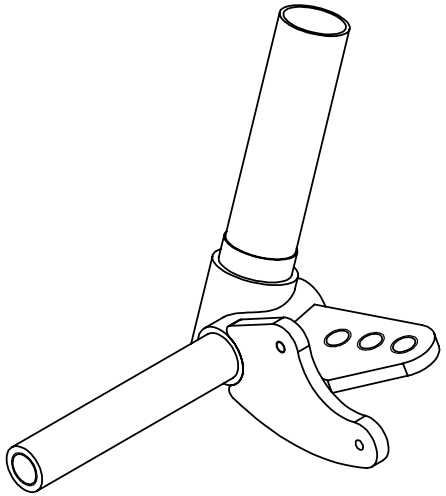

TEAM 9 HUMAN POWERED VEHICLE CHALLENGE

UNLESS OTHERWISE SPECIFIED:
DIMENSIONS ARE IN INCHES
GENERAL SURFACE FINISH 125
TOLERANCES:
FRACTIONAL ±1/16
ANGULAR: ± 0.5°
TWO PLACE DECIMAL ± .03
THREE PLACE DECIMAL ± .005

MATERIAL
6061-T6 (SS)

FINISH

COMMENTS:
KNUCKLE ASSEMBLY

DO NOT SCALE DRAWING

DRAWN BY:
ALEX HAWLEY

TITLE:
KNUCKLES

SIZE
A

DATE DRAWN
12/12/2013

SCALE: 1:3 | WEIGHT: 0.62 | SHEET 3 OF 3

82

5 4 3 2 1

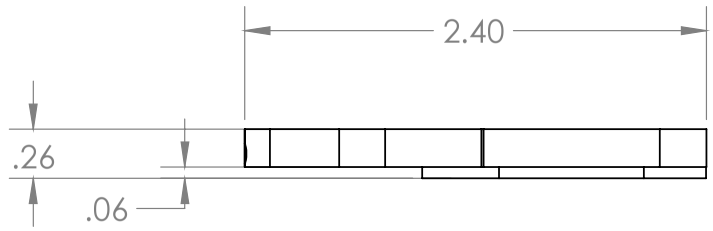

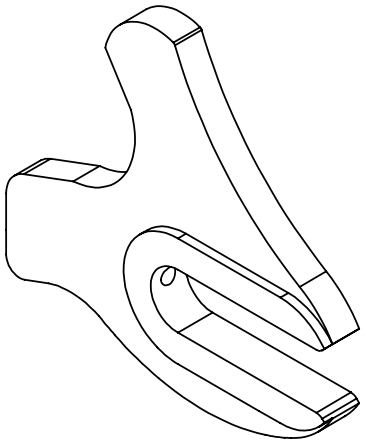

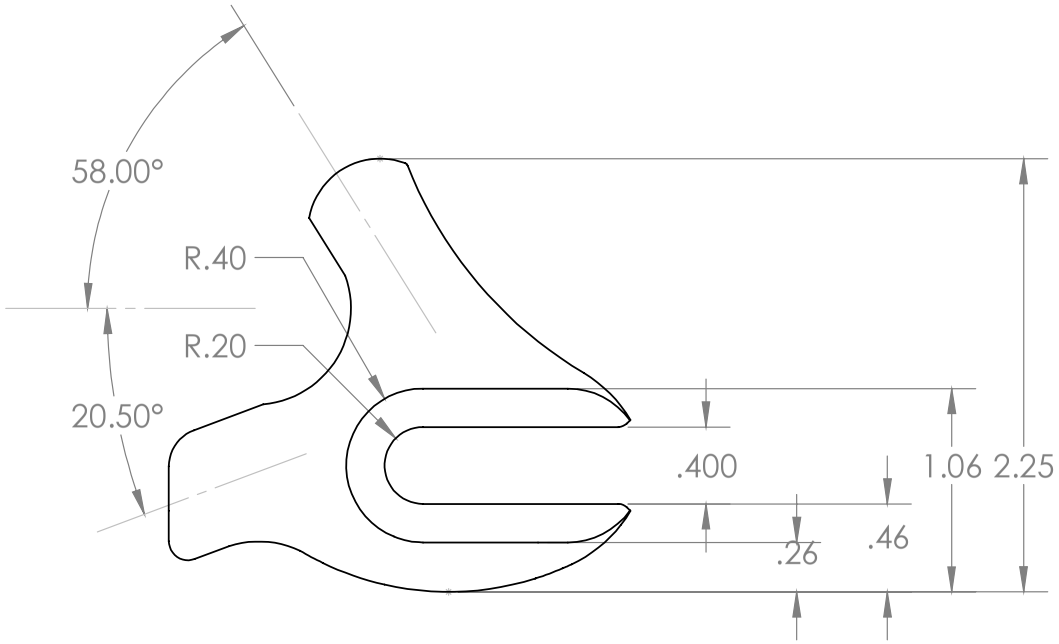

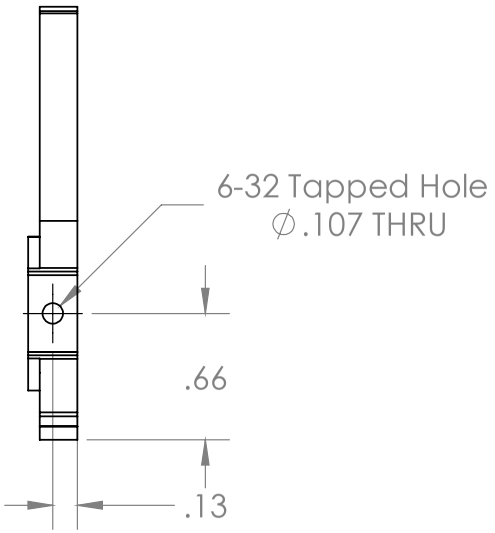

TEAM 9 HUMAN POWERED VEHICLE CHALLENGE

UNLESS OTHERWISE SPECIFIED:
DIMENSIONS ARE IN INCHES
GENERAL SURFACE FINISH 125
TOLERANCES:
FRACTIONAL ±1/16
ANGULAR: ± 0.5°
TWO PLACE DECIMAL ± .03
THREE PLACE DECIMAL ± .005

MATERIAL
6061-T6 (SS)

FINISH

COMMENTS:
This part will be machinced in a CNC machine. The code will be produced with a program called CAMWORKS.

DO NOT SCALE DRAWING

DRAWN BY:
KEVIN MONTOYA

TITLE:
LEFT DROPOUT

SIZE
A

DATE DRAWN
12/12/2013

SCALE: 1:1 | WEIGHT: 0.05 lbs | SHEET 1 OF 1

5 4 3 2 1

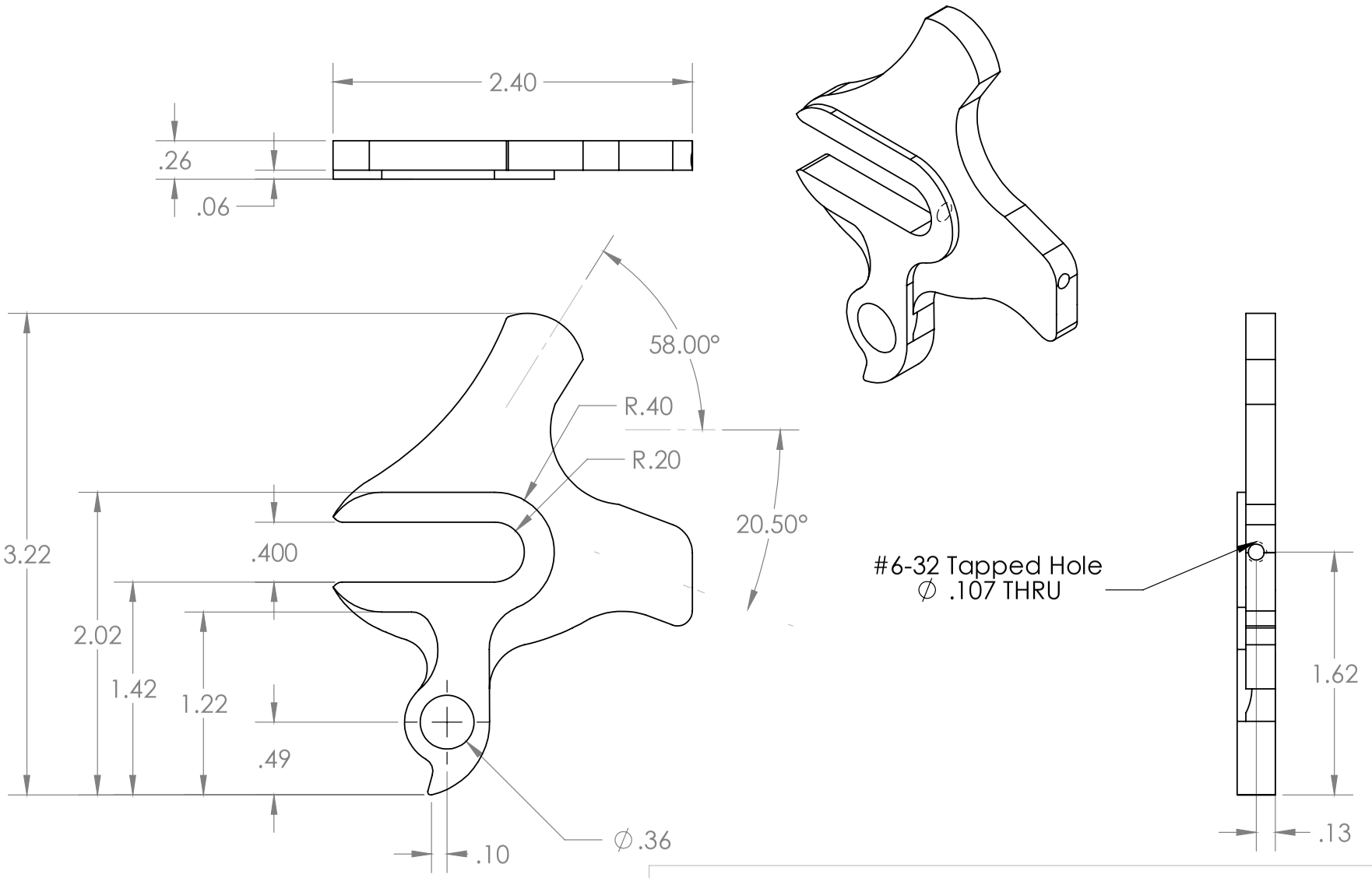

TEAM 9 HUMAN POWERED VEHICLE CHALLENGE

UNLESS OTHERWISE SPECIFIED:
DIMENSIONS ARE IN INCHES
GENERAL SURFACE FINISH 125
TOLERANCES:
FRACTIONAL ±1/16
ANGULAR: ± 0.5°
TWO PLACE DECIMAL ± .03
THREE PLACE DECIMAL ± .005

MATERIAL
6061-T6 (SS)

FINISH

COMMENTS:
This part will be machinced in a CNC machine. The code will be produced with a program called CAMWORKS.

DO NOT SCALE DRAWING

DRAWN BY:
KEVIN MONTOYA

TITLE:
RIGHT DROPOUT

SIZE
A

DATE DRAWN
12/12/2013

SCALE: 1:1 | WEIGHT: 0.06 lbs | SHEET 1 OF 1

84

5 4 3 2 1

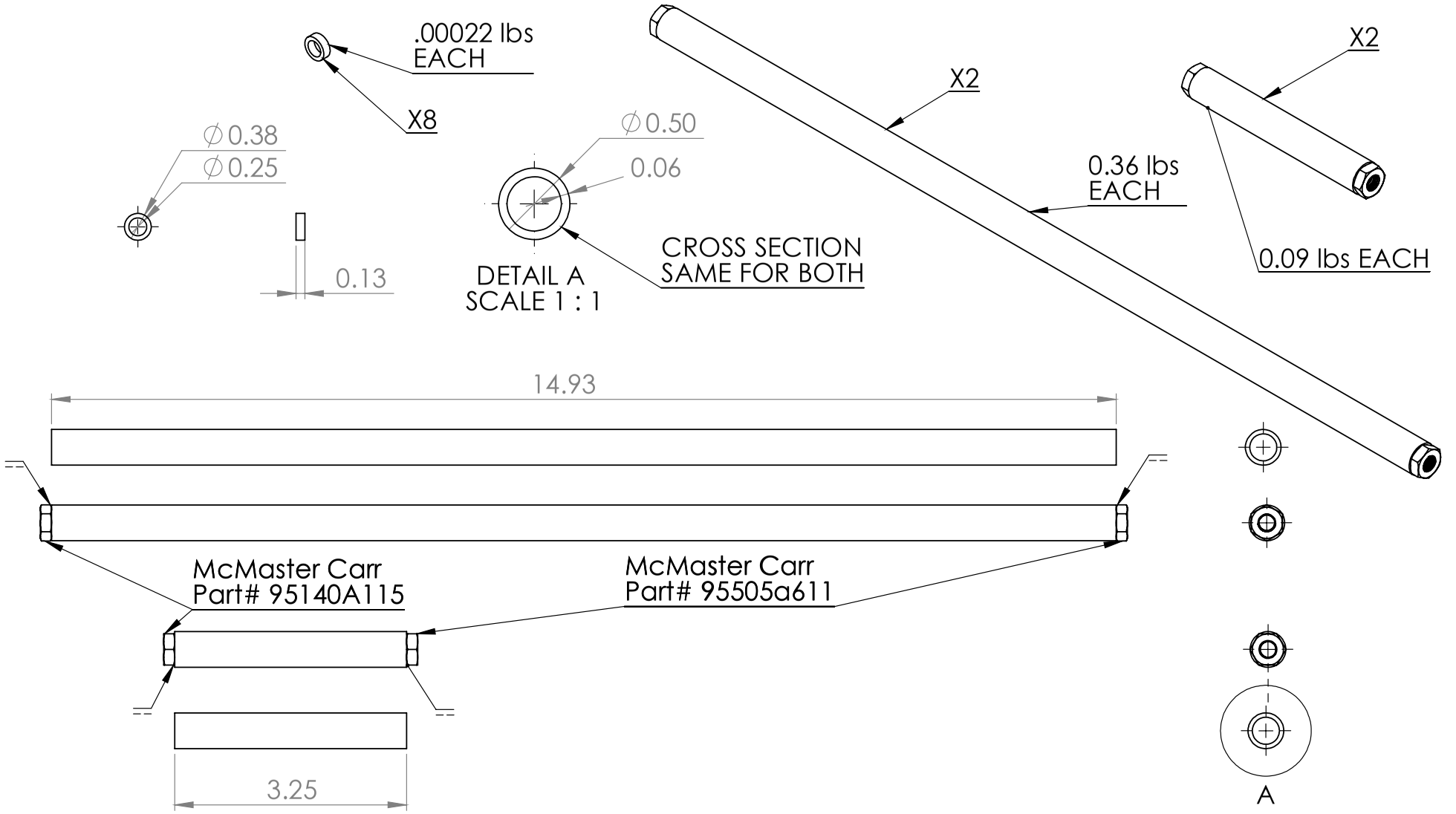

TEAM 9 HUMAN POWERED VEHICLE CHALLENGE

UNLESS OTHERWISE SPECIFIED:
DIMENSIONS ARE IN INCHES
GENERAL SURFACE FINISH 125
TOLERANCES:
FRACTIONAL ±1/16
ANGULAR: ± 0.5°
TWO PLACE DECIMAL ± .03
THREE PLACE DECIMAL ± .005

MATERIAL
4130 CHROMOLY

FINISH

COMMENTS:

DO NOT SCALE DRAWING

DRAWN BY:
ALEX HAWLEY

TITLE:
Linkages and Spacers

SIZE
A

DATE DRAWN
12/10/2013

SCALE: 1:2 | WEIGHT: 0.46 lbs | SHEET 1 OF 1

85

SolidWorks Student Edition.
For Academic Use Only.

5 4 3 2 1

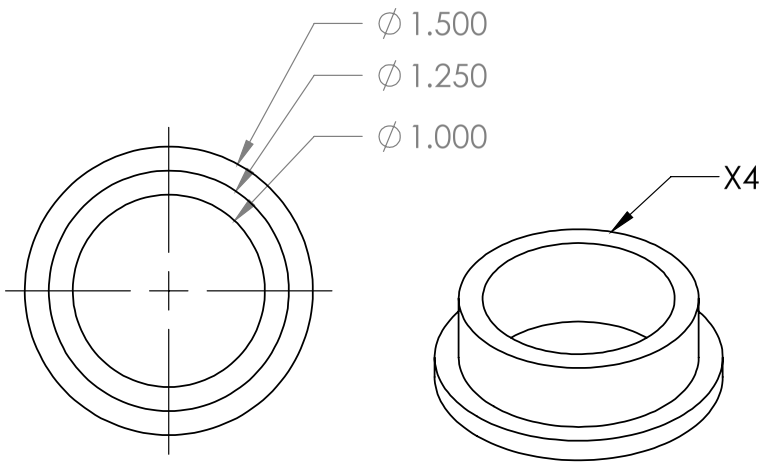

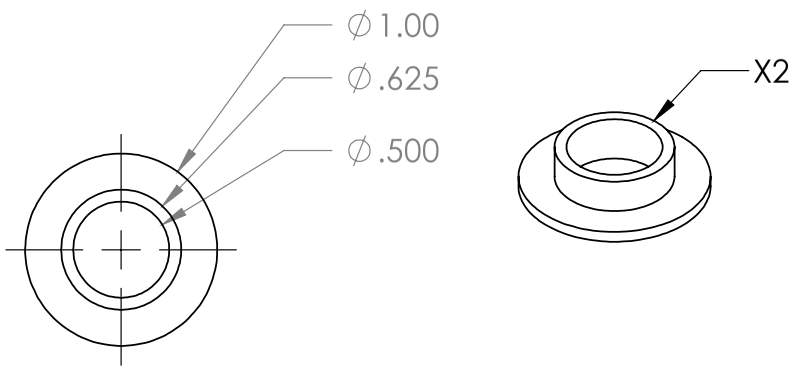

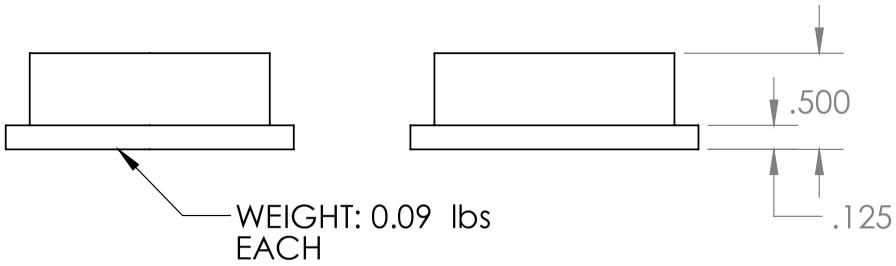

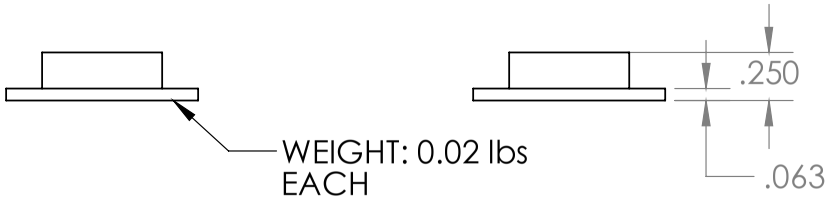

TEAM 9 HUMAN POWERED VEHICLE CHALLENGE

UNLESS OTHERWISE SPECIFIED:
DIMENSIONS ARE IN INCHES
GENERAL SURFACE FINISH 125
TOLERANCES:
FRACTIONAL ±1/16
ANGULAR: ± 0.5°
TWO PLACE DECIMAL ± .03
THREE PLACE DECIMAL ± .005

MATERIAL
Bronze (Alloy 936)

FINISH

COMMENTS:

DO NOT SCALE DRAWING

DRAWN BY:
KEVIN MONTOYA

TITLE:
STEERING BUSHINGS

SIZE
A

DATE DRAWN
12/12/2013

SCALE: 1:1 | WEIGHT: 0.4 lbs | SHEET 1 OF 1

5 4 3 2 1

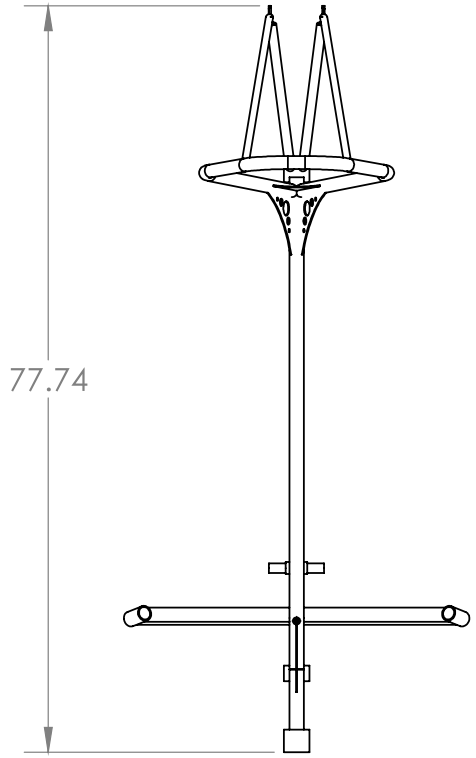

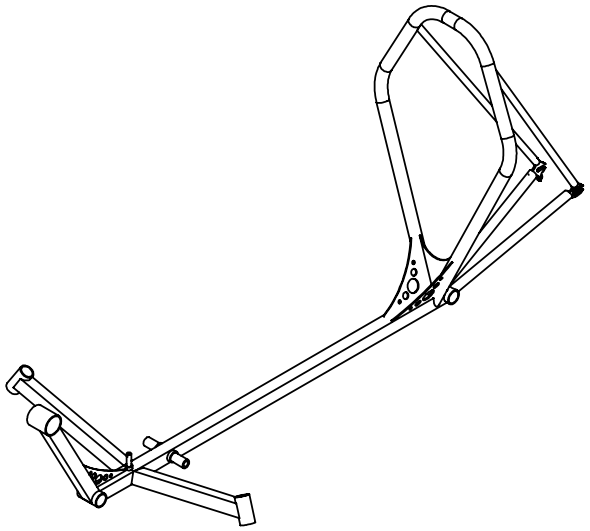

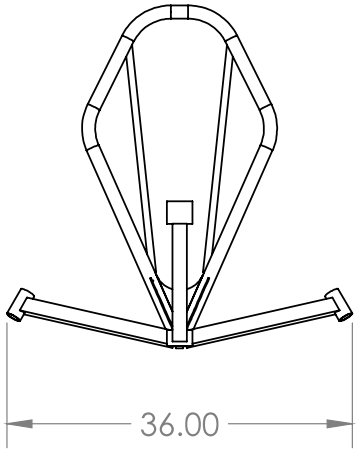

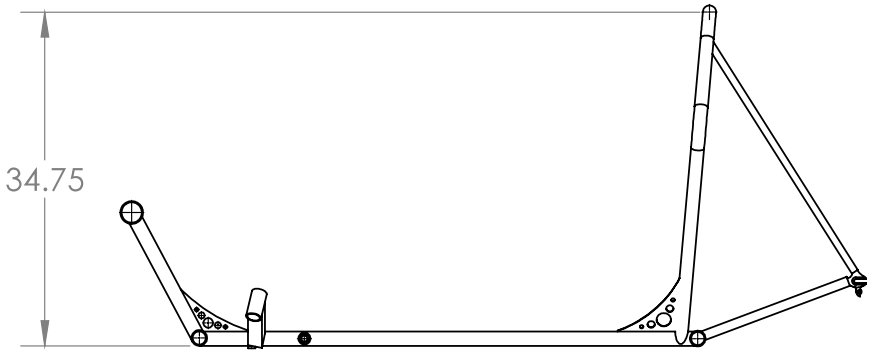

TEAM 9 HUMAN POWERED VEHICLE CHALLENGE

UNLESS OTHERWISE SPECIFIED:
DIMENSIONS ARE IN INCHES
GENERAL SURFACE FINISH 125
TOLERANCES:
FRACTIONAL ±1/16
ANGULAR: ± 0.5°
TWO PLACE DECIMAL ± .03
THREE PLACE DECIMAL ± .005

MATERIAL
6061-T6 (SS)

FINISH

COMMENTS:
Frame for 2013-2014 HPVC Capstone

Designed and Created by Matt Gerlich

Sketches completed by Kevin Montoya

DO NOT SCALE DRAWING

DRAWN BY:
KEVIN MONTOYA

TITLE:
FRAME

SIZE
A

DATE DRAWN
12/12/2013

SCALE: 1:20 | WEIGHT: 14.50 lbs | SHEET 1 OF 14

87

5 4 3 2 1

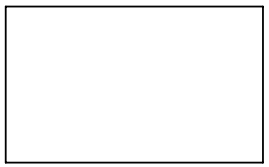

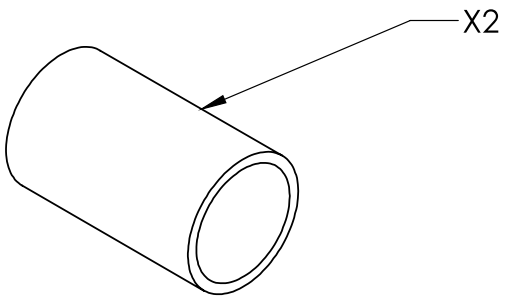

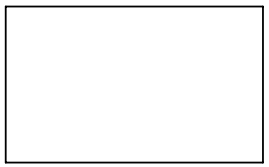

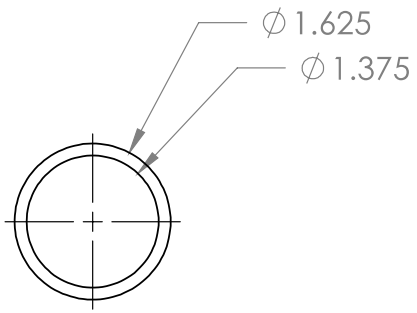

TEAM 9 HUMAN POWERED VEHICLE CHALLENGE

UNLESS OTHERWISE SPECIFIED:
DIMENSIONS ARE IN INCHES
GENERAL SURFACE FINISH 125
TOLERANCES:
FRACTIONAL ±1/16
ANGULAR: ± 0.5°
TWO PLACE DECIMAL ± .03
THREE PLACE DECIMAL ± .005

MATERIAL
6061-T6 (SS)

FINISH

COMMENTS:

DO NOnot SCALE DRAWING

DRAWN BY:
KEVIN MONTOYA

TITLE:
FRAME

SIZE
A

DATE DRAWN
12/12/2013

SCALE: 1:2

WEIGHT: 14.50 lbs

SHEET 2 OF 14

88

5 4 3 2 1

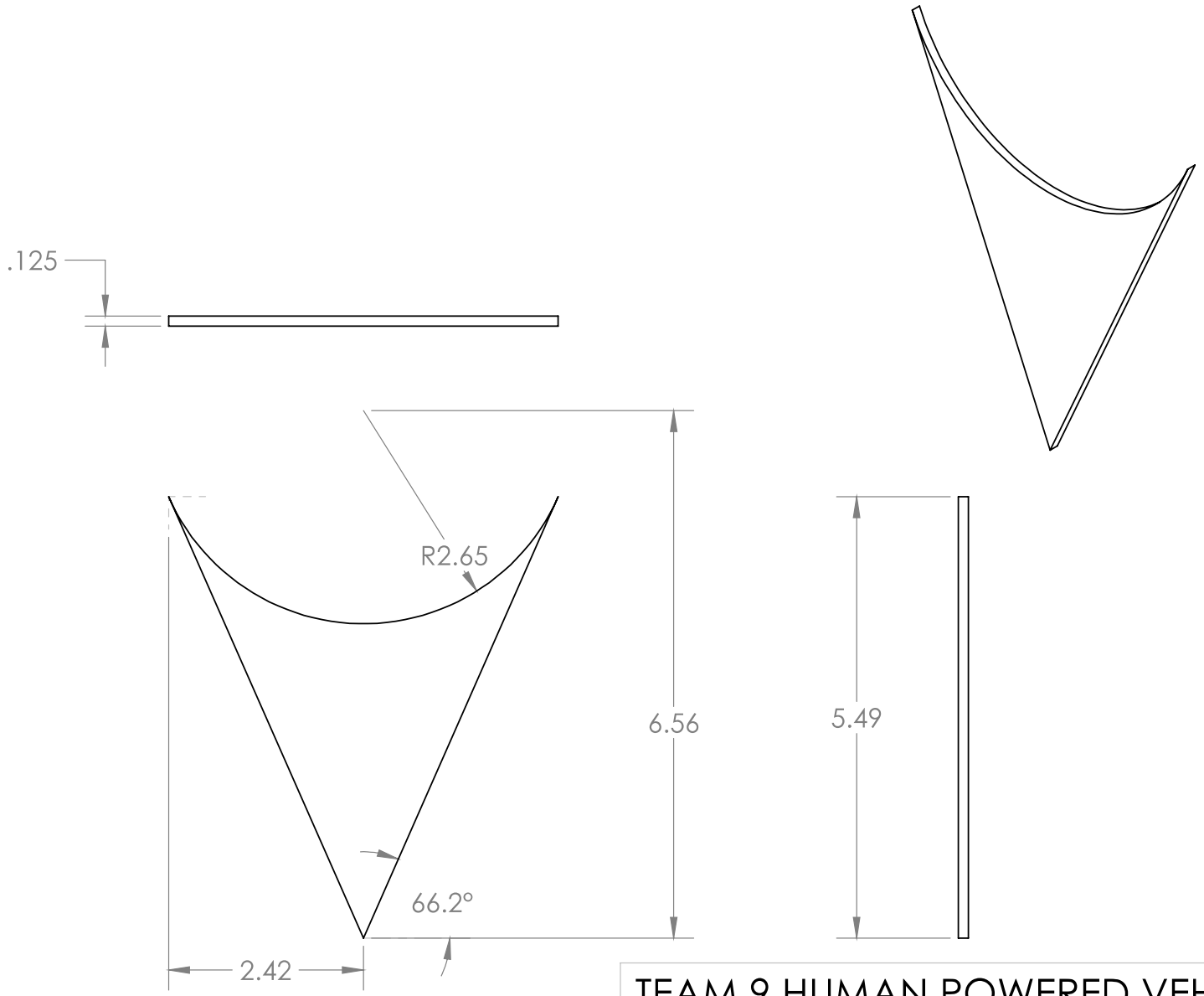

TEAM 9 HUMAN POWERED VEHICLE CHALLENGE

UNLESS OTHERWISE SPECIFIED:
DIMENSIONS ARE IN INCHES
GENERAL SURFACE FINISH 125
TOLERANCES:
FRACTIONAL ±1/16
ANGULAR: ± 0.5°
TWO PLACE DECIMAL ± .03
THREE PLACE DECIMAL ± .005

MATERIAL
6061-T6 (SS)

FINISH

COMMENTS:

DO NOT SCALE DRAWING

DRAWN BY:
KEVIN MONTOYA

TITLE:
FRAME

SIZE
A

DATE DRAWN
12/12/2013

SCALE: 1:2

WEIGHT: 14.50 lbs

SHEET 3 OF 14

68

5 4 3 2 1

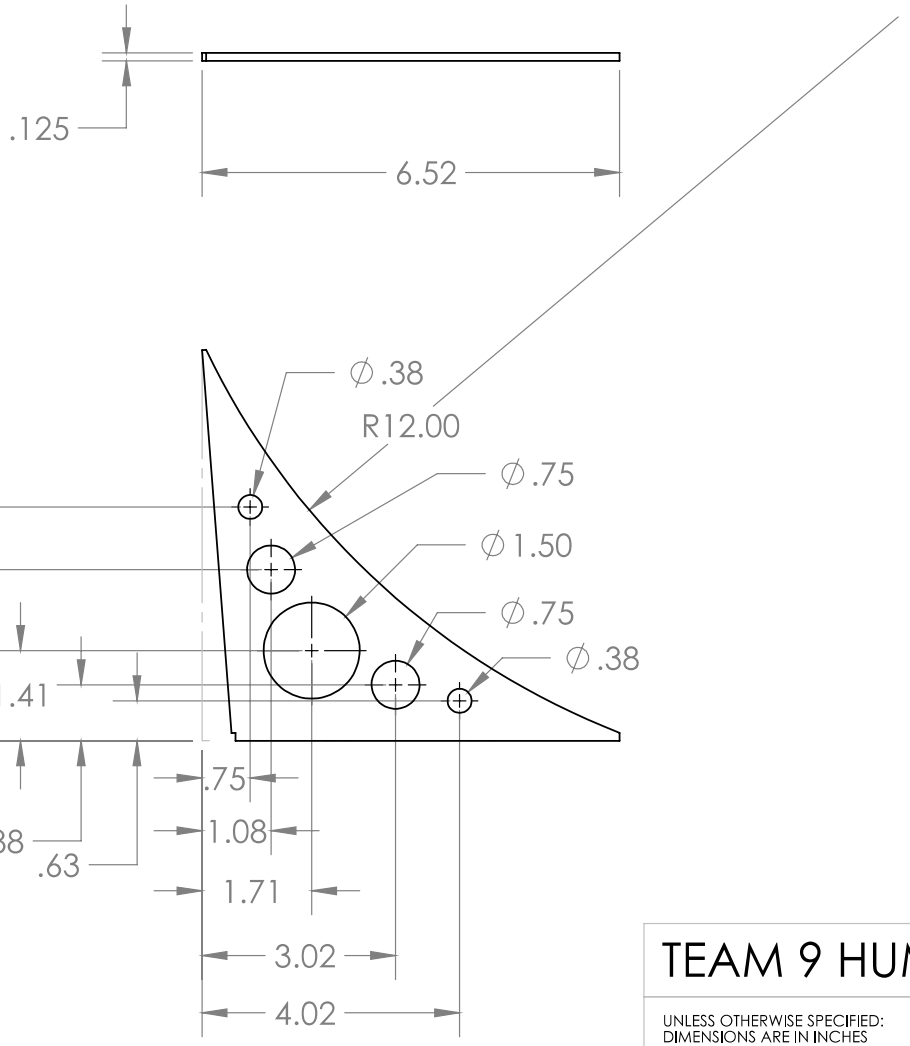

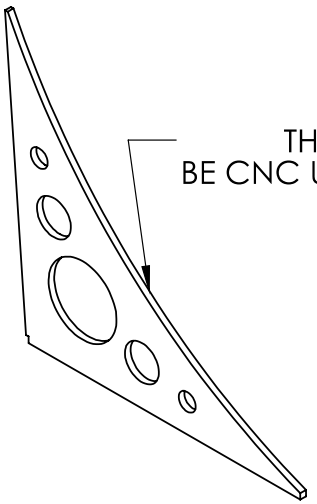

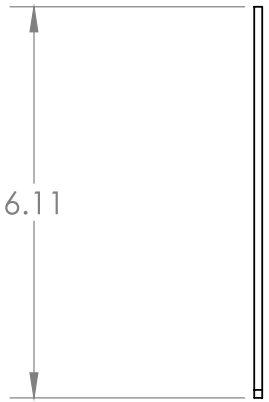

TEAM 9 HUMAN POWERED VEHICLE CHALLENGE

UNLESS OTHERWISE SPECIFIED:
DIMENSIONS ARE IN INCHES
GENERAL SURFACE FINISH 125
TOLERANCES:
FRACTIONAL ±1/16
ANGULAR: ± 0.5°
TWO PLACE DECIMAL ± .03
THREE PLACE DECIMAL ± .005

MATERIAL
6061-T6 (SS)

FINISH

COMMENTS:

DO NOT SCALE DRAWING

DRAWN BY:
KEVIN MONTOYA

TITLE:
FRAME

SIZE
A

DATE DRAWN
12/12/2013

SCALE: 1:3 | WEIGHT: 14.50 lbs | SHEET 4 OF 14

06

5 4 3 2 1

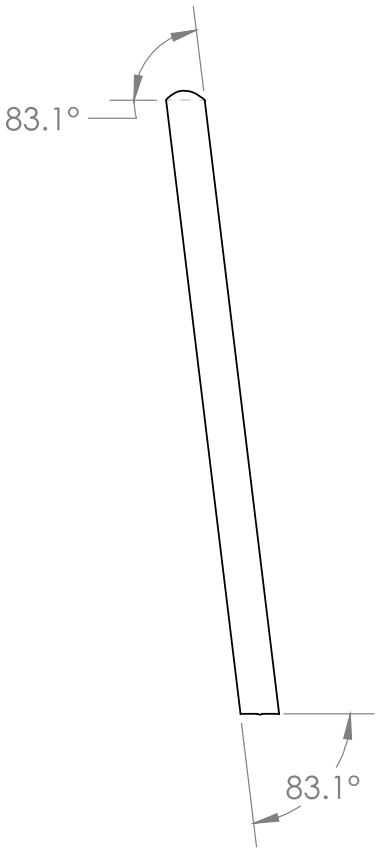

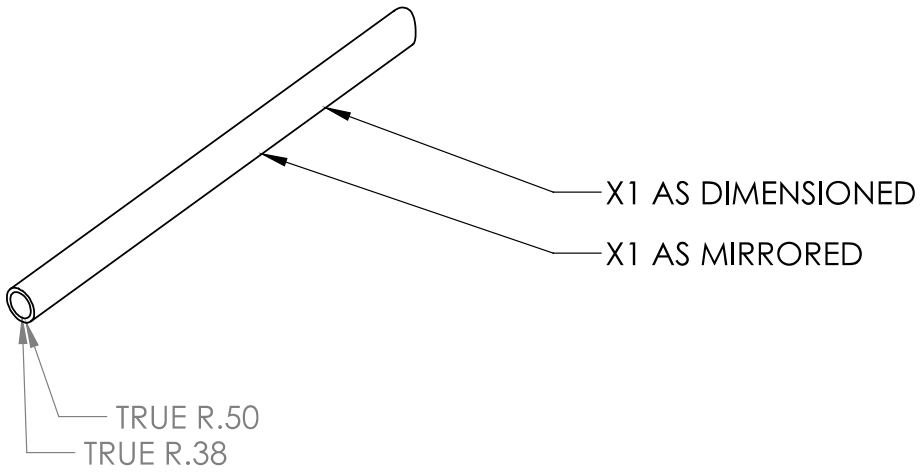

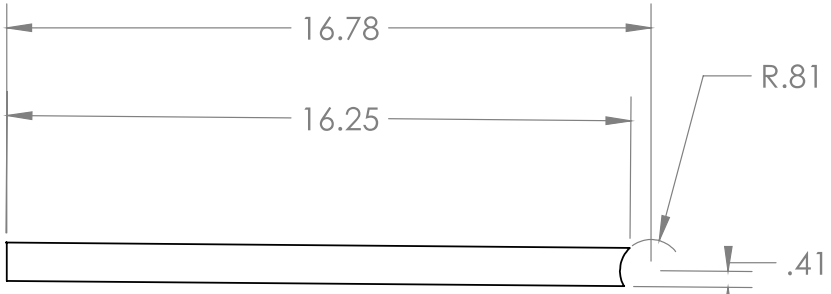

TEAM 9 HUMAN POWERED VEHICLE CHALLENGE

UNLESS OTHERWISE SPECIFIED: DIMENSIONS ARE IN INCHES GENERAL SURFACE FINISH 125 TOLERANCES: FRACTIONAL ±1/16 ANGULAR: ± 0.5° TWO PLACE DECIMAL ± .03 THREE PLACE DECIMAL ± .005	COMMENTS:	DRAWN BY: KEVIN MONTOYA
		TITLE: FRAME
MATERIAL 6061-T6 (SS)		SIZE A / DATE DRAWN 12/12/2013
FINISH	DO NOT SCALE DRAWING	SCALE: 1:5 / WEIGHT: 14.50 lbs / SHEET 5 OF 14

91

5 4 3 2 1

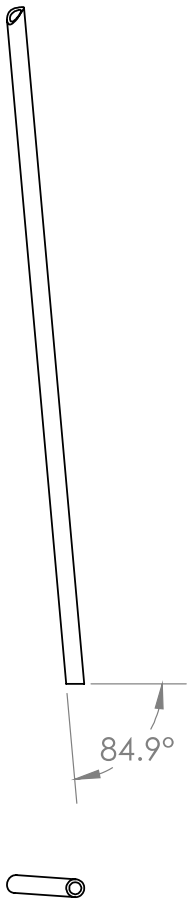

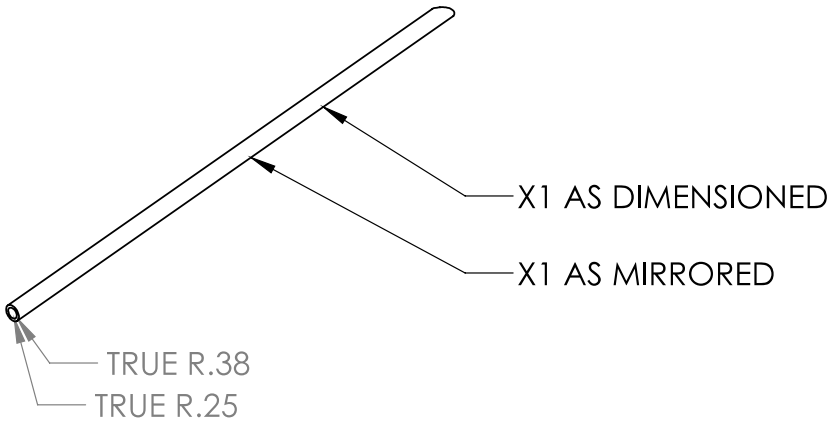

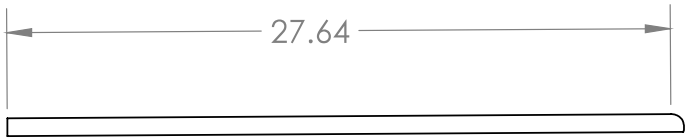

TEAM 9 HUMAN POWERED VEHICLE CHALLENGE

UNLESS OTHERWISE SPECIFIED:
DIMENSIONS ARE IN INCHES
GENERAL SURFACE FINISH 125
TOLERANCES:
FRACTIONAL ±1/16
ANGULAR: ± 0.5°
TWO PLACE DECIMAL ± .03
THREE PLACE DECIMAL ± .005

MATERIAL
6061-T6 (SS)

FINISH

COMMENTS:

DO NOT SCALE DRAWING

DRAWN BY:
KEVIN MONTOYA

TITLE:
FRAME

SIZE
A

DATE DRAWN
12/12/2013

SCALE: 1:8

WEIGHT: 14.50 lbs

SHEET 6 OF 14

92

5 4 3 2 1

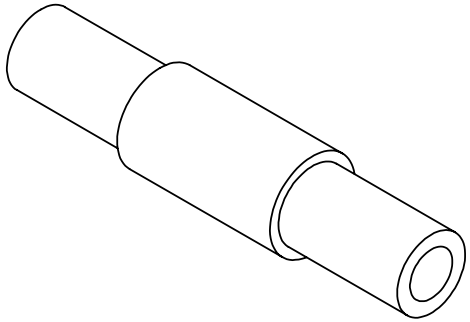

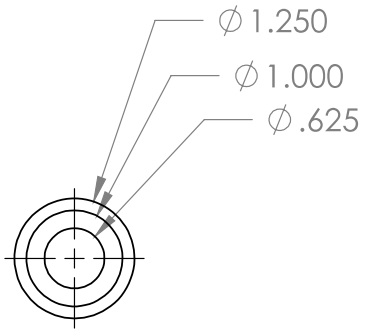

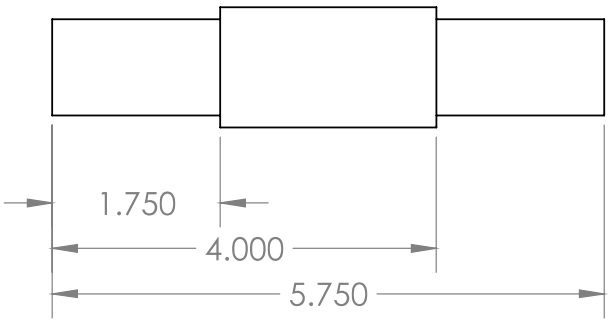

TEAM 9 HUMAN POWERED VEHICLE CHALLENGE

UNLESS OTHERWISE SPECIFIED:
DIMENSIONS ARE IN INCHES
GENERAL SURFACE FINISH 125
TOLERANCES:
FRACTIONAL ±1/16
ANGULAR: ± 0.5°
TWO PLACE DECIMAL ± .03
THREE PLACE DECIMAL ± .005

MATERIAL
6061-T6 (SS)

FINISH

COMMENTS:

DO NOT SCALE DRAWING

DRAWN BY:
KEVIN MONTOYA

TITLE:
FRAME

SIZE
A

DATE DRAWN
12/12/2013

SCALE: 1:2

WEIGHT: 14.50 lbs

SHEET 7 OF 14

93

5 4 3 2 1

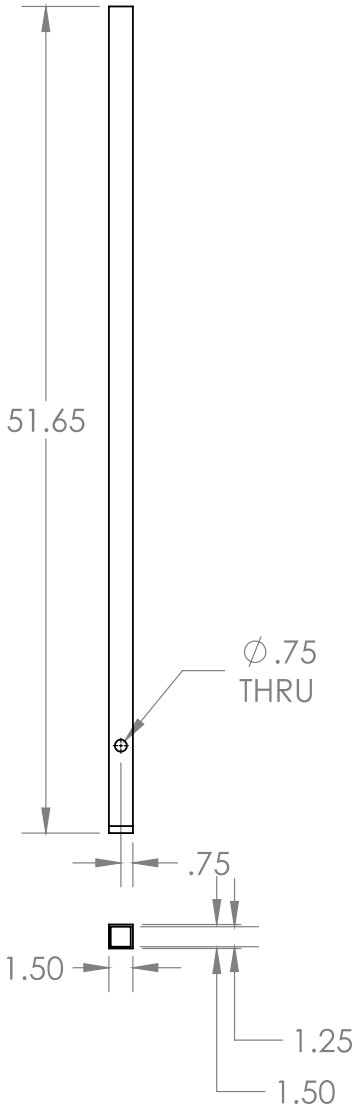

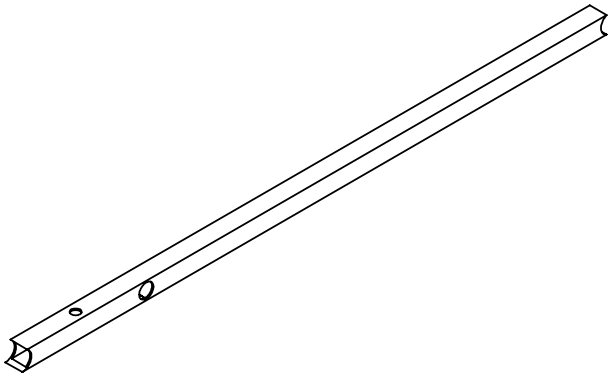

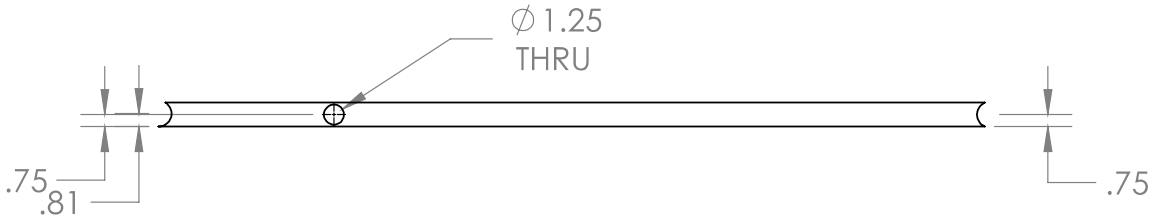

TEAM 9 HUMAN POWERED VEHICLE CHALLENGE

UNLESS OTHERWISE SPECIFIED:
DIMENSIONS ARE IN INCHES
GENERAL SURFACE FINISH 125
TOLERANCES:
FRACTIONAL ±1/16
ANGULAR: ± 0.5°
TWO PLACE DECIMAL ± .03
THREE PLACE DECIMAL ± .005

MATERIAL
6061-T6 (SS)

FINISH

COMMENTS:

DO NOT SCALE DRAWING

DRAWN BY:
KEVIN MONTOYA

TITLE:
FRAME

SIZE
A

DATE DRAWN
12/12/2013

SCALE: 1:12 | WEIGHT: 14.50 lbs | SHEET 8 OF 14

94

5 4 3 2 1

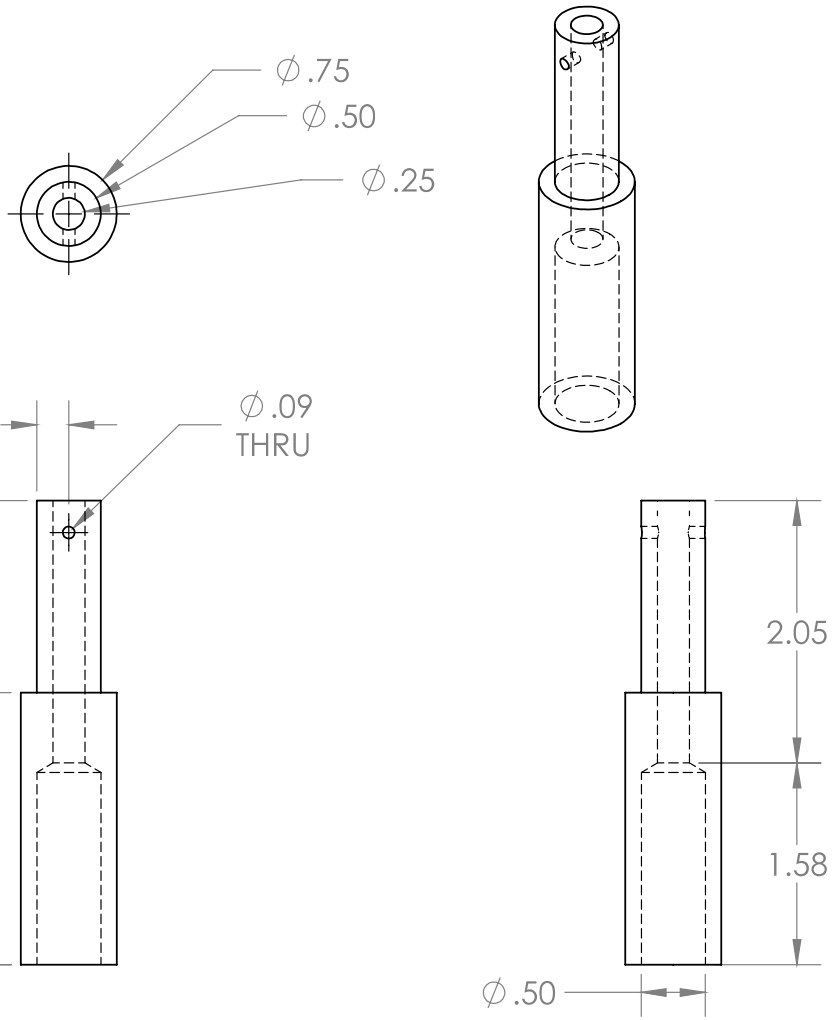

TEAM 9 HUMAN POWERED VEHICLE CHALLENGE

UNLESS OTHERWISE SPECIFIED:
DIMENSIONS ARE IN INCHES
GENERAL SURFACE FINISH 125
TOLERANCES:
FRACTIONAL ±1/16
ANGULAR: ± 0.5°
TWO PLACE DECIMAL ± .03
THREE PLACE DECIMAL ± .005

MATERIAL
6061-T6 (SS)

FINISH

COMMENTS:

DO NOT SCALE DRAWING

DRAWN BY:
KEVIN MONTOYA

TITLE:
FRAME

SIZE
A

DATE DRAWN
12/12/2013

SCALE: 2:3

WEIGHT: 14.50 lbs

SHEET 9 OF 14

95

5 4 3 2 1

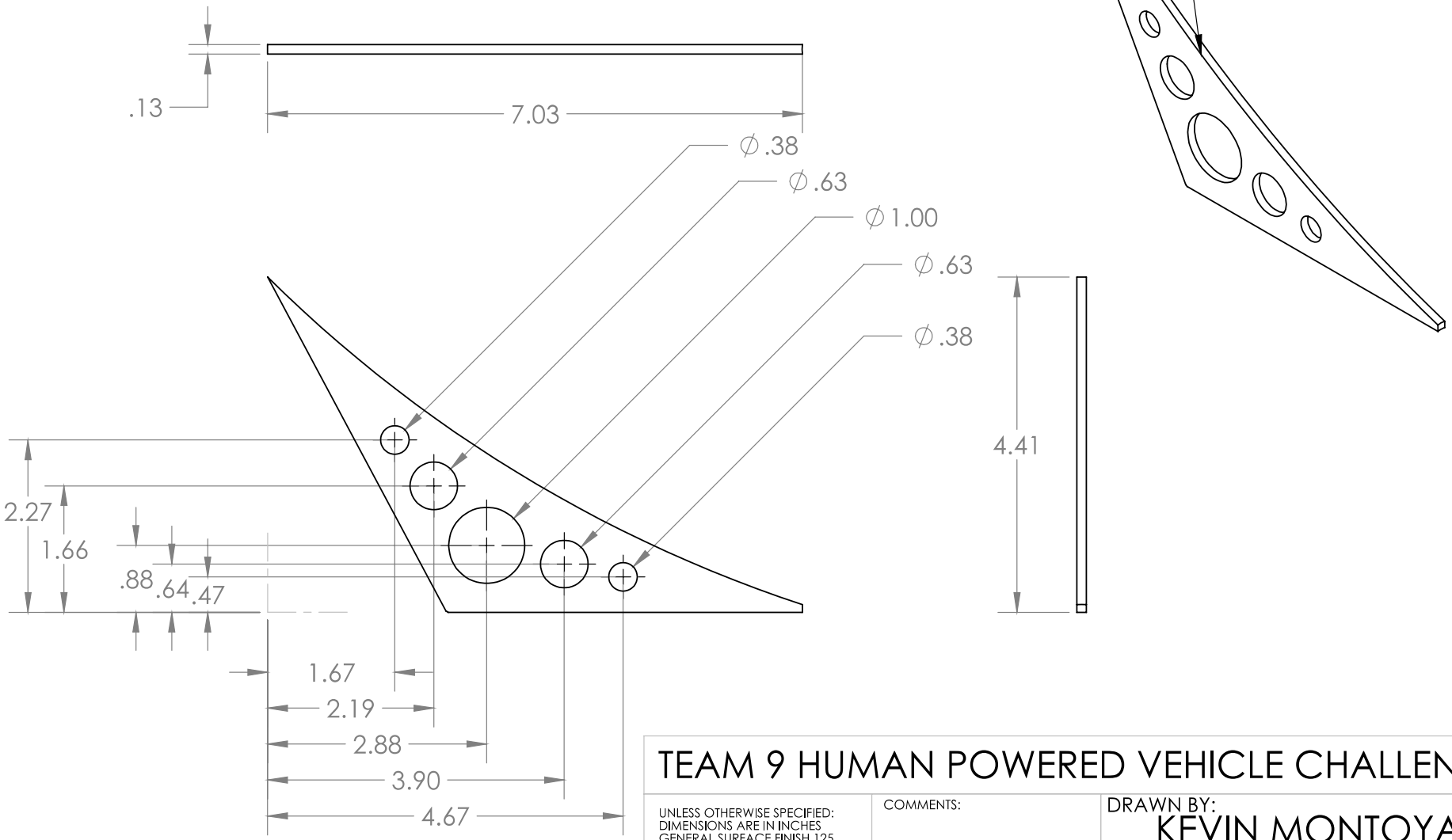

TEAM 9 HUMAN POWERED VEHICLE CHALLENGE

UNLESS OTHERWISE SPECIFIED:
DIMENSIONS ARE IN INCHES
GENERAL SURFACE FINISH 125
TOLERANCES:
FRACTIONAL ±1/16
ANGULAR: ± 0.5°
TWO PLACE DECIMAL ± .03
THREE PLACE DECIMAL ± .005

MATERIAL
6061-T6 (SS)

FINISH

COMMENTS:

DO NOT SCALE DRAWING

DRAWN BY:
KEVIN MONTOYA

TITLE:
FRAME

SIZE
A

DATE DRAWN
12/12/2013

SCALE: 1:2

WEIGHT: 14.50 lbs

SHEET 10 OF 14

96

5 4 3 2 1

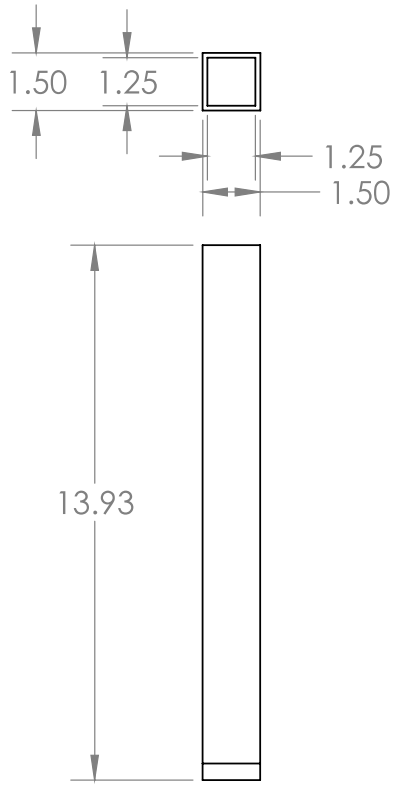

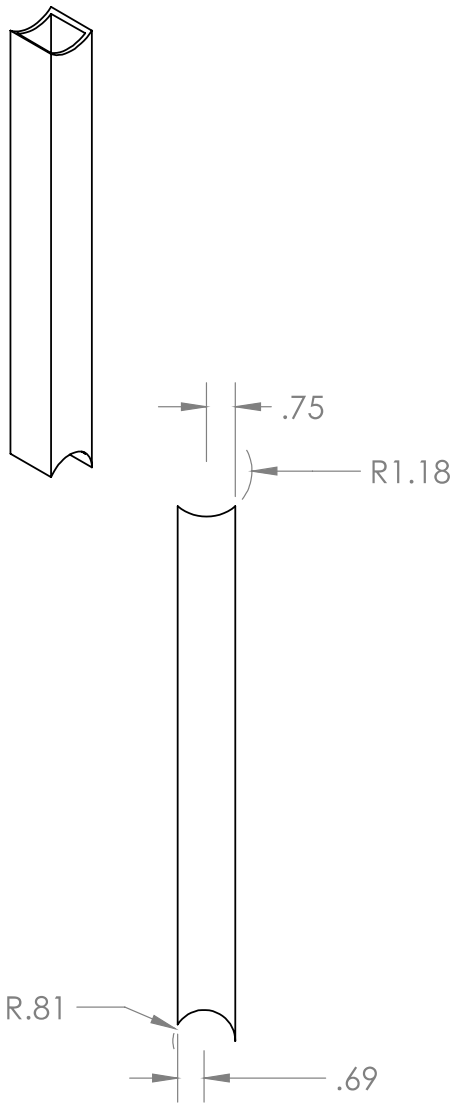

TEAM 9 HUMAN POWERED VEHICLE CHALLENGE

UNLESS OTHERWISE SPECIFIED:
DIMENSIONS ARE IN INCHES
GENERAL SURFACE FINISH 125
TOLERANCES:
FRACTIONAL ±1/16
ANGULAR: ± 0.5°
TWO PLACE DECIMAL ± .03
THREE PLACE DECIMAL ± .005

MATERIAL
6061-T6 (SS)

FINISH

COMMENTS:

DO NOT SCALE DRAWING

DRAWN BY:
KEVIN MONTOYA

TITLE:
FRAME

SIZE
A

DATE DRAWN
12/12/2013

SCALE: 1:5

WEIGHT: 14.50 lbs

SHEET 11 OF 14

97

5 4 3 2 1

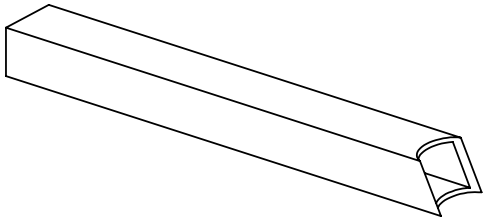

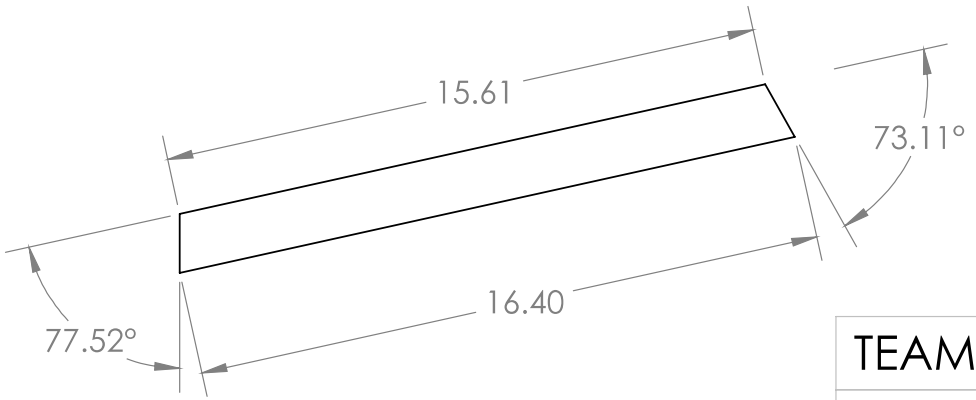

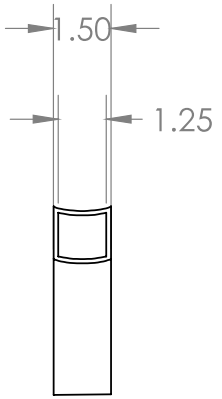

TEAM 9 HUMAN POWERED VEHICLE CHALLENGE

UNLESS OTHERWISE SPECIFIED:
DIMENSIONS ARE IN INCHES
GENERAL SURFACE FINISH 125
TOLERANCES:
FRACTIONAL ±1/16
ANGULAR: ± 0.5°
TWO PLACE DECIMAL ± .03
THREE PLACE DECIMAL ± .005

MATERIAL
6061-T6 (SS)

FINISH

COMMENTS:

DO NOT SCALE DRAWING

DRAWN BY:
KEVIN MONTOYA

TITLE:
FRAME

SIZE
A

DATE DRAWN
12/12/2013

SCALE: 1:5

WEIGHT: 14.50 lbs

SHEET 12 OF 14

86

5 4 3 2 1

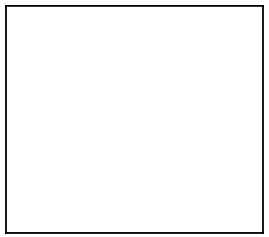

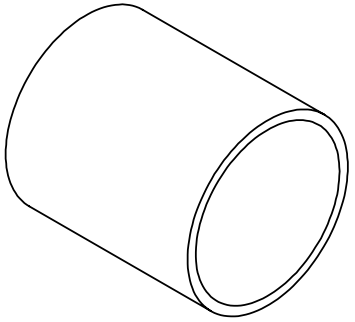

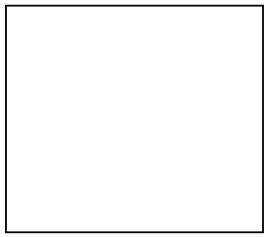

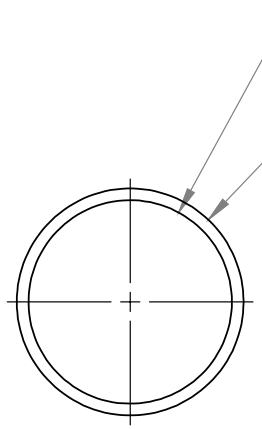

2.677

TEAM 9 HUMAN POWERED VEHICLE CHALLENGE

UNLESS OTHERWISE SPECIFIED:
DIMENSIONS ARE IN INCHES
GENERAL SURFACE FINISH 125
TOLERANCES:
FRACTIONAL ±1/16
ANGULAR: ± 0.5°
TWO PLACE DECIMAL ± .03
THREE PLACE DECIMAL ± .005

MATERIAL
6061-T6 (SS)

FINISH

COMMENTS:

DO NOT SCALE DRAWING

DRAWN BY:
KEVIN MONTOYA

TITLE:
FRAME

SIZE
A

DATE DRAWN
12/12/2013

SCALE: 1:2

WEIGHT: 14.50 lbs

SHEET 13 OF 14

66

5 4 3 2 1

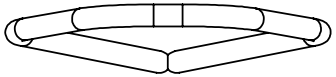

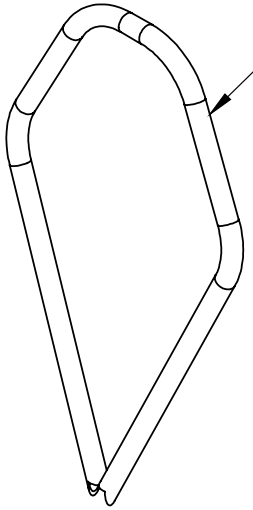

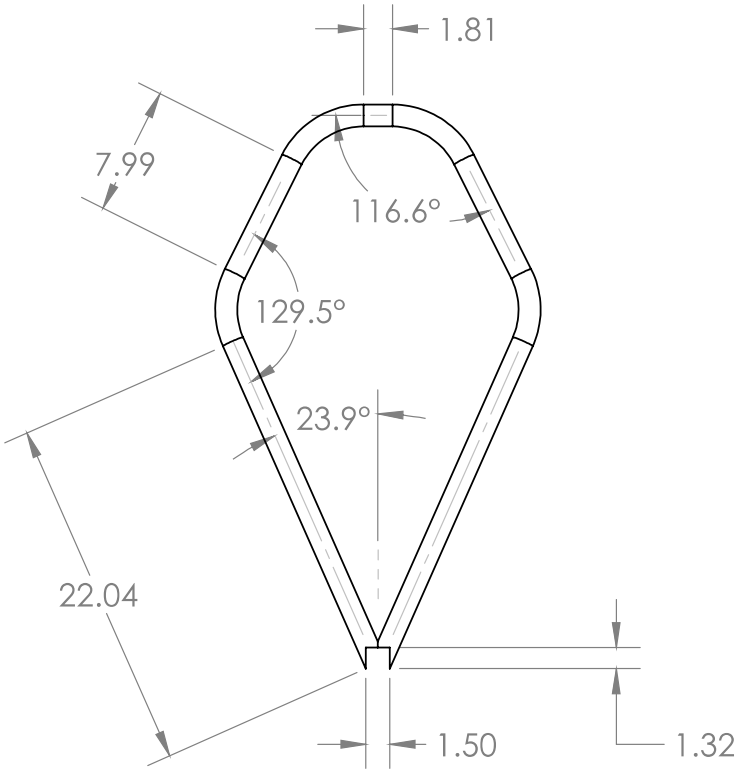

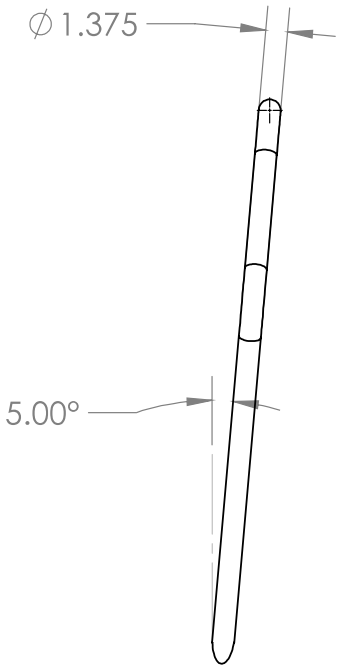

TEAM 9 HUMAN POWERED VEHICLE CHALLENGE

UNLESS OTHERWISE SPECIFIED:
DIMENSIONS ARE IN INCHES
GENERAL SURFACE FINISH 125
TOLERANCES:
FRACTIONAL ±1/16
ANGULAR: ± 0.5°
TWO PLACE DECIMAL ± .03
THREE PLACE DECIMAL ± .005

MATERIAL
6061-T6 (SS)

FINISH

COMMENTS:

DO NOT SCALE DRAWING

DRAWN BY:
KEVIN MONTOYA

TITLE:
FRAME

SIZE
A

DATE DRAWN
12/12/2013

SCALE: 1:12 | WEIGHT: 14.50 lbs | SHEET 14 OF 14

100

5 4 3 2 1

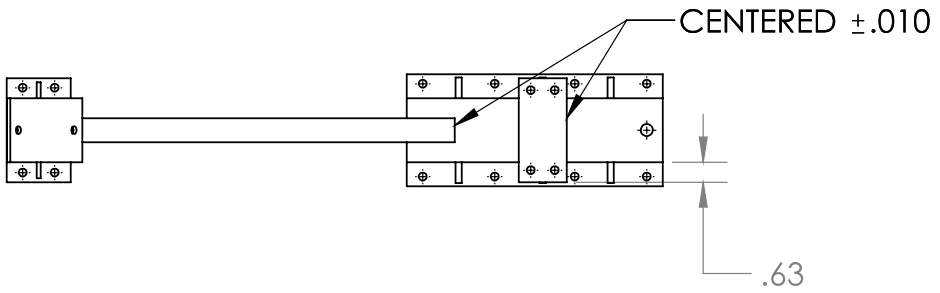

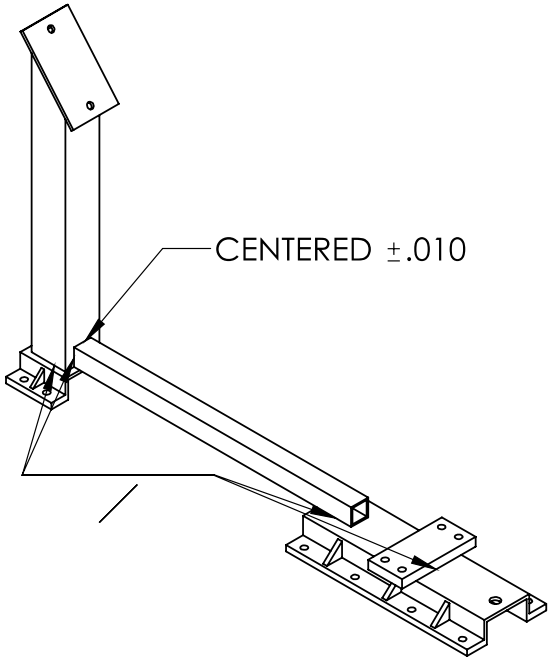

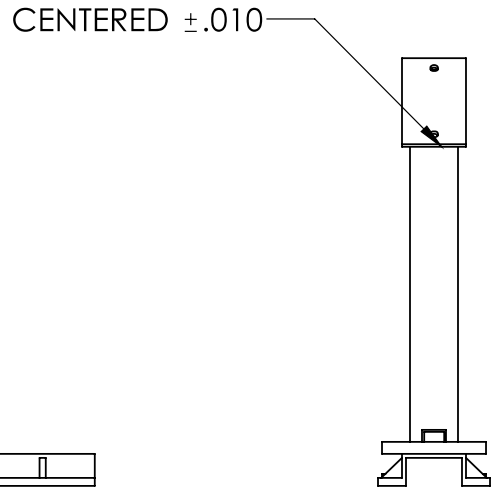

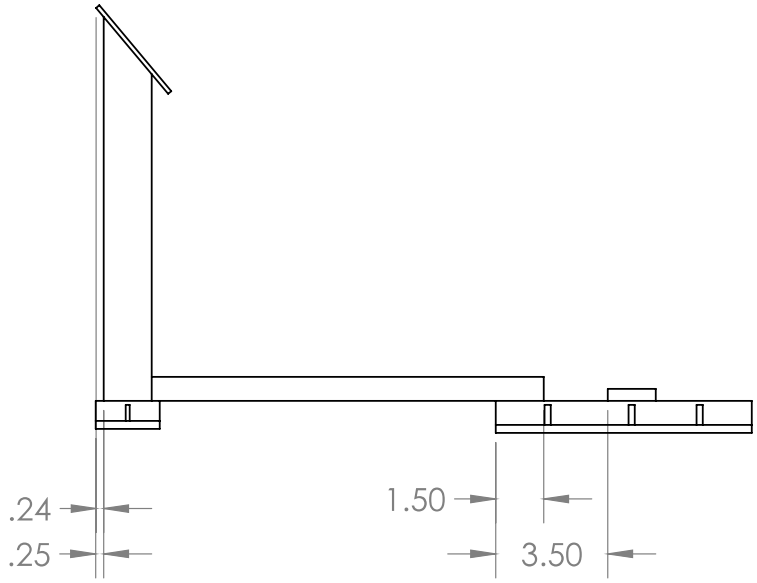

TEAM 9 HUMAN POWERED VEHICLE CHALLENGE

UNLESS OTHERWISE SPECIFIED:
DIMENSIONS ARE IN INCHES
GENERAL SURFACE FINISH 125
TOLERANCES:
FRACTIONAL ±1/16
ANGULAR: ± 0.5°
TWO PLACE DECIMAL ± .03
THREE PLACE DECIMAL ± .005

MATERIAL
6061-T6 (SS)

FINISH

COMMENTS:

DO NOT SCALE DRAWING

DRAWN BY:
KEVIN MONTOYA

TITLE:
SEAT BRACKET

SIZE
A

DATE DRAWN
12/12/2013

SCALE: 1:6 | WEIGHT: 2.02 | SHEET 1 OF 7

101

5 4 3 2 1

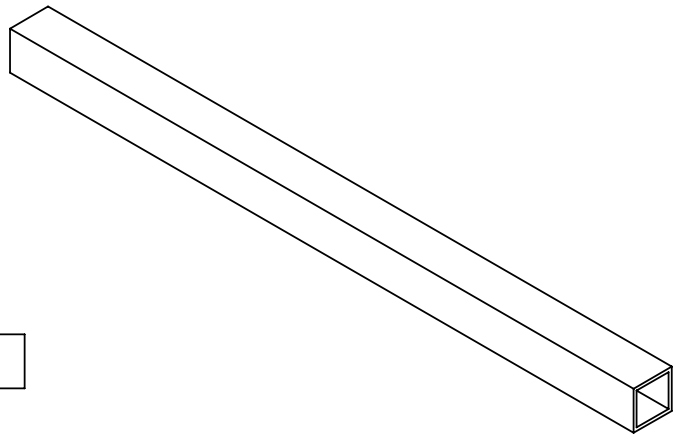

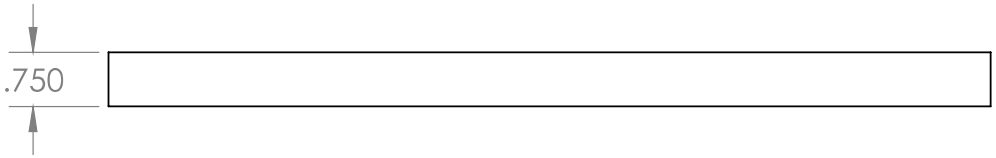

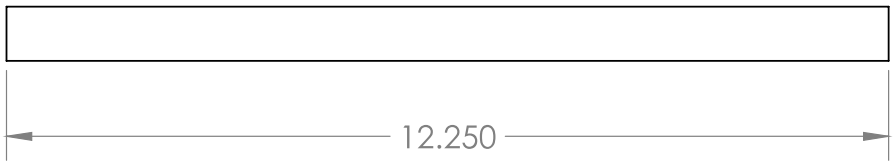

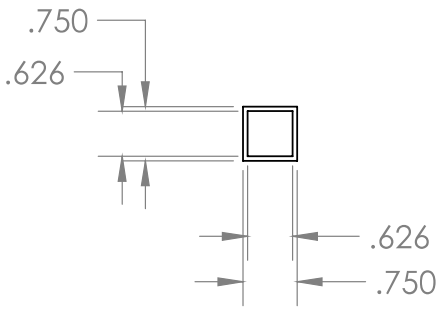

TEAM 9 HUMAN POWERED VEHICLE CHALLENGE

UNLESS OTHERWISE SPECIFIED:
DIMENSIONS ARE IN INCHES
GENERAL SURFACE FINISH 125
TOLERANCES:
FRACTIONAL ±1/16
ANGULAR: ± 0.5°
TWO PLACE DECIMAL ± .03
THREE PLACE DECIMAL ± .005

MATERIAL
6061-T6 (SS)

FINISH

COMMENTS:

DO NOT SCALE DRAWING

DRAWN BY:
KEVIN MONTOYA

TITLE:
SEAT BRACKET

SIZE
A

DATE DRAWN
12/12/2013

SCALE: 3:8

WEIGHT: 2.02

SHEET 2 OF 7

102

5 4 3 2 1

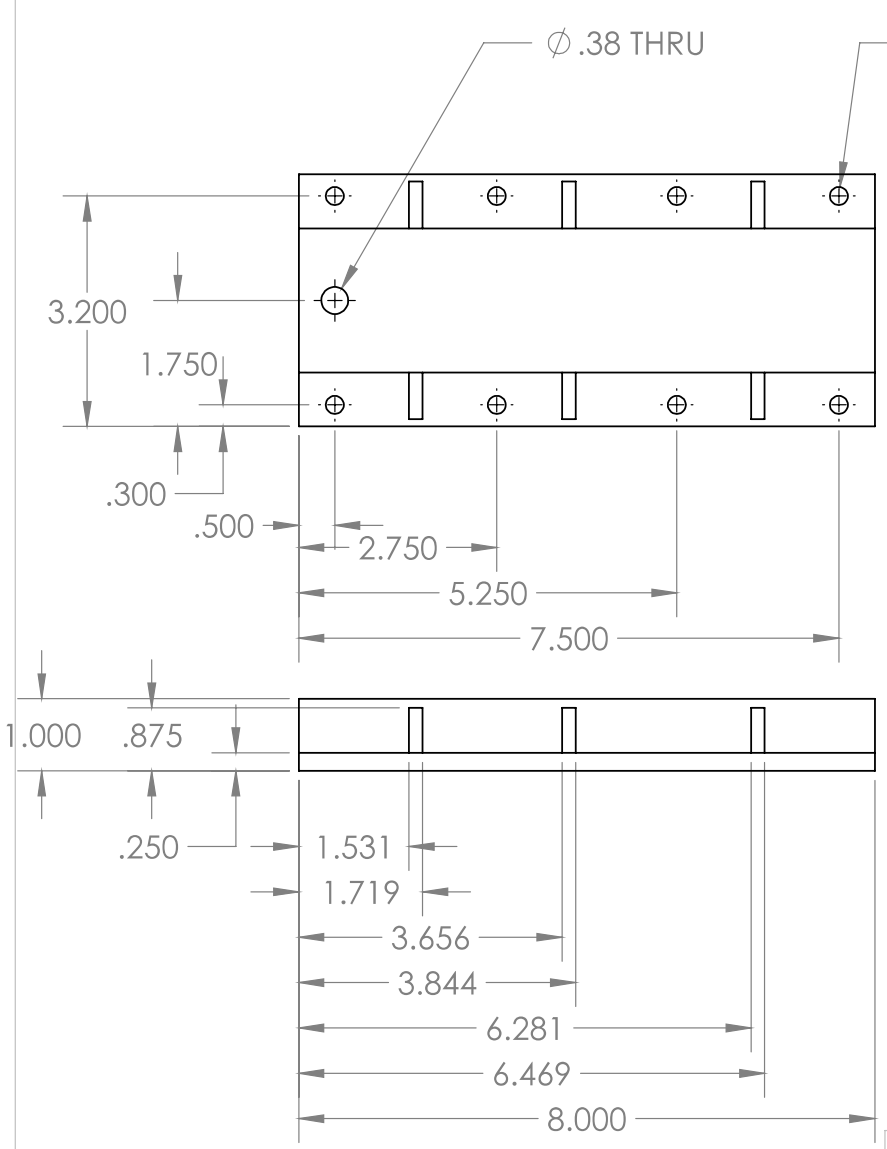

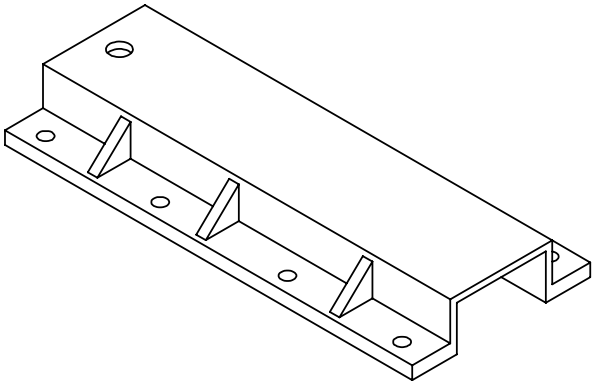

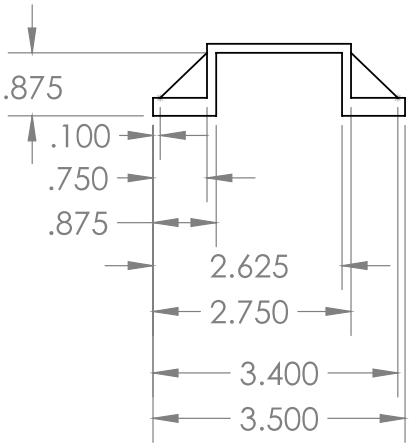

TEAM 9 HUMAN POWERED VEHICLE CHALLENGE

UNLESS OTHERWISE SPECIFIED:
DIMENSIONS ARE IN INCHES
GENERAL SURFACE FINISH 125
TOLERANCES:
FRACTIONAL ±1/16
ANGULAR: ± 0.5°
TWO PLACE DECIMAL ± .03
THREE PLACE DECIMAL ± .005

MATERIAL
6061-T6 (SS)

FINISH

COMMENTS:

DO NOT SCALE DRAWING

DRAWN BY:
KEVIN MONTOYA

TITLE:
SEAT BRACKET

SIZE
A

DATE DRAWN
12/12/2013

SCALE: 3:8

WEIGHT: 2.02

SHEET 3 OF 7

103

5 4 3 2 1

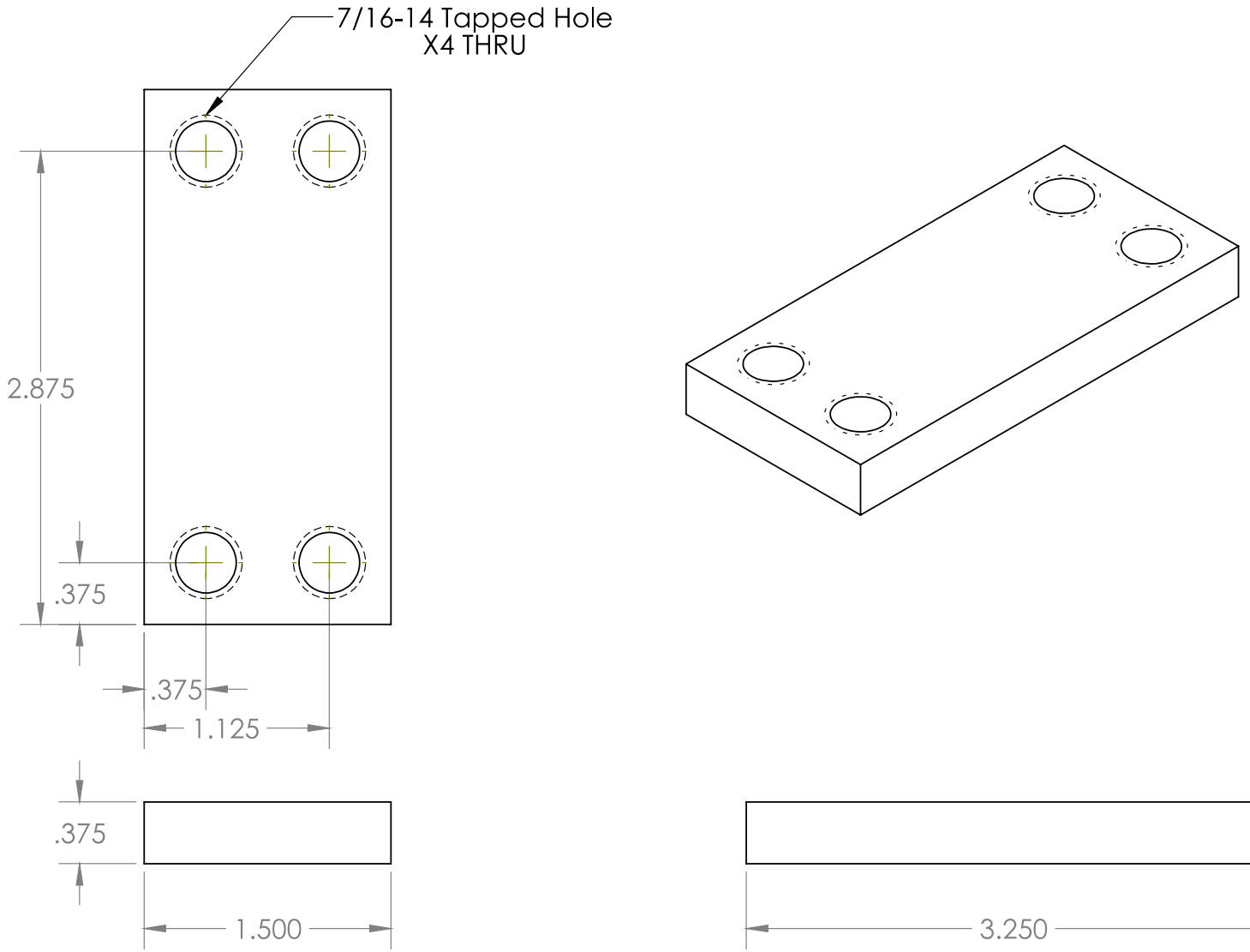

TEAM 9 HUMAN POWERED VEHICLE CHALLENGE

UNLESS OTHERWISE SPECIFIED:
DIMENSIONS ARE IN INCHES
GENERAL SURFACE FINISH 125
TOLERANCES:
FRACTIONAL ±1/16
ANGULAR: ± 0.5°
TWO PLACE DECIMAL ± .03
THREE PLACE DECIMAL ± .005

MATERIAL
6061-T6 (SS)

FINISH

COMMENTS:

DO NOT SCALE DRAWING

DRAWN BY:
KEVIN MONTOYA

TITLE:
SEAT BRACKET

SIZE
A

DATE DRAWN
12/12/2013

SCALE: 1:1

WEIGHT: 2.02

SHEET 4 OF 7

104

5 4 3 2 1

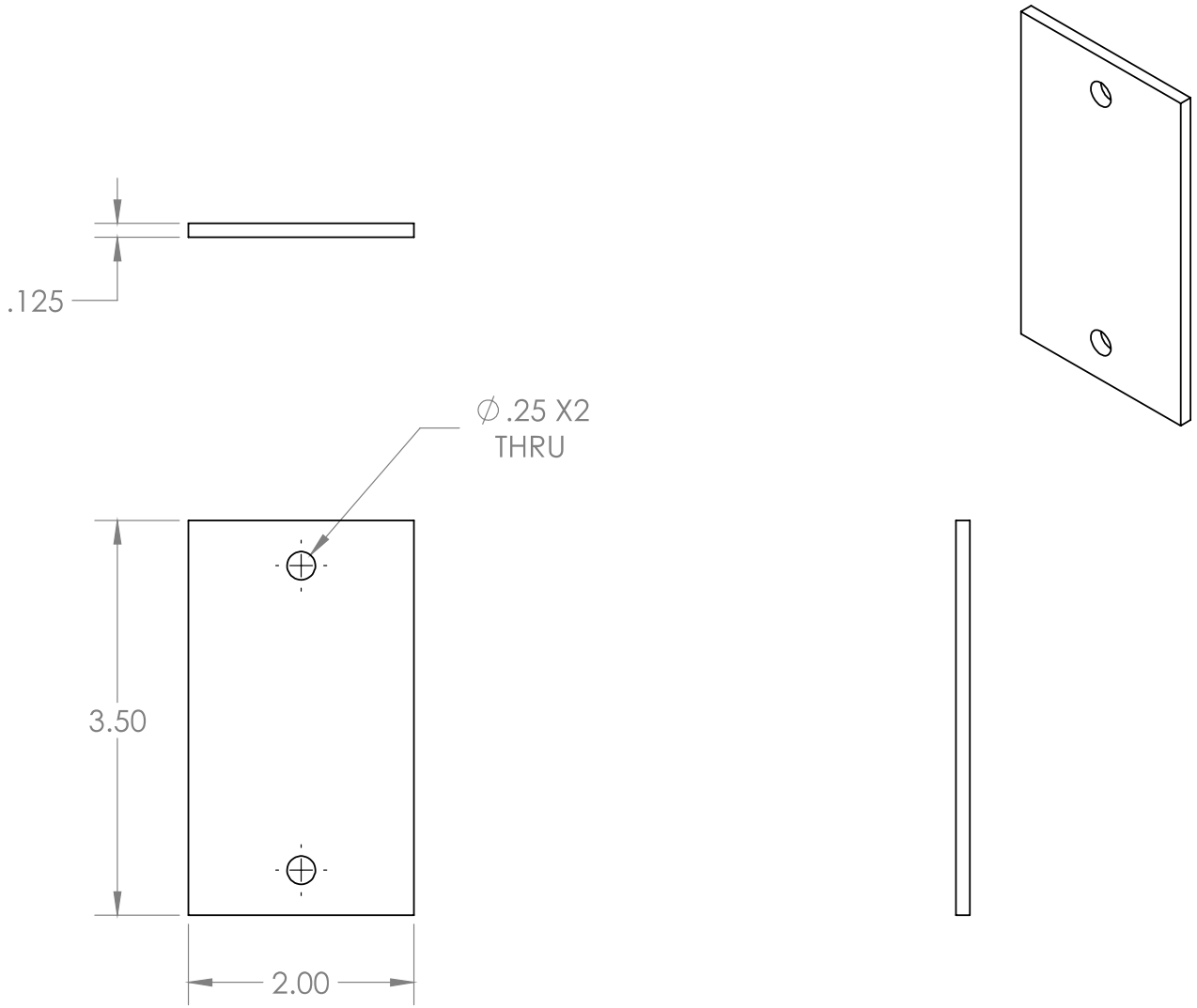

TEAM 9 HUMAN POWERED VEHICLE CHALLENGE

UNLESS OTHERWISE SPECIFIED: DIMENSIONS ARE IN INCHES GENERAL SURFACE FINISH 125 TOLERANCES: FRACTIONAL ±1/16 ANGULAR: ± 0.5° TWO PLACE DECIMAL ± .03 THREE PLACE DECIMAL ± .005	COMMENTS:	DRAWN BY: KEVIN MONTOYA	
		TITLE: SEAT BRACKET	
		SIZE A	DATE DRAWN 12/12/2013
MATERIAL 6061-T6 (SS)			
FINISH	DO NOT SCALE DRAWING	SCALE: 5:8	WEIGHT: 2.02 / SHEET 5 OF 7

105

5 4 3 2 1

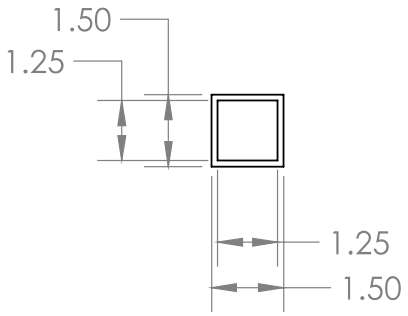

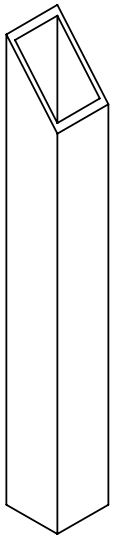

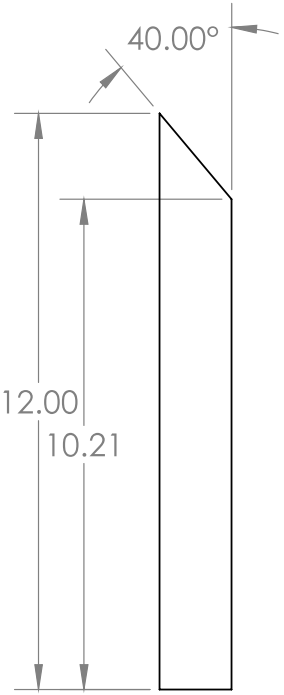

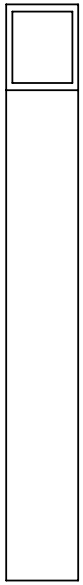

TEAM 9 HUMAN POWERED VEHICLE CHALLENGE

UNLESS OTHERWISE SPECIFIED:
DIMENSIONS ARE IN INCHES
GENERAL SURFACE FINISH 125
TOLERANCES:
FRACTIONAL ±1/16
ANGULAR: ± 0.5°
TWO PLACE DECIMAL ± .03
THREE PLACE DECIMAL ± .005

MATERIAL
6061-T6 (SS)

FINISH

COMMENTS:

DO NOT SCALE DRAWING

DRAWN BY:
KEVIN MONTOYA

TITLE:
SEAT BRACKET

SIZE
A

DATE DRAWN
12/12/2013

SCALE: 1:4

WEIGHT: 2.02

SHEET 6 OF 7

106

5 4 3 2 1

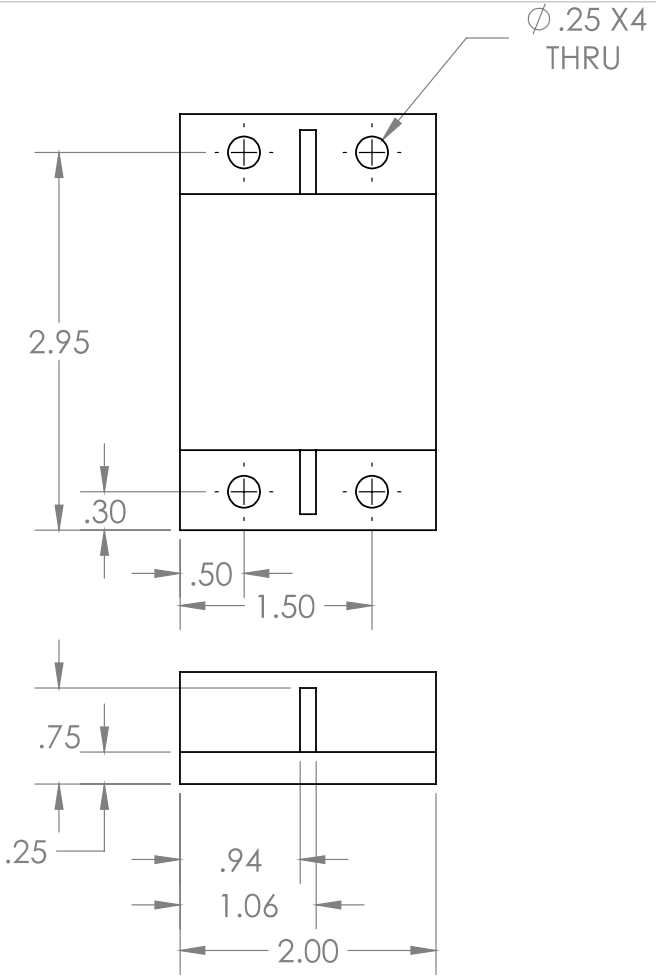

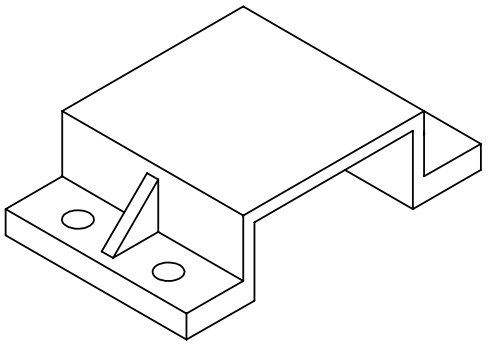

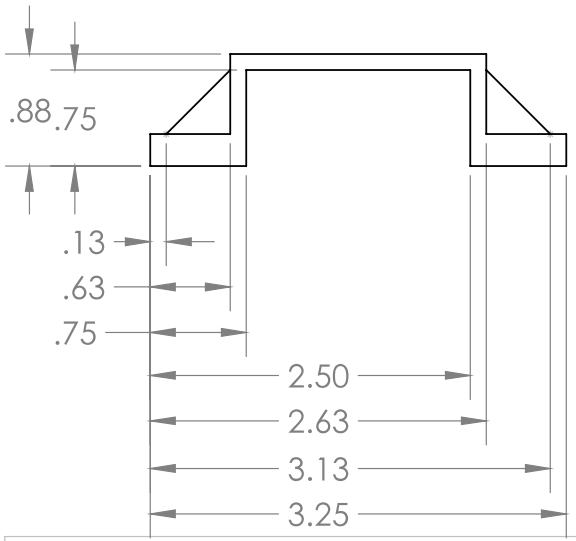

TEAM 9 HUMAN POWERED VEHICLE CHALLENGE

UNLESS OTHERWISE SPECIFIED:
DIMENSIONS ARE IN INCHES
GENERAL SURFACE FINISH 125
TOLERANCES:
FRACTIONAL ±1/16
ANGULAR: ± 0.5°
TWO PLACE DECIMAL ± .03
THREE PLACE DECIMAL ± .005

MATERIAL
6061-T6 (SS)

FINISH

COMMENTS:

DO NOT SCALE DRAWING

DRAWN BY:
KEVIN MONTOYA

TITLE:
SEAT BRACKET

SIZE
A

DATE DRAWN
12/12/2013

SCALE: 2:3

WEIGHT: 2.02

SHEET 7 OF 7

107

5 4 3 2 1

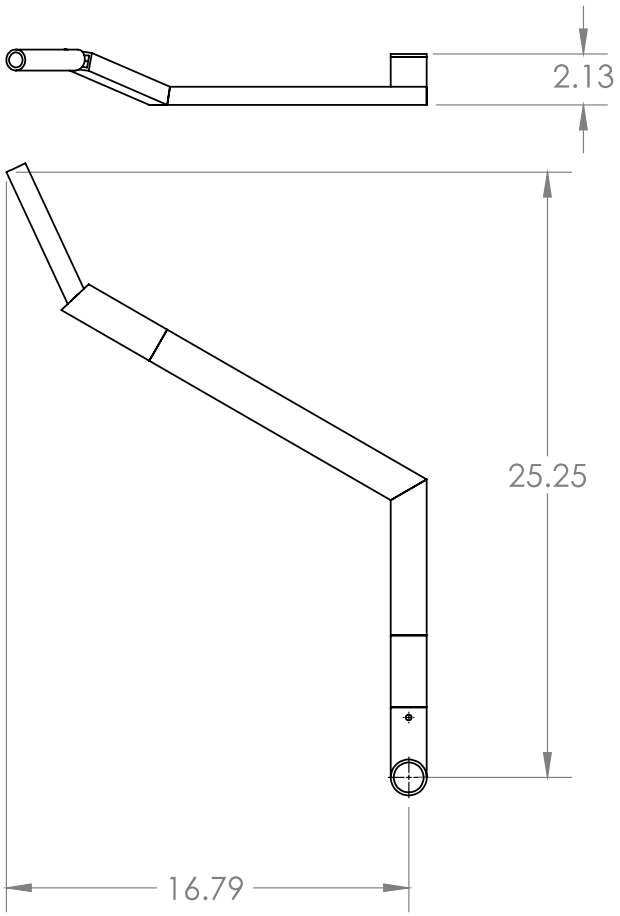

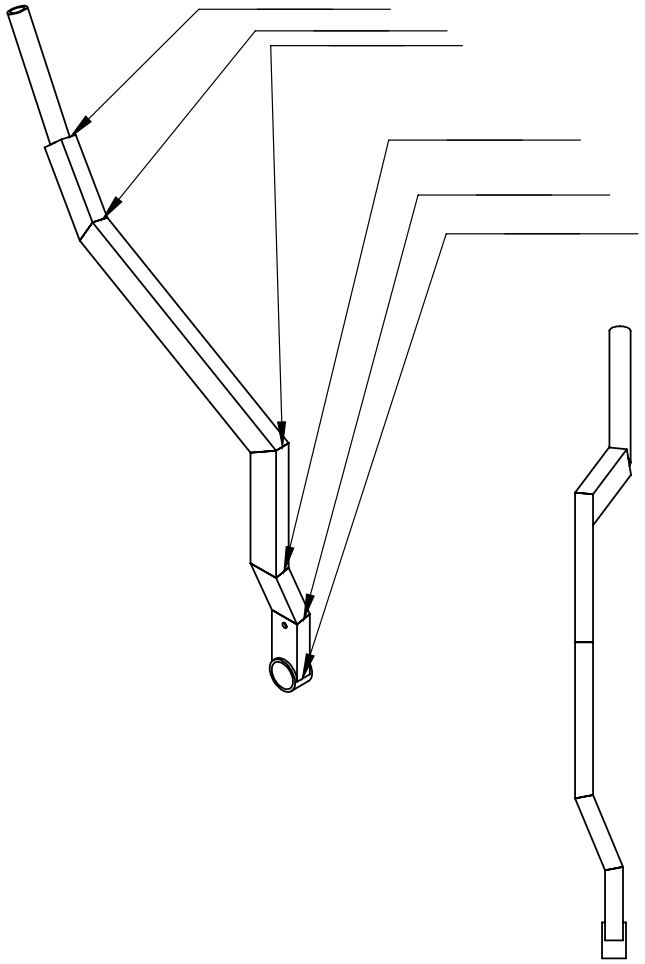

TEAM 9 HUMAN POWERED VEHICLE CHALLENGE

UNLESS OTHERWISE SPECIFIED:
DIMENSIONS ARE IN INCHES
GENERAL SURFACE FINISH 125
TOLERANCES:
FRACTIONAL ±1/16
ANGULAR: ± 0.5°
TWO PLACE DECIMAL ± .03
THREE PLACE DECIMAL ± .005

MATERIAL
6061-T6 (SS)

FINISH

COMMENTS:

DO NOT SCALE DRAWING

DRAWN BY:
KEVIN MONTOYA

TITLE:
STEERING ARMS

SIZE
A

DATE DRAWN
12/12/2013

SCALE: 1:8 | WEIGHT: 1.59 lbs | SHEET 1 OF 9

108

5 4 3 2 1

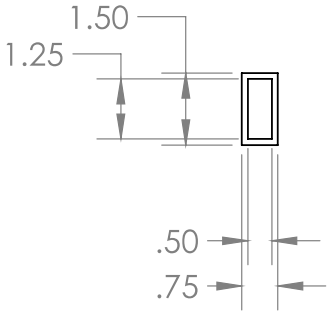

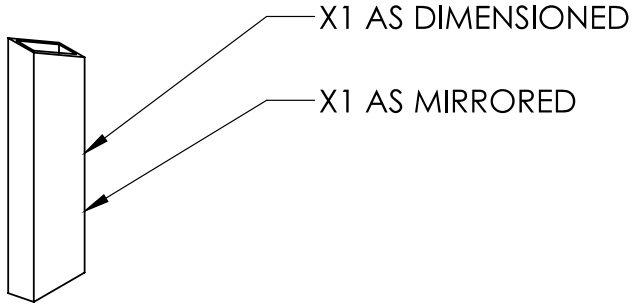

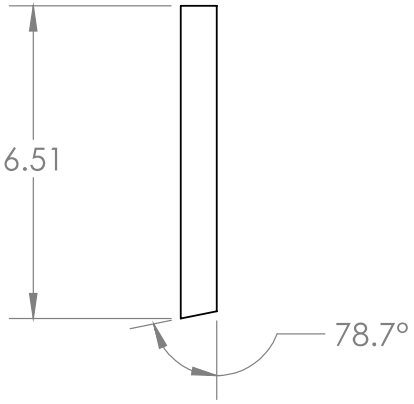

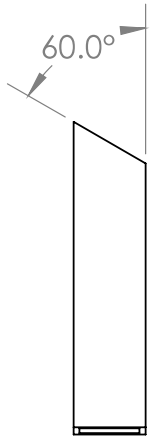

TEAM 9 HUMAN POWERED VEHICLE CHALLENGE

UNLESS OTHERWISE SPECIFIED:
DIMENSIONS ARE IN INCHES
GENERAL SURFACE FINISH 125
TOLERANCES:
FRACTIONAL ±1/16
ANGULAR: ± 0.5°
TWO PLACE DECIMAL ± .03
THREE PLACE DECIMAL ± .005

MATERIAL
6061-T6 (SS)

FINISH

COMMENTS:

DO NOT SCALE DRAWING

DRAWN BY:
KEVIN MONTOYA

TITLE:
STEERING ARMS

SIZE
A

DATE DRAWN
12/12/2013

SCALE: 1:4 | WEIGHT: 1.59 lbs | SHEET 2 OF 9

5 4 3 2 1

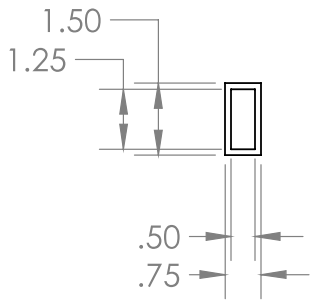

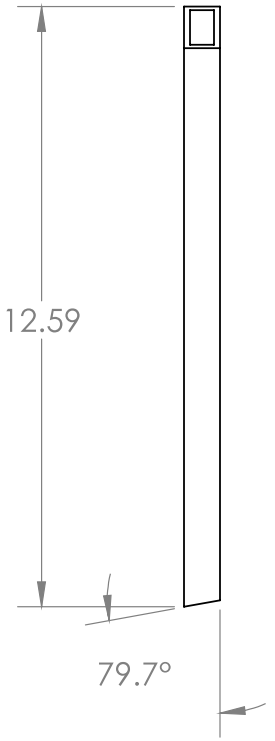

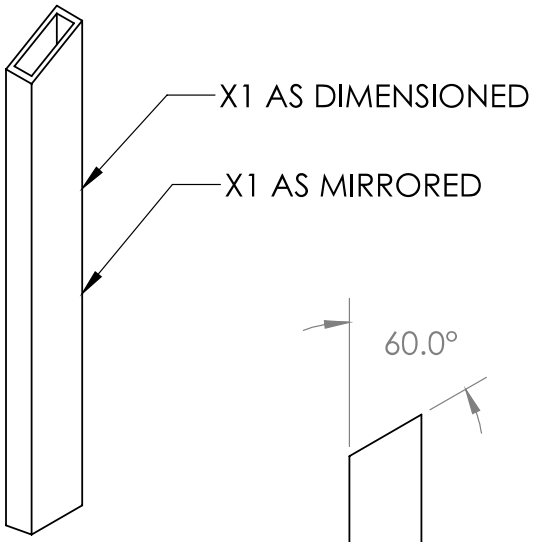

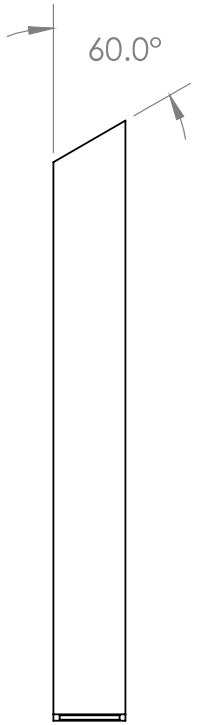

TEAM 9 HUMAN POWERED VEHICLE CHALLENGE

UNLESS OTHERWISE SPECIFIED:
DIMENSIONS ARE IN INCHES
GENERAL SURFACE FINISH 125
TOLERANCES:
FRACTIONAL ±1/16
ANGULAR: ± 0.5°
TWO PLACE DECIMAL ± .03
THREE PLACE DECIMAL ± .005

MATERIAL
6061-T6 (SS)

FINISH

COMMENTS:

DO NOT SCALE DRAWING

DRAWN BY:
KEVIN MONTOYA

TITLE:
STEERING ARMS

SIZE
A

DATE DRAWN
12/12/2013

SCALE: 1:4 | WEIGHT: 1.59 lbs | SHEET 3 OF 9

110

5 4 3 2 1

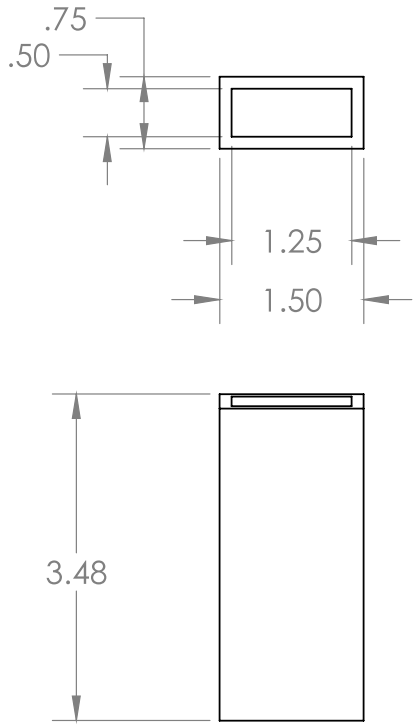

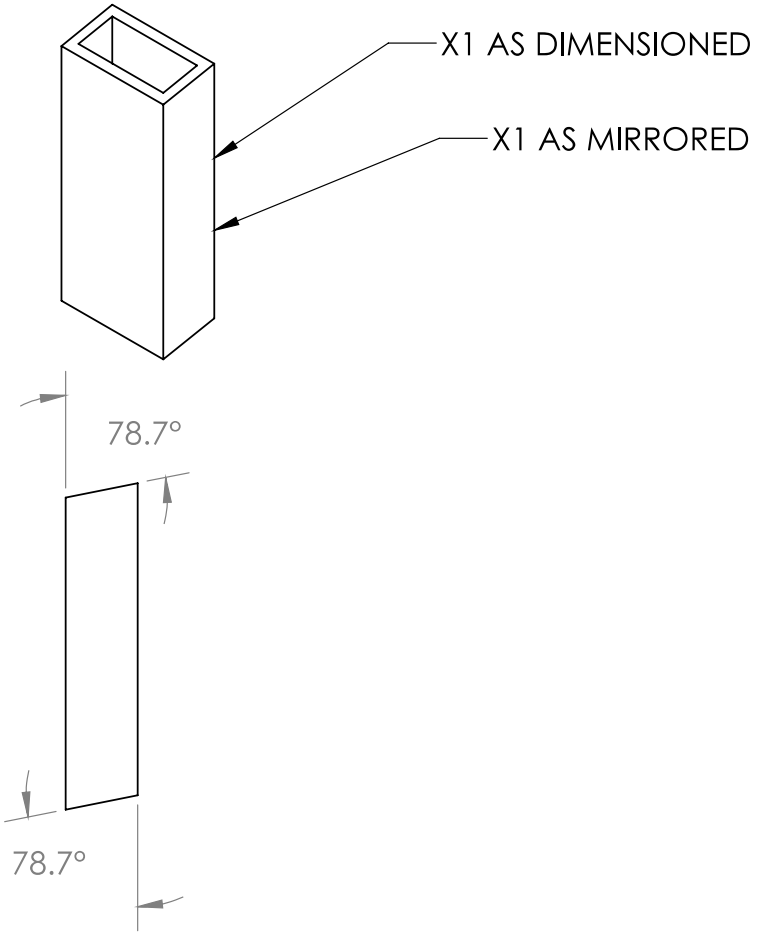

TEAM 9 HUMAN POWERED VEHICLE CHALLENGE

UNLESS OTHERWISE SPECIFIED:
DIMENSIONS ARE IN INCHES
GENERAL SURFACE FINISH 125
TOLERANCES:
FRACTIONAL ±1/16
ANGULAR: ± 0.5°
TWO PLACE DECIMAL ± .03
THREE PLACE DECIMAL ± .005

MATERIAL
6061-T6 (SS)

FINISH

COMMENTS:

DO NOT SCALE DRAWING

DRAWN BY:
KEVIN MONTOYA

TITLE:
STEERING ARMS

SIZE
A

DATE DRAWN
12/12/2013

SCALE: 1:2 | WEIGHT: 1.59 lbs | SHEET 4 OF 9

111

5 4 3 2 1

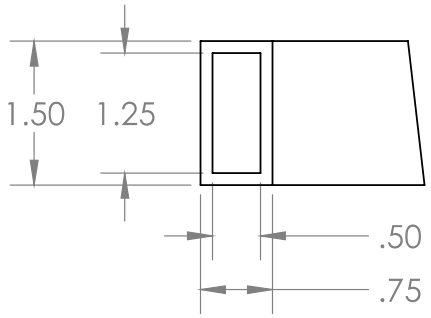

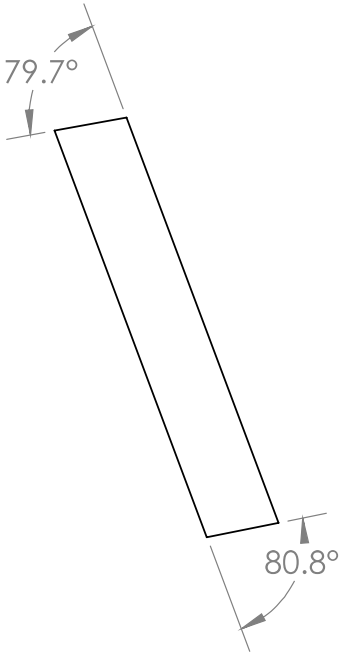

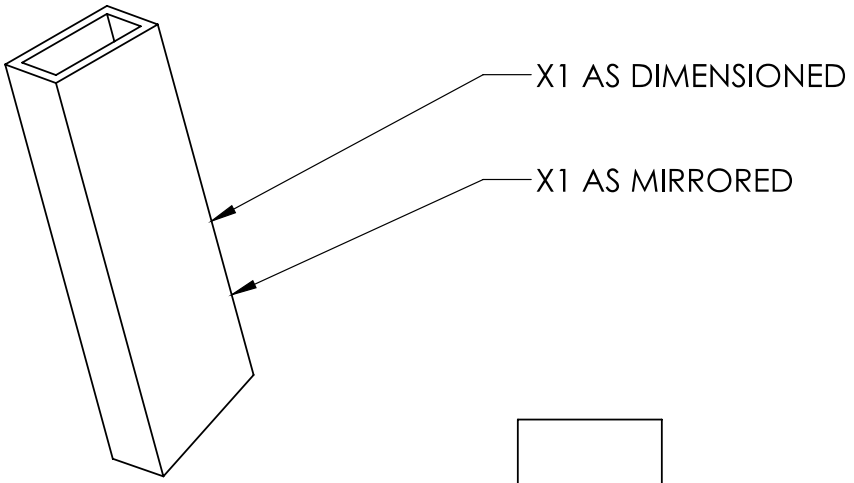

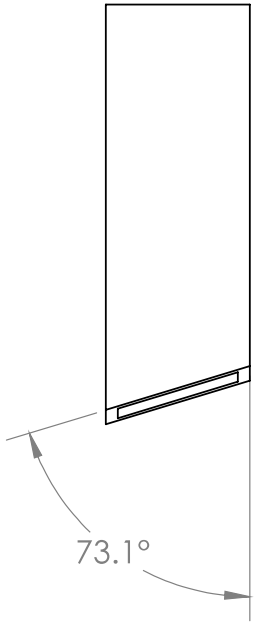

TEAM 9 HUMAN POWERED VEHICLE CHALLENGE

UNLESS OTHERWISE SPECIFIED:
DIMENSIONS ARE IN INCHES
GENERAL SURFACE FINISH 125
TOLERANCES:
FRACTIONAL ±1/16
ANGULAR: ± 0.5°
TWO PLACE DECIMAL ± .03
THREE PLACE DECIMAL ± .005

MATERIAL
6061-T6 (SS)

FINISH

COMMENTS:

DO NOT SCALE DRAWING

DRAWN BY:
KEVIN MONTOYA

TITLE:
STEERING ARMS

SIZE
A

DATE DRAWN
12/12/2013

SCALE: 1:2

WEIGHT: 1.59 lbs

SHEET 5 OF 9

112

5 4 3 2 1

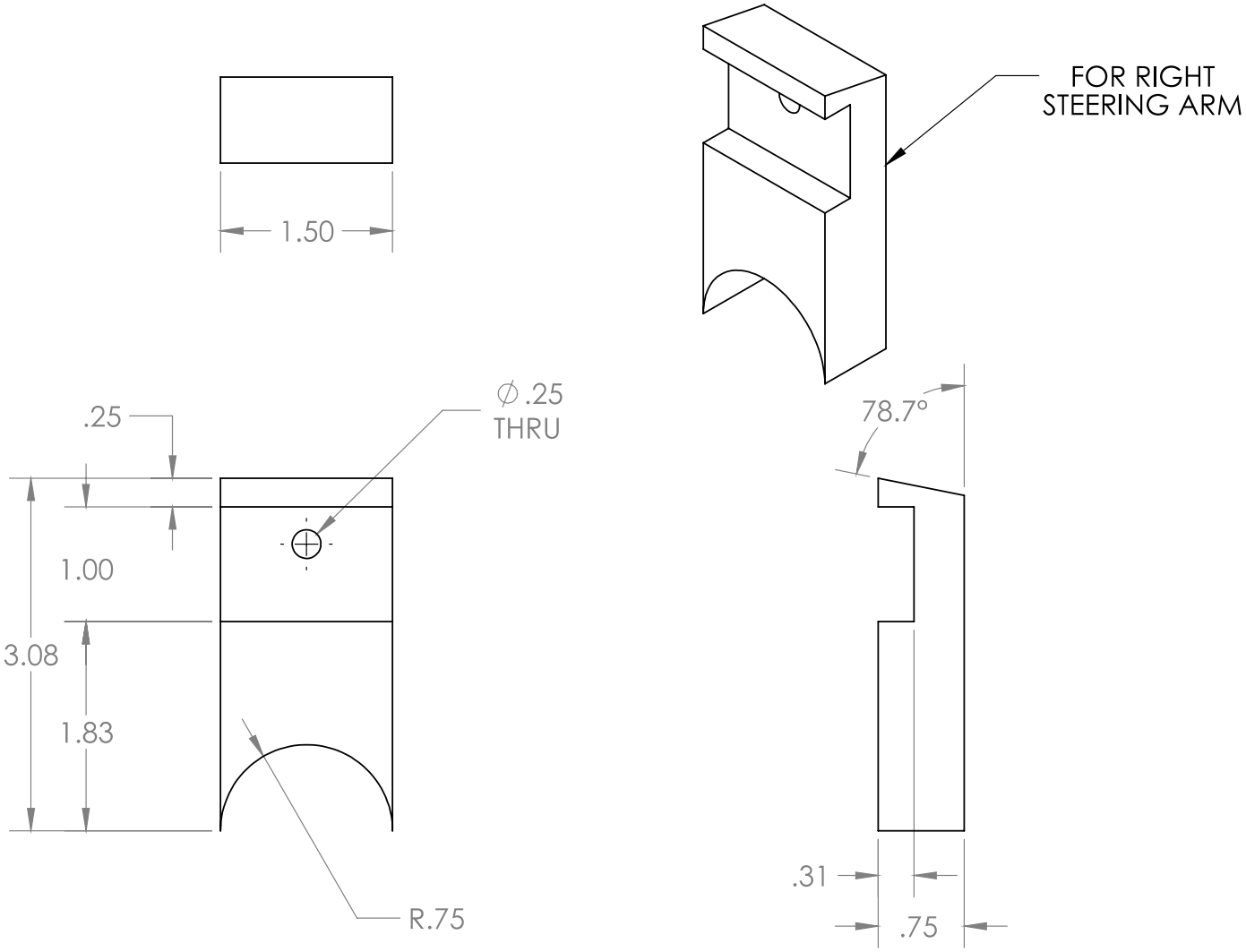

TEAM 9 HUMAN POWERED VEHICLE CHALLENGE

UNLESS OTHERWISE SPECIFIED:
DIMENSIONS ARE IN INCHES
GENERAL SURFACE FINISH 125
TOLERANCES:
FRACTIONAL ±1/16
ANGULAR: ± 0.5°
TWO PLACE DECIMAL ± .03
THREE PLACE DECIMAL ± .005

MATERIAL
6061-T6 (SS)

FINISH

COMMENTS:

DO NOT SCALE DRAWING

DRAWN BY:
KEVIN MONTOYA

TITLE:
STEERING ARMS

SIZE
A

DATE DRAWN
12/12/2013

SCALE: 2:3

WEIGHT: 1.59 lbs

SHEET 6 OF 9

5 4 3 2 1

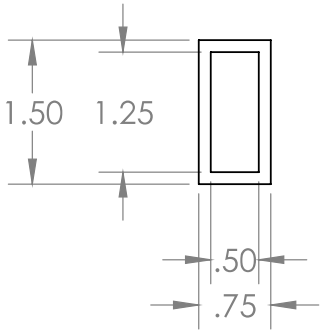

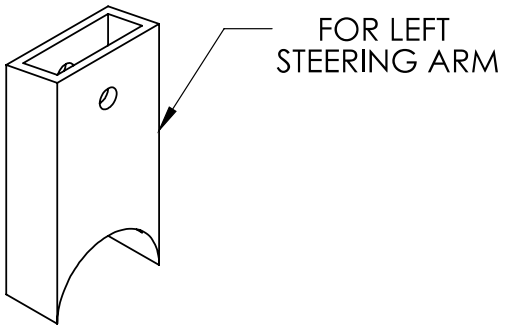

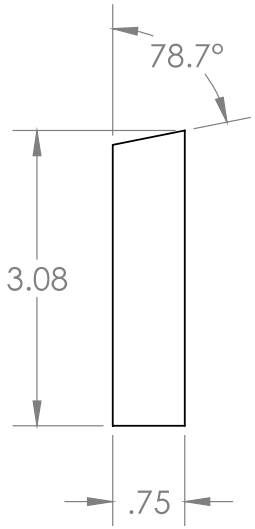

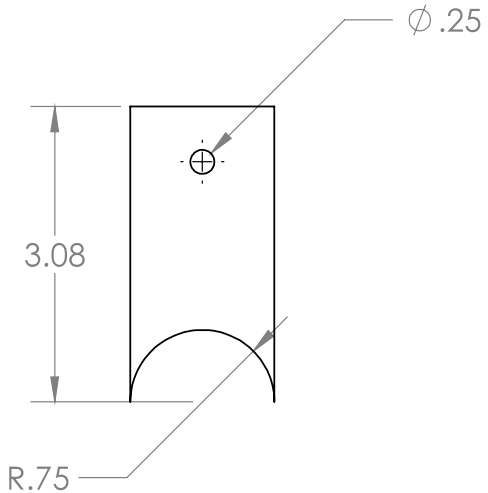

TEAM 9 HUMAN POWERED VEHICLE CHALLENGE

UNLESS OTHERWISE SPECIFIED:
DIMENSIONS ARE IN INCHES
GENERAL SURFACE FINISH 125
TOLERANCES:
FRACTIONAL ±1/16
ANGULAR: ± 0.5°
TWO PLACE DECIMAL ± .03
THREE PLACE DECIMAL ± .005

MATERIAL
6061-T6 (SS)

FINISH

COMMENTS:

DO NOT SCALE DRAWING

DRAWN BY:
KEVIN MONTOYA

TITLE:
STEERING ARMS

SIZE
A

DATE DRAWN
12/12/2013

SCALE: 1:2 | WEIGHT: 1.59 lbs | SHEET 7 OF 9

5 4 3 2 1

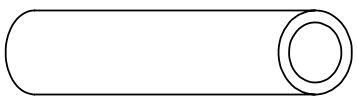

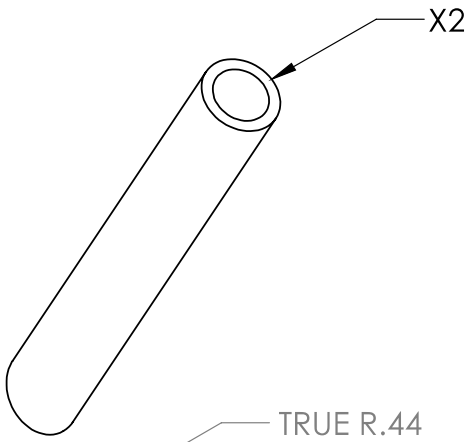

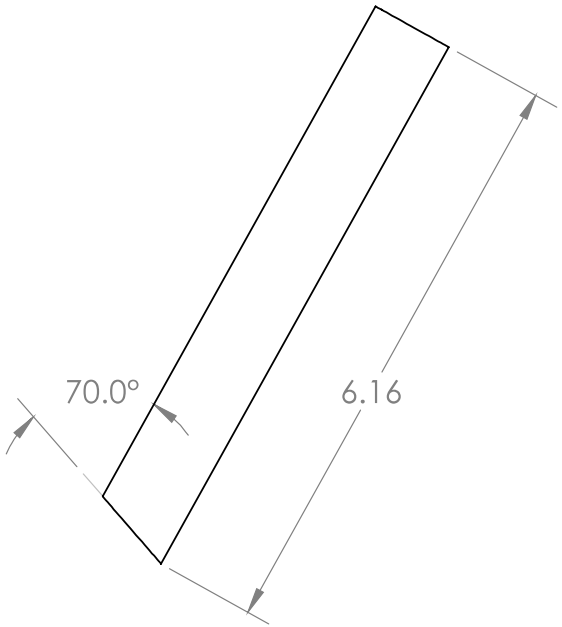

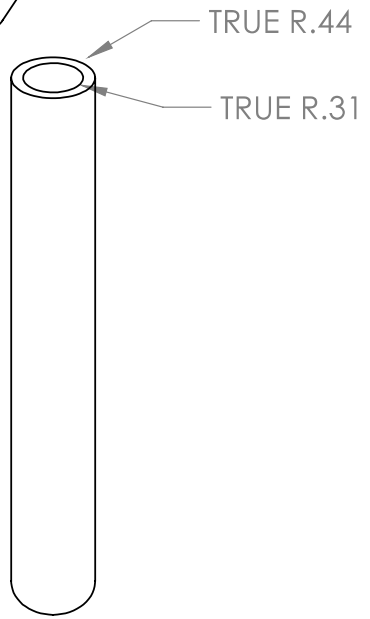

TEAM 9 HUMAN POWERED VEHICLE CHALLENGE

UNLESS OTHERWISE SPECIFIED:
DIMENSIONS ARE IN INCHES
GENERAL SURFACE FINISH 125
TOLERANCES:
FRACTIONAL ±1/16
ANGULAR: ± 0.5°
TWO PLACE DECIMAL ± .03
THREE PLACE DECIMAL ± .005

MATERIAL
6061-T6 (SS)

FINISH

COMMENTS:

DO NOT SCALE DRAWING

DRAWN BY:
KEVIN MONTOYA

TITLE:
STEERING ARMS

SIZE
A

DATE DRAWN
12/12/2013

SCALE: 1:2 | WEIGHT: 1.59 lbs | SHEET 8 OF 9

115

5 4 3 2 1

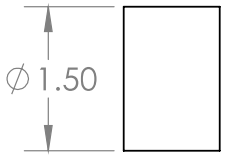

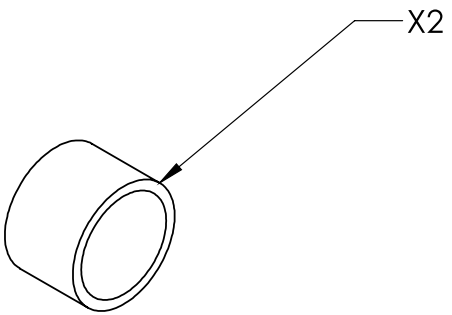

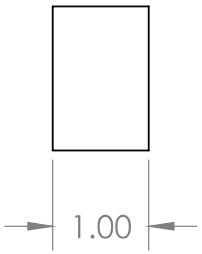

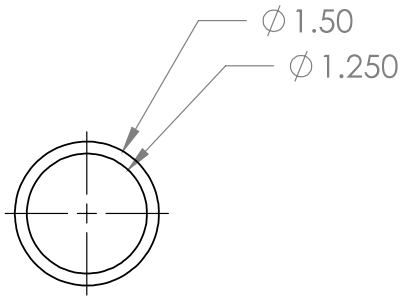

TEAM 9 HUMAN POWERED VEHICLE CHALLENGE

UNLESS OTHERWISE SPECIFIED:
DIMENSIONS ARE IN INCHES
GENERAL SURFACE FINISH 125
TOLERANCES:
FRACTIONAL ±1/16
ANGULAR: ± 0.5°
TWO PLACE DECIMAL ± .03
THREE PLACE DECIMAL ± .005

MATERIAL
6061-T6 (SS)

FINISH

COMMENTS:

DO NOT SCALE DRAWING

DRAWN BY:
KEVIN MONTOYA

TITLE:
STEERING ARMS

SIZE
A

DATE DRAWN
12/12/2013

SCALE: 1:2 | WEIGHT: 1.59 lbs | SHEET 9 OF 9

5 4 3 2 1

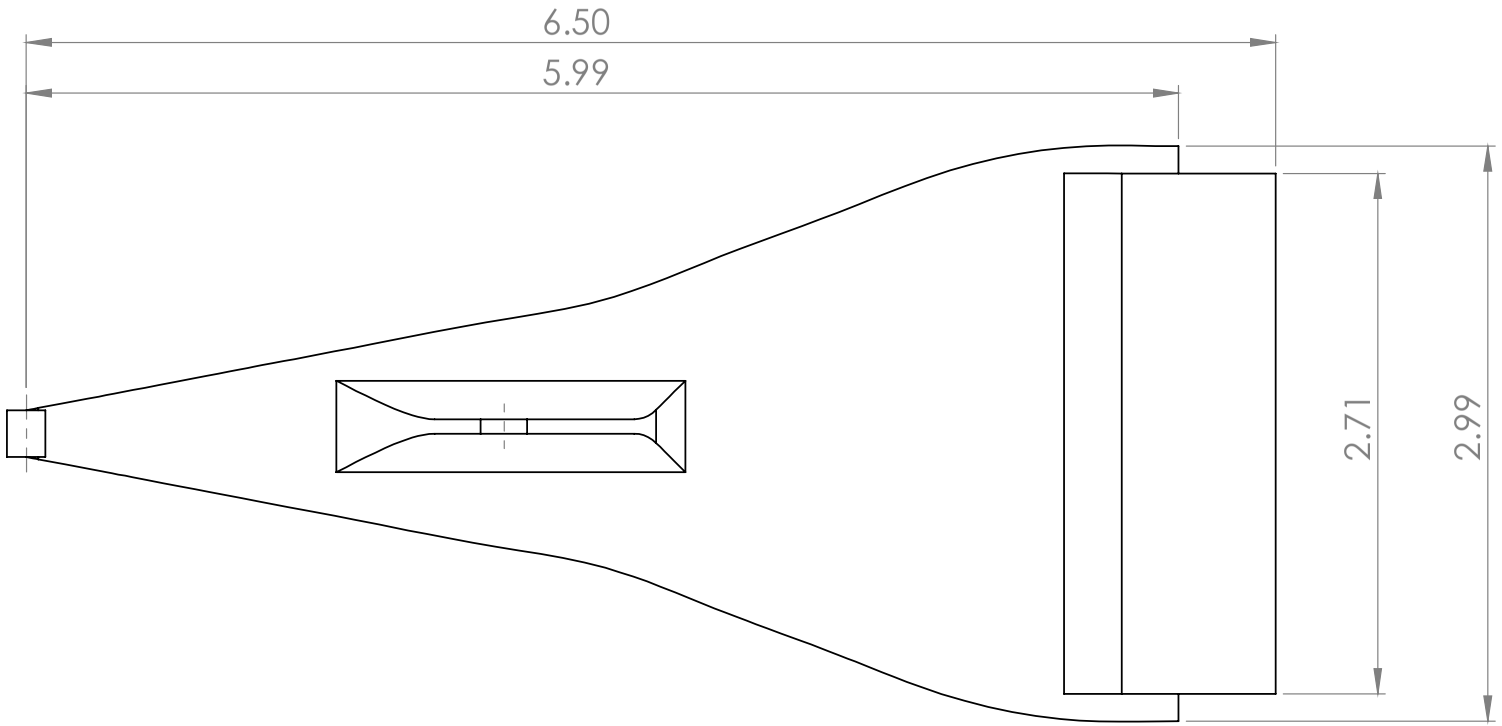

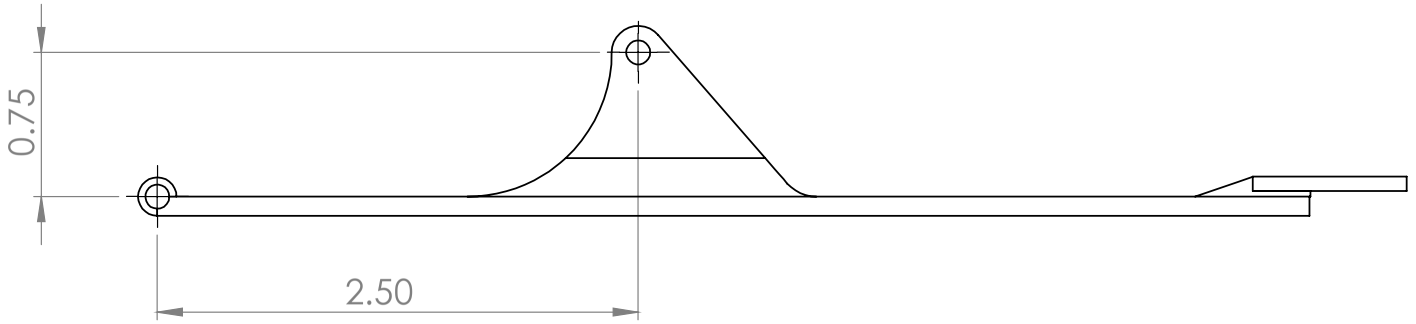

TEAM 9 HUMAN POWERED VEHICLE CHALLENGE

UNLESS OTHERWISE SPECIFIED:
DIMENSIONS ARE IN INCHES
GENERAL SURFACE FINISH 125
TOLERANCES:
FRACTIONAL ±1/16
ANGULAR: ± 0.5°
TWO PLACE DECIMAL ± .03
THREE PLACE DECIMAL ± .005

MATERIAL
ABS

FINISH

COMMENTS:
FDM Rapid Prototyped Part

DO NOT SCALE DRAWING

DRAWN BY: Erik Nelson

TITLE: Closing Duct Flap

SIZE **A**

DATE DRAWN 12/8/2013

SCALE: 1:1 | WEIGHT: 0.05 | SHEET 1 OF 1

117

5 4 3 2 1

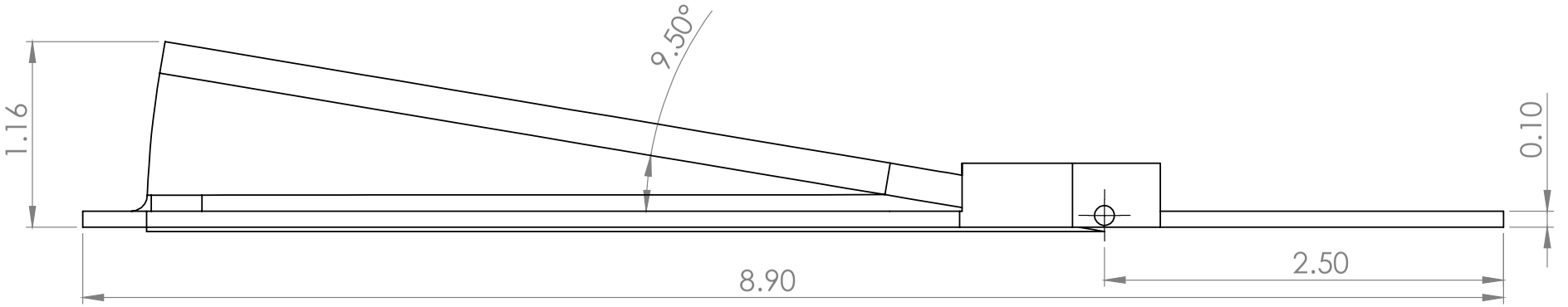

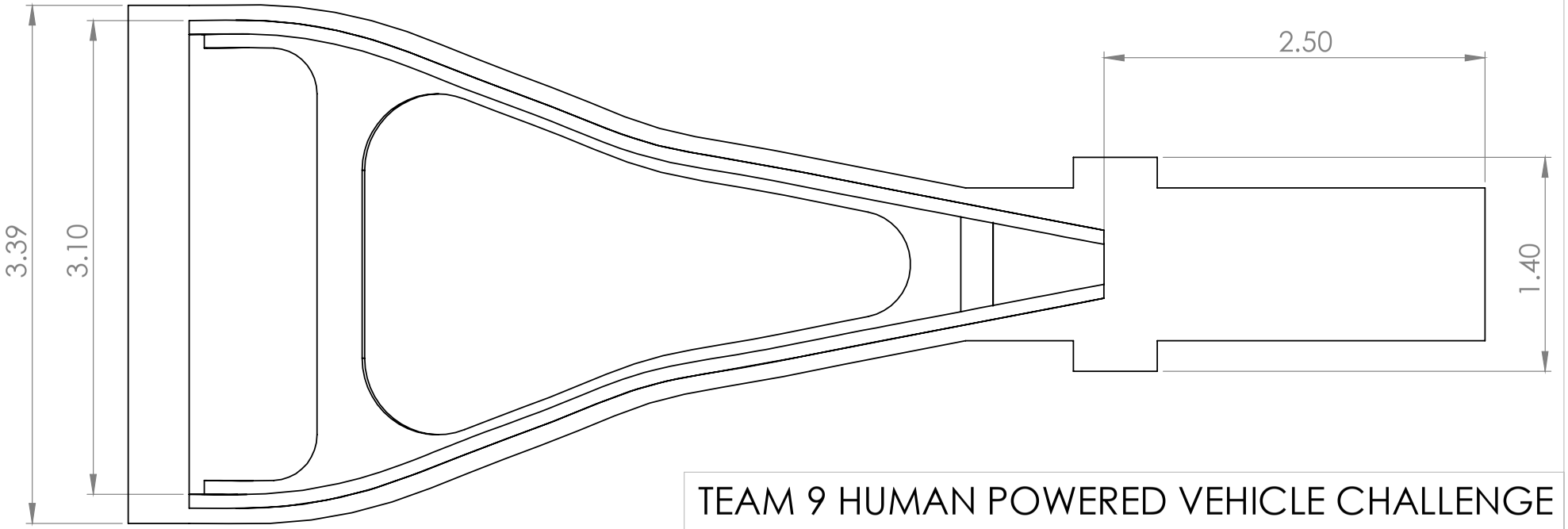

TEAM 9 HUMAN POWERED VEHICLE CHALLENGE

UNLESS OTHERWISE SPECIFIED:
DIMENSIONS ARE IN INCHES
GENERAL SURFACE FINISH 125
TOLERANCES:
FRACTIONAL ±1/16
ANGULAR: ± 0.5°
TWO PLACE DECIMAL ± .03
THREE PLACE DECIMAL ± .005

MATERIAL
ABS

FINISH

COMMENTS:
FDM Rapid Prototyped Part

DO NOT SCALE DRAWING

DRAWN BY:
Erik Nelson

TITLE:
Closing Duct Frame

SIZE
A

DATE DRAWN
12/8/2013

SCALE: 1:1

WEIGHT: 0.07

SHEET 1 OF 1

118

5 4 3 2 1

APPENDIX B – PROJECT PLANNING

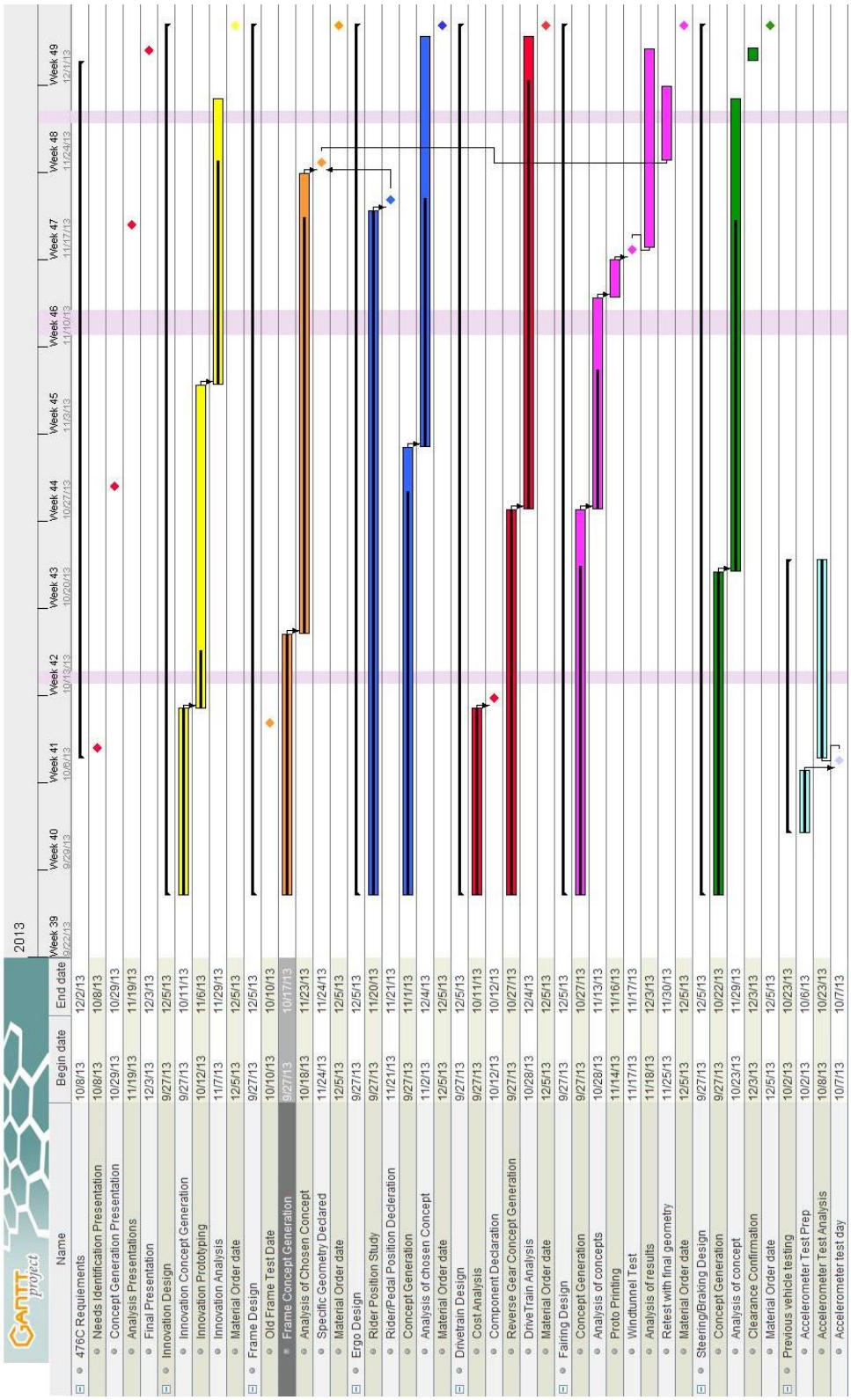

Fall Gantt Chart

Spring Gantt Chart

APPENDIX C – ANALYSIS DATA

ACCELEROMETER DATA

- Test 1 is a run at low speed towards two .75inch tall wood slats - accelerometers on rear axle the maximum applied force for test 1 is 222.5 LBS
- Test 2 is a run at high speed towards two .75inch tall wood slats - accelerometers on rear axle the maximum applied force for test 2 is 243.8 LBS
- Test 3 is a run at high speed towards two .75inch tall wood slats - accelerometers on front axle the maximum applied force for test 3 is 271.8 LBS
- Test 4 is a run at high speed towards two .75inch tall wood slats - accelerometers on mid belly of bike the maximum applied force for test 4 is 182.6 LBS

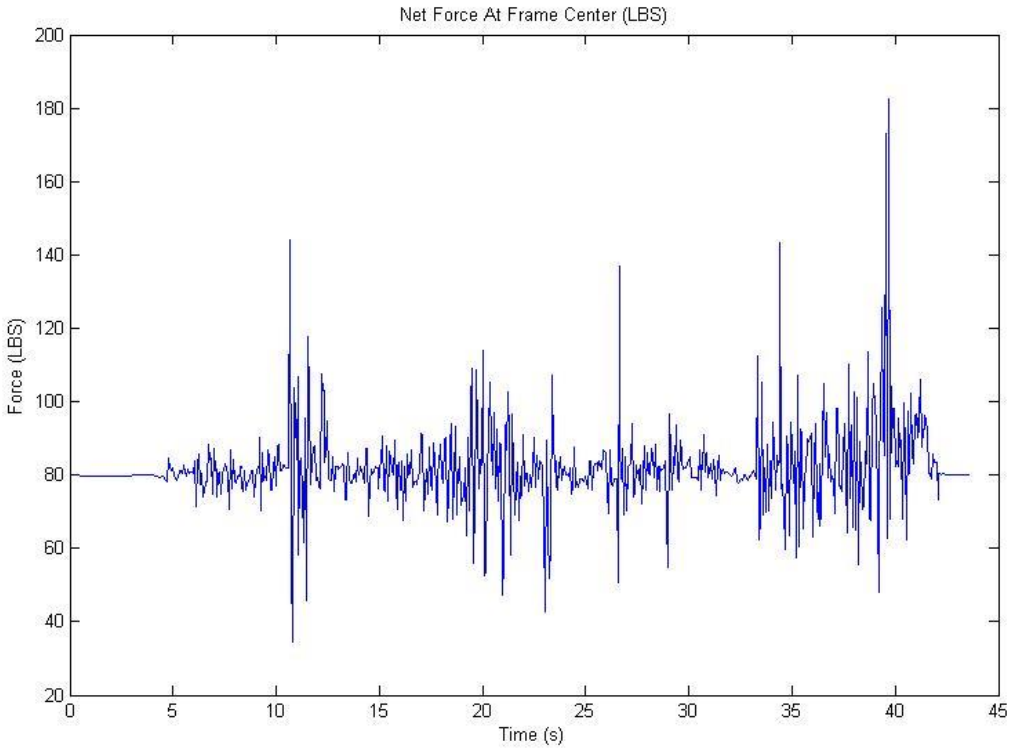

Force on Center Tube

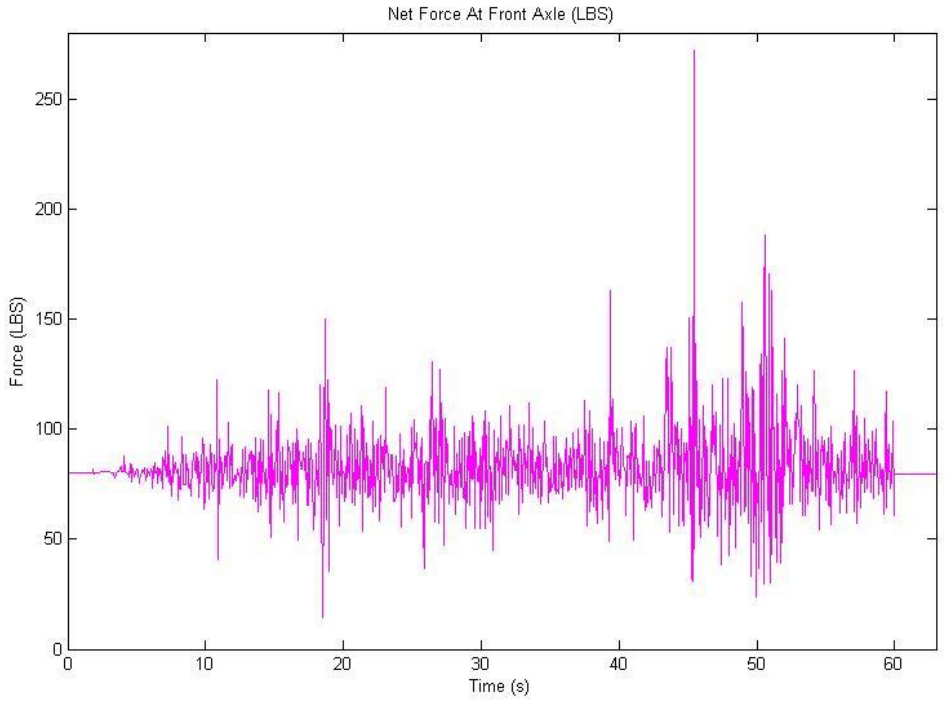

Force on Front Axle

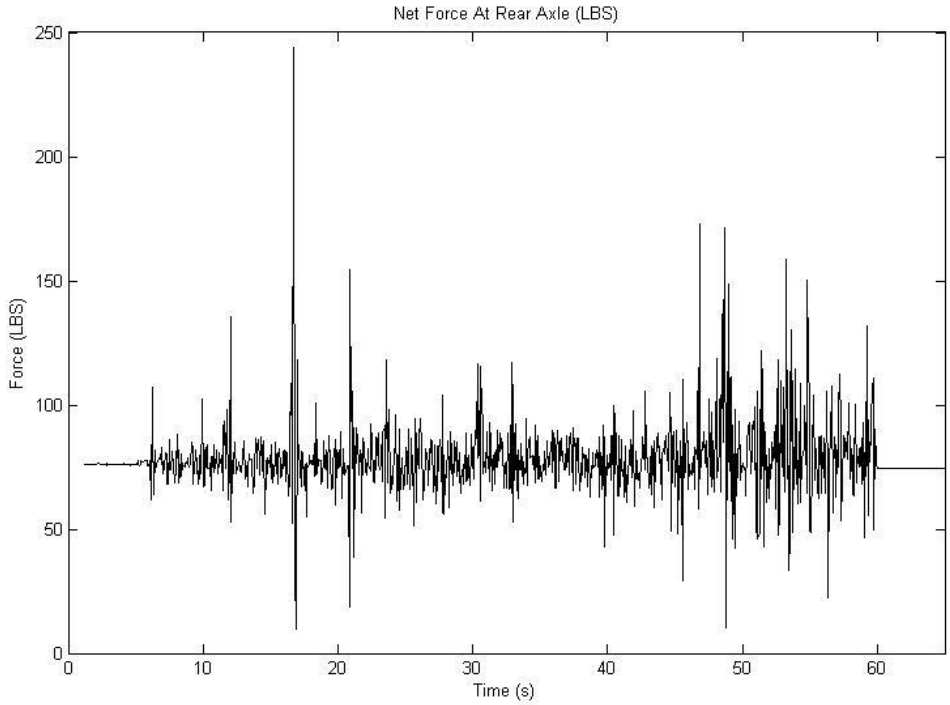

Force on Rear Axle

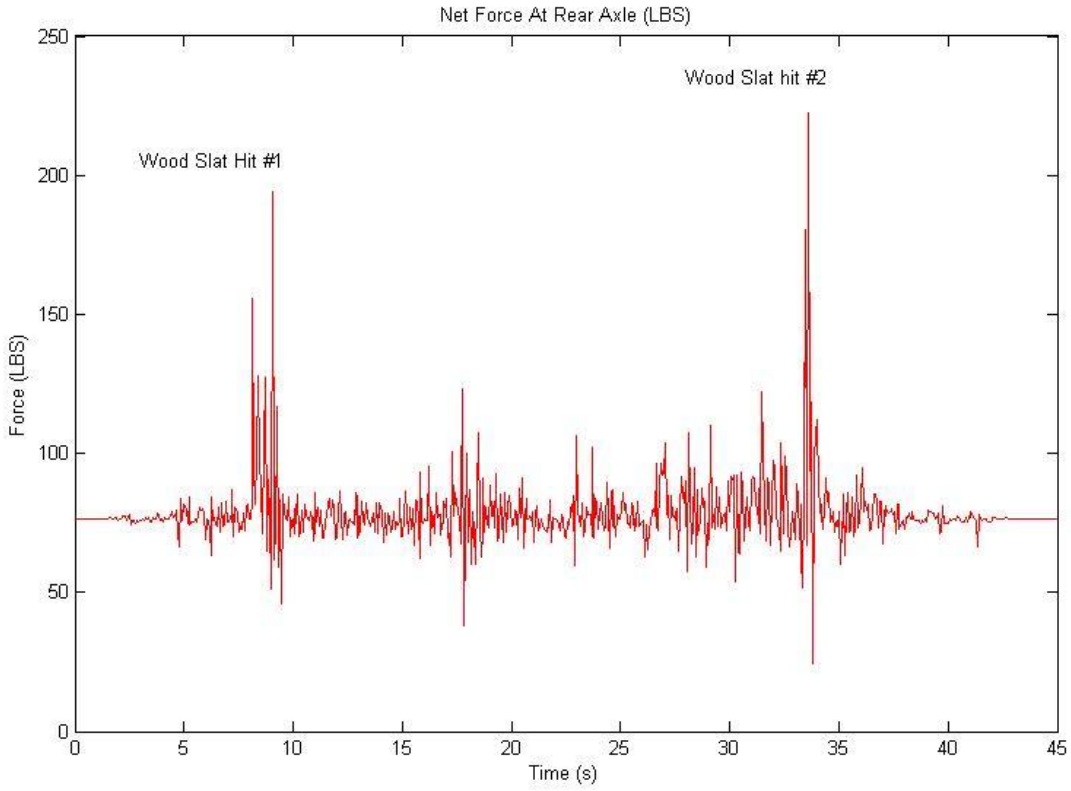

Force on Rear Axle Over Rumble Strip

COEFFICIENT OF DRAG RESULTS

Change in Length

Length (in)	Width (in)	Height (in)	Speed (in/s)	Force (lbf)	Area (in^2)	C_d
96	18	33	704	0.4572	595.12	0.033
102	18	33	704	0.3775	579.41	0.028
108	18	33	704	0.3897	576.73	0.029
96	18	37	704	0.5995	681.54	0.038
102	18	37	704	0.4110	670.37	0.026
108	18	37	704	0.5400	670.51	0.035
96	18	39	704	0.6008	727.01	0.036
102	18	39	704	0.4123	751.53	0.024
108	18	39	704	0.5919	718.78	0.036
96	20	33	704	0.3215	624.85	0.022
102	20	33	704	0.3020	611.54	0.021
108	20	33	704	0.3198	600.8	0.023
96	20	37	704	0.5132	716.58	0.031
102	20	37	704	0.4957	702.1	0.030
108	20	37	704	0.4895	701.49	0.030
96	20	39	704	0.5913	763.3	0.033
102	20	39	704	0.5336	755.25	0.030
108	20	39	704	0.5085	750.21	0.029
96	22	33	704	0.3878	662.26	0.025
102	22	33	704	0.4633	651.16	0.031
108	22	33	704	0.3926	633.91	0.027
96	22	37	704	0.5417	760.07	0.031
102	22	37	704	0.5659	753.55	0.032
108	22	37	704	0.4376	740.06	0.025
96	22	39	704	0.6102	809.7	0.032
102	22	39	704	0.5902	805.48	0.032
108	22	39	704	0.4914	792.63	0.027
96	24	33	704	0.4520	700.15	0.028
102	24	33	704	0.3914	683.3	0.025
108	24	33	704	0.3361	678.4	0.021
96	24	37	704	0.6170	803.72	0.033
102	24	37	704	0.5126	790.64	0.028
108	24	37	704	0.5767	788.48	0.032
96	24	39	704	0.7177	855.92	0.036
102	24	39	704	0.5843	844.81	0.030
108	24	39	704	0.5251	845.19	0.027

Change in Width

Length (in)	Width (in)	Height (in)	Speed (in/s)	Force (lbf)	Area (in^2)	C_d
96	18	33	704	0.4572	595.12	0.033
96	20	33	704	0.3215	624.85	0.022
96	22	33	704	0.3878	662.26	0.025
96	24	33	704	0.4520	700.15	0.028
96	18	37	704	0.5995	681.54	0.038
96	20	37	704	0.5132	716.58	0.031
96	22	37	704	0.5417	760.07	0.031
96	24	37	704	0.6170	803.72	0.033
96	18	39	704	0.6008	727.01	0.036
96	20	39	704	0.5913	763.3	0.033
96	22	39	704	0.6102	809.7	0.032
96	24	39	704	0.7177	855.92	0.036
102	18	33	704	0.3775	579.41	0.028
102	20	33	704	0.3020	611.54	0.021
102	22	33	704	0.4633	651.16	0.031
102	24	33	704	0.3914	683.3	0.025
102	18	37	704	0.4110	670.37	0.026
102	20	37	704	0.4957	702.1	0.030
102	22	37	704	0.5659	753.55	0.032
102	24	37	704	0.5126	790.64	0.028
102	18	39	704	0.4123	751.53	0.024
102	20	39	704	0.5336	755.25	0.030
102	22	39	704	0.5902	805.48	0.032
102	24	39	704	0.5843	844.81	0.030
108	18	33	704	0.3897	576.73	0.029
108	20	33	704	0.3198	600.8	0.023
108	22	33	704	0.3926	633.91	0.027
108	24	33	704	0.3361	678.4	0.021
108	18	37	704	0.5400	670.51	0.035
108	20	37	704	0.4895	701.49	0.030
108	22	37	704	0.4376	740.06	0.025
108	24	37	704	0.5767	788.48	0.032
108	18	39	704	0.5919	718.78	0.036
108	20	39	704	0.5085	750.21	0.029
108	22	39	704	0.4914	792.63	0.027
108	24	39	704	0.5251	845.19	0.027

Change in Height

Length (in)	Width (in)	Height (in)	Speed (in/s)	Force (lbf)	Area (in^2)	C_d
96	18	33	704	0.4572	595.12	0.033
96	18	37	704	0.5995	681.54	0.038
96	18	39	704	0.6008	727.01	0.036
96	20	33	704	0.3215	624.85	0.022
96	20	37	704	0.5132	716.58	0.031
96	20	39	704	0.5913	763.3	0.033
96	22	33	704	0.3878	662.26	0.025
96	22	37	704	0.5417	760.07	0.031
96	22	39	704	0.6102	809.7	0.032
96	24	33	704	0.4520	700.15	0.028
96	24	37	704	0.6170	803.72	0.033
96	24	39	704	0.7177	855.92	0.036
102	18	33	704	0.3775	579.41	0.028
102	18	37	704	0.4110	670.37	0.026
102	18	39	704	0.4123	751.53	0.024
102	20	33	704	0.3020	611.54	0.021
102	20	37	704	0.4957	702.1	0.030
102	20	39	704	0.5336	755.25	0.030
102	22	33	704	0.4633	651.16	0.031
102	22	37	704	0.5659	753.55	0.032
102	22	39	704	0.5902	805.48	0.032
102	24	33	704	0.3914	683.3	0.025
102	24	37	704	0.5126	790.64	0.028
102	24	39	704	0.5843	844.81	0.030
108	18	33	704	0.3897	576.73	0.029
108	18	37	704	0.5400	670.51	0.035
108	18	39	704	0.5919	718.78	0.036
108	20	33	704	0.3198	600.8	0.023
108	20	37	704	0.4895	701.49	0.030
108	20	39	704	0.5085	750.21	0.029
108	22	33	704	0.3926	633.91	0.027
108	22	37	704	0.4376	740.06	0.025
108	22	39	704	0.4914	792.63	0.027
108	24	33	704	0.3361	678.4	0.021
108	24	37	704	0.5767	788.48	0.032
108	24	39	704	0.5251	845.19	0.027

RIDER POSITION STUDY DATA

3 Minute Test at 130°							
	Average Power (W)	Max Power (W)	Average Heart Rate (BPM)	Average Cadence (RPM)	Energy Expended (Kj)	Rider Weight (Kg)	Power To Weight
Alex	195	312	177	68	35	83.9	2.32
Erik	251	439	164	97	47	70.3	3.57
Heather	172	301	164	80	32	58.96	2.92
Phillip	140	521	160	87	27	86.2	1.62
Kevin	245	443	166	94	44	83.9	2.92
Matt	175	311	163	85	33	63.5	2.76

3 Minute Test at 122°							
	Average Power (W)	Max Power (W)	Average Heart Rate (BPM)	Average Cadence (RPM)	Energy Expended (Kj)	Rider Weight (Kg)	Power To Weight
Alex	229	492	189	70	42	83.9	2.73
Erik	307	426	174	101	55	70.3	4.37
Heather	154	491	170	91	28	58.96	2.61
Phillip	159	382	164	93	29	86.2	1.84
Kevin	242	406	175	91	47	83.9	2.88
Matt	174	230	158	90	31	63.5	2.74

3 Minute test at 115°							
	Average Power (W)	Max Power (W)	Average Heart Rate (BPM)	Average Cadence (RPM)	Energy Expended (Kj)	Rider Weight (Kg)	Power To Weight
Alex	194	361	183	69	35	83.9	2.31
Erik	287	381	165	95	53	70.3	4.08
Heather	131	503	169	84	25	58.96	2.22
Phillip	131	427	164	89	25	86.2	1.52
Kevin	244	422	175	98	45	83.9	2.91
Matt	188	319	139	93	34	63.5	2.96